Recombinant protein immobilisation and display by alginate

A thesis presented in partial fulfilment of the
requirements of the degree of
Master of Science
in
Microbiology
at Massey University, Palmerston North,
New Zealand

Andrew Jameson

2016

ABSTRACT

Biopolymers are a diverse group of organic materials with important applications in a number of industries. Their ability to adsorb and encapsulate compounds has been widely utilised in both biotechnologies and pharmaceuticals. In the last decade, biopolymers have been given new and enhanced functionality, including the separation and purification of compounds. This field is of increasing relevance as advances in the bacterial cell culture process have improved productivity in the biomanufacturing industry, with the establishment of several bacterial host cell lines and optimised protein production systems. This increase in upstream productivity is leading to bottlenecks in downstream processing as current technology platforms reach their limits of throughput and scalability. While previous studies have generated functionalised protein biopolymers using polyhydroxyalkanoate (PHA) biopolyester beads, very few studies have examined the commercially significant biopolymer alginate. Alginate is an exopolysaccharide produced by algae and some bacteria, and is widely utilised in food, pharmaceutical, and biomedical industries because of its stabilising, haemostatic, biocompatible properties and its modifiable structure. In this study, a partially functional alginate-binding recombinant protein was produced, which contained an α-amylase domain from *Bacillus licheniformis* (BLA) translationally fused to the alginate-binding domain of *Pseudomonas aeruginosa* AlgX – an alginate acetyltransferase. An Ssp DnaB mini-intein was included between BLA and AlgX to facilitate recovery of BLA, following immobilisation and display on the surface of alginate. However, aberrant activity of the intein caused total cleavage of the recombinant protein between its BLA and AlgX domains before it could be recovered from the protein production system. Additionally, the absence of a key cysteine residue in the alginate-binding domain prevented the formation of a disulfide bond, which is an essential structural element for the folding and functionality of this region. While this study was unable to overcome intein hyperactivity, functional analysis of the BLA domain showed consistent and significant levels of α-amylase activity, leading to a positive outlook for the functionality of a full-length recombinant protein if proper intein activity can be restored and the necessary cysteine included. In this way, alginate could be specifically functionalised with a desired protein, and in turn, alginate beads could be used for the separation and enrichment of target proteins.

ACKNOWLEDGEMENTS

First and foremost, my gratitude goes to my supervisor, Dr. Bernd Rehm. Thank you for the opportunity, the challenges, the exceptional work environment, and for the understanding and patience when I floundered. I wasn't always the best student, sometimes not even a decent one, but you never gave up on me, and for that I'm in your debt.

My deepest appreciation to my co-supervisor Dr. Zoe Jordens for always believing in me. It was your enthusiasm and confidence that convinced me to pursue postgrad, and without you I would not be writing this today at the conclusion of my Masters of Science.

Thank you, Dr. Fata Moradali. Not content with just completing your PhD and multiple publications, you had to help a struggling MSc student find their footing in the lab and be their mentor throughout their project. Your efforts, assistance and good spirits enriched my years at Massey University. My one regret is that my research was unable to generate a paper, in which all your hard work could be properly recognised as a co-author. However, this thesis is a testament to your guidance, and I am forever grateful.

I would like to thank my family. To Dad, you were a bastion of patience and calm on those bad days when nothing seemed to go right, and you were unquestioning in your support and advice. To Mom, your endless supply of love and study aids made our home a warm and welcoming place after a long day (week) at Massey. And for my sisters, I will miss the breakfasts and coffees together, your love and encouragement were a constant. I love you all.

A heartfelt thank you to the Rehm lab and PolyBatics groups. Too many to name, too great to leave out. Each of you made the lab my home-away-from-home. From the reagents being cooked up in the lab, the discussions around the table at lunch, or the comradery from working well into the night, every one of you enlivened my postgraduate experience, and I will sincerely miss you all.

To my friends, thank you for enduring the endless rants about my project. You saw me at my worst, and still gave me your best.

My appreciation goes out to Massey University and the Institute of Fundamental Sciences. You provided a supportive and collegial workplace for my postgrad; and finally fixed the WiFi connection in the reading room, God bless. Importantly, there are people of IFS that I wish to personally thank. To Ann Truter, you provided the greatest assistance to all my bureaucratic fumblings. I offer my gratitude for your patience when I took an eternity to respond to emails. To Dr. Kathryn Stowell, your care and diligence to the postgraduate students of IFS is inspiring, and I do not know if I would have finished postgrad without your compassion and support. To Trevor Loo, I will always appreciate your guidance and technical expertise with gel filtration chromatography; you made one of the most confusing and frustrating experiences look effortless. And finally to the people of the Massey Genome Service, thank you all for your exceptional work sequencing my twice-damned plasmids and genes.

Speaking of cursed idols, thank you to the University of Otago and the Centre for Protein Research for your tireless efforts to ruin my day with peptidase S8. I wish I could have given you my actual recombinant protein to analyse, but I do sincerely appreciate your work on those damnable proteases.

Finally, to my partner Javier, thank you for your unconditional love and support these last two-and-a-half years. You picked me up and dusted me off after each stumble, and stood by my side and faced down every problem and obstacle. Without you, I wouldn’t have made it. You deserve the world.

TABLE OF CONTENTS

LIST OF ABBREVIATIONS

A full list of abbreviations.

˚C	Degree Celsius
A	Absorbance
AGE	Agarose gel electrophoresis
Ap	Ampicillin
APS	Ammonium persulfate
BLA	*Bacillus licheniformis* α-amylase
bp	Base pairs
BSA	Bovine serum albumin
Δ	Delta (deleted)
DMSO	Dimethyl sulfoxide
DNA	Deoxyribonucleic acid
dNTPs	Deoxyribonucleotide triphosphates
dsDNA	Double-stranded deoxyribonucleic acid
DTT	Dithiothreitol
ETOH	Ethanol
EDTA	Ethylenediaminetetraacetic acid
g	Gram/gravity
GDP	Guanine diphosphate
His-tag	Polyhistidine-tag
HRP	Horse radish peroxidase
kbp	Kilo base pairs
kDa	Kilodaltons
λ	Lambda phage
LB	Luria-Bertani (broth)
MOPS	3-(N-morpholino)propanesulfonic acid
MW	Molecular weight
OD	Optical density

ORF	Open reading frame
PBS	Phosphate-buffered saline
PCR	Polymerase chain reaction
PEG	Polyethylene glycol
REase	Restriction endonuclease
RNAase	Ribonuclease
Rpm	Rotations/revolutions per minute
SDS	Sodium dodecyl sulfate
SDS-PAGE	Sodium dodecyl sulfate polyacrylamide gel electrophoresis
TB	Terrific Broth
TBE	Tris-borate-EDTA buffer
TBST	Tris-buffered saline and Tween 20
Tet	Tetracycline
TEMED	Tetramethylethylenediamine
T_m	Primer melting temperature
Tris	Trishydroxymethylaminomethane
vol	Volume
v/v	Volume per volume
w/v	Weight per volume

LIST OF FIGURES

LIST OF TABLES

CHAPTER ONE
INTRODUCTION

Biopolymers are a diverse group of organic materials with important applications in a number of industries. Their ability to adsorb and encapsulate compounds has been widely utilised in both biotechnologies and pharmaceuticals (Leonard *et al.*, 2013, Ramadas *et al.*, 2000, Shimoyama *et al.*, 2012). In the last decade, biopolymers have been given new and enhanced functionality, including the separation and purification of compounds (Grage and Rehm, 2008, Hay *et al.*, 2015). This field is of increasing relevance as advances in the bacterial cell culture process have improved productivity in the biomanufacturing industry, with the establishment of several bacterial host cell lines and optimised protein production systems. This increase in upstream productivity is leading to bottlenecks in downstream processing as current technology platforms reach their limits of throughput and scalability (Gottschalk, 2008, Langer, 2012).

Chromatography remains a valuable tool in the separation and purification of proteins, and has a leading role in downstream processing of therapeutic proteins, especially antibodies. However, there are limitations to chromatography brought about by capacity, as more product results in higher production costs in a near linear fashion. Due to the capacity and cost constraints of chromatography, there has been interest for a 'low-tech' non-chromatographic alternative for downstream processing in the biomanufacturing industry (Langer, 2012). One area of research being explored is the production and immobilisation of functional recombinant proteins onto carrier materials. Carrier materials such as biopolymers have potentially greater capacity than chromatography columns, and specifically bind the target compound (Grage and Rehm, 2008, Hay *et al.*, 2015). While previous studies have used polyhydroxyalkanoate (PHA) biopolyester beads to immobilise recombinant proteins fused to the PHA-binding protein PHA synthase (PhaC), there have been few studies done using other biopolymers, such as alginate. Alginate is the collective term for a group of polysaccharides produced by brown seaweed and a few bacteria, and is a highly versatile, modifiable

biomaterial extensively utilised in textile, food, pharmaceutical and biomedical industries (Rehm, 2010).

In this chapter I first describe chromatography and an alternative protein separation method (Section 1.1). In Section 1.2, I expound on the structure, biosynthesis and applications of alginate. I then review the components of a recombinant protein design, including the alginate binding protein AlgX (Section 1.3), α-amylase (Section 1.4), and Ssp DnaB mini-intein (Section 1.5). In Section 1.6, I evaluate *Bacillus megaterium* for recombinant protein production. Finally, I outline the aims and objectives (Section 1.7) and hypotheses of the study (Section 1.8).

1.1 Chromatographic protein purification and a potential separation alternative

1.1.1 Liquid chromatography

Chromatography is the collective term for a set of techniques used to separate a mixture by distributing its components between two phases: a stationary phase that remains fixed in place, and a mobile phase that carries the mixture through the medium. Because of the difference in factors such as the solubility and size of certain components in the mobile phase, and the strength of their affinities for the stationary phase, some components will move faster than others, thus facilitating separation.

Liquid chromatography is a type of chromatography, in which the mobile phase is a liquid, and is frequently used in the separation and purification of proteins from a mixture. Separation can be based on affinity between the protein and specific molecules in the stationary phase (affinity chromatography), interactions between the charge of the resin and the charge of the protein (ion exchange chromatography or IEC), or the size of the protein versus the pore size of the column (size exclusion chromatography or SEC). Affinity chromatography is used in the purification of proteins bound with tags, such as His-tags, biotin or antigens, or by the protein's affinity for a metal (Zn, Cu, Fe, Ni, etc.). While this form of chromatography is very specific, it is not very robust and over time the resins may need to be replaced. Additionally, there can be sample losses due to improper elution of the bound protein. IEC uses an ion exchange mechanism to separate proteins based on their respective charges, in which functional groups on the stationary phase resin interact with oppositely charged groups of the compound to be retained. IEC is less specific than affinity chromatography, but it is more robust, and the protein does not need to be modified after purification as is often the case with affinity-based tags. Finally, SEC separates proteins according to their size, in which smaller proteins are able to enter the pores of the media used and are removed from the flow of the mobile phase. The residence time for these proteins depends on their effective size, whereas larger proteins that are excluded from these pores undergo no retention and are the first to be eluted. SEC has the advantage that there is no sample loss. However, it suffers from relatively low resolving power compared with other

chromatography techniques, in which there must be a 10% difference in molecular mass between different proteins to achieve good resolution (Skoog, 2006).

The advantages of chromatography for protein separation are its simple methods and generally high resolving power, which allows for separation of components from a complex mixture. Although chromatography resins have benefitted from improved dynamic binding capacity, advancements in chromatographic operations have not kept pace with the significant enhancements in protein production, including in bacterial cell culture. This disparity between chromatographic separation throughput and increasing protein production levels is likely to grow over time. While upstream processes cannot exceed cell density and protein solubility limitations, there is still much room for improvement in protein production, leading to an upward trend for recombinant protein batch volume that will need downstream processing. While larger columns that are capable of accommodating larger batch volumes are as reliable and robust as smaller columns, there is no economy of scale. The additional cost of resins, buffers, and other consumables currently outstrips any savings made by increasing productivity (Gottschalk, 2008, Langer, 2012). Furthermore, long-term operations with multiple bind-and-elute cycles require meticulous cleaning to prevent progressive fouling and microbial contamination (Gottschalk, 2008). This is typical in chromatographic operations where certain techniques only partially purify proteins, such as IEC, which requires additional cycles and different column-types to achieve purification. SEC has similar limitations as it requires combination with other HPLC techniques to achieve high purity of the desired protein.

The capacity and cost limitations of chromatography, coupled with the multiple steps and cycles necessary to achieve high purity of product has fuelled research towards a single-step non-chromatographic alternative for protein purification. One innovative technique is the one-step production of recombinant proteins that are immobilised by a carrier material.

1.1.2 One-step production of immobilised recombinant protein

One of the earlier studies looking at the potential of recombinant protein-specific immobilisation and display by carrier materials focussed on polyhydroxyalkanoate (PHA), and

PHA synthase (PhaC), a key enzyme in the formation of PHA beads (Grage and Rehm, 2008). Polyhydroxyalkanoate is a biopolyester produced by bacterial fermentation of sugars and lipids, and is deposited in the form of highly refractive granules within the cell. PhaC is embedded in the outer phospholipid monolayer of PHA during its synthesis (Uchino *et al.*, 2007). Recombinant protein-displaying PHA beads were generated by the overproduction of a target protein genetically fused to the PHA synthase gene (*phaC*) (Hay *et al.*, 2015). These recombinant protein polymer beads were successfully used for laboratory-scale protein purification, and demonstrated an enrichment process for recombinant protein. Similarly, the high-density display of functional protein at the inclusion surface of polyhydroxybutyrate (PHB) was adapted to the production of pure recombinant protein (Grage *et al.*, 2011). The inclusion of a cleavage site such as an enterokinase (EK) or a self-cleaving module such as modified sortase A (Srt A) between PhaC and the target protein allowed for recovery of the target protein. After isolation of PHA beads, the target protein could be specifically cleaved off by EK digestion or induction of Srt A, resulting in purified protein.

This technique of recombinant protein production and immobilisation by PHA beads has been adapted for other target proteins. In a study by Rasiah and Rehm (2009), an α-amylase was successfully used as the target protein of a recombinant PhaC fusion protein, demonstrating activity equal to free α-amylase. Furthermore, PHB beads have been used to display multiple antigens with potential diagnostic and therapeutic applications (Chen *et al.*, 2014, Parlane *et al.*, 2015).

While protein display on biopolyester beads has been studied and applied, there exist alternative biomaterials available that have yet to be explored for their capacity to specifically immobilise and display recombinant proteins on their surface. One such alternative is the exopolysaccharide alginate. An alginate-binding recombinant protein could act as a proof-of-concept, and open up further research into the potential of alginate in polymer-assisted protein purification.

1.2 Alginate structure, biosynthesis and applications

Alginate is a linear, anionic exopolysaccharide consisting of β-D-mannuronic acid and its C5-epimer α-L-guluronic acid, which are linked via β-1,4-glycosidic bonds in alternating

sequences or in homopolymeric blocks. The block copolymers can be arranged as consecutive guluronate residues (G-blocks), consecutive mannuronate residues (M-blocks) or as alternating mannuronate and guluronate residues (MG-blocks) (Figure 1) (Rehm, 2010, Remminghorst and Rehm, 2006).

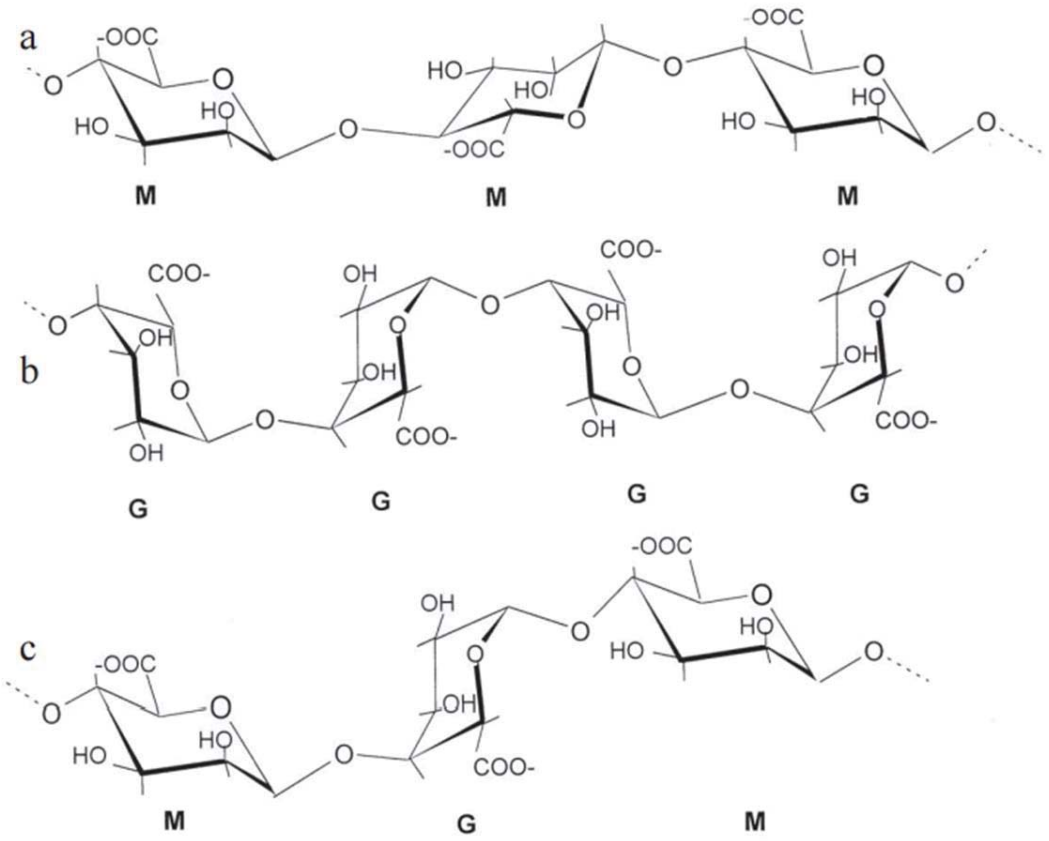

Figure 1. Chemical structure of alginate. Alginate is a linear anionic co-polymer of β-D-mannuronic acid and its C5-epimer α-L-guluronic acid, which are linked via β-1,4-glycosidic bonds in alternating sequences or in homopolymeric blocks. The block copolymers can be arranged as consecutive mannuronate residues (M-blocks) (a), consecutive guluronate residues (G-blocks) (b), or as alternating mannuronate and guluronate residues (MG-blocks) (c) (Rehm, 2010).

While commercially farmed alginate is almost exclusively isolated from brown seaweeds (*Phaeophyceae*), alginate is also synthesised by species of the two bacterial genera *Pseudomonas* and *Azotobacter*. Algal alginates suffer from seasonal heterogeneity in composition and material properties, which distinguishes them from bacterial alginates. Bacterial alginate is restricted, however, due to prohibitive costs of commercial production.

Bacterial alginates have been shown to have a high capacity for chemical modification both *in vivo* and *in vitro*, allowing for greater tensile strength, increased water retention and resistance to tear (Boyd and Chakrabarty, 1995, Hay *et al.*, 2013). There are so far eight *Pseudomonas* species capable of alginate biosynthesis: *P. aeruginosa*, *P. syringae*, *P. fluorescens, P. putida*, *P. brassicacaerum, P. mendonica, P. alkylphenolia,* and *P. entomophila*. In contrast, only one species of *Azotobacter*, *A. vinelandii*, has been shown to produce alginate (Riley *et al.*, 2013). *A. vinelandii* is of particular significance as it is a non-pathogenic source of bacterial alginate and alginate-binding protein genes. While alginate biosynthesis in *P. aeruginosa* has been widely studied, the role of this bacterial species as an important opportunistic human pathogen should be considered when selecting a genetic source for potential biotechnological and pharmaceutical applications, as it may complicate product licensing requirements.

The alginate biosynthetic gene cluster characterised in *P. aeruginosa* has been studied as the model for alginate production and regulation. The gene cluster contains sequences for *algD, alg8*, *alg44, algK, algE, algG, algX, algL, algI, algJ, algF,* and *algA,* and acts as an operon controlled by the *algD* promoter (Chitnis and Ohman, 1993). Alginate biosynthesis takes place in the bacterial cytoplasm where fructose-6-phosphate is converted to GDP-mannuronic acid (the subunit comprising alginate) through the activity of AlgA (a bifunctional enzyme known as a phosphomannose isomerase and GDP-mannose pyrophosphorylase), AlgC (phosphomannomutase), and AlgD (GDP-mannose dehydrogenase) (Figure 2) (Franklin *et al.*, 2011, Robles-Price *et al.*, 2004). While the initial steps of alginate biosynthesis have been thoroughly studied, the later steps are still being elucidated and characterised. An as yet to be identified transporter shuttles the alginate intermediate across the inner membrane into the periplasmic space. GDP-mannuronic acid is polymerised at the inner membrane into polymannuronic acid blocks by the polymerase and co-polymerase, Alg8 and Alg44 (Rehman *et al.*, 2013). The newly formed polymer is subsequently modified in two ways. AlgG, a mannuronan C5 epimerase, partially epimerises the mannuronic acid residues into guluronic acid (Franklin *et al.*, 1994). AlgF, AlgI, and AlgJ acetylate some of the mannuronic acid residues, which improves water retention in the final alginate polymer (Franklin and Ohman, 1993, Franklin and Ohman, 1996). The mature alginate polymer will consist of varying amounts of polyM, polyG, and polyMG blocks, with some of the mannuronic acid residues

acetylated. AlgE appears to act as an anion channel, and is therefore considered to be the outer membrane protein involved in transporting the alginate polymer into the extracellular space (Rehm *et al.*, 1994).

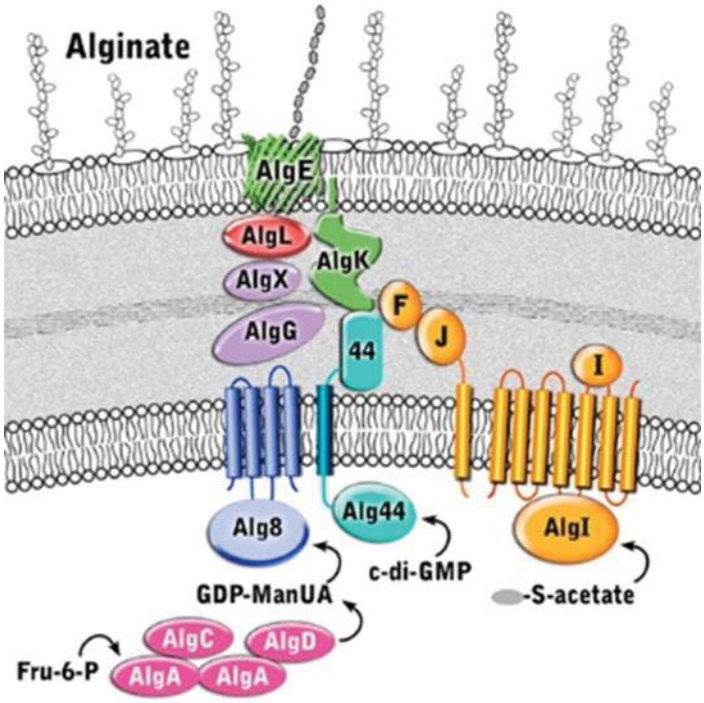

Figure 2. Bacterial alginate biosynthesis model. Alginate biosynthesis begins in the cytoplasm where AlgA, AlgC, and AlgD convert fructose-6-phosphate into GDP-mannuronic acid. The alginate intermediate is transported across the inner membrane into the periplasm, at which stage Alg8 and Alg44 polymerise GDP-mannuronic acid into polymannuronic acid blocks. The polymer is further modified by AlgG, which partially epimerises the mannuronic acid residues into guluronic acid, while some mannuronic acid is acetylated by AlgF, AlgI, AlgJ, and AlgX. AlgL interacts with the transporter protein scaffold formed by AlgG, AlgK and AlgX, and also has lyase activity, which breaks down alginate polymer. AlgE is an outer membrane anion channel that transports the alginate polymer into the extracellular space (Franklin *et al.*, 2011).

AlgL (alginate lyase) has an unknown role in alginate biosynthesis, although its presence has been shown to be necessary for alginate production and it is considered to be a regulator of alginate biosynthesis (Albrecht and Schiller, 2005, Shankar *et al.*, 1995). A proposed role for AlgL is the recognition and degradation of improperly formed alginate polymers into their subunits for recycling in the periplasm (Svanem *et al.*, 2001). Another study has suggested

AlgL could be part of a transporter protein scaffold along with AlgG, AlgK and AlgX, which protects and shuttles the alginate polymer across the periplasmic space (Albrecht and Schiller, 2005). Since the role of this scaffold is to protect the polymer from lyase activity, it is possible that both these models are correct as an alginate polymer that does not form a proper complex with the scaffold will be exposed and vulnerable to AlgL-facilitated breakdown. Following production and secretion into the extracellular space, alginate interacts with the environment and forms complex structures through cross-linkage with divalent cations.

Bacterial alginate is produced in response to environmental conditions and is one of the major components in biofilm formation in alginate-producing bacteria. The exopolysaccharide aids in protecting the bacteria from harmful compounds, such as antibiotics and other biocides, and from abiotic stresses, such as pH, by forming a mechanical barrier. The ability for alginate to bind several times its own volume of water, coupled with a slow rate of desiccation, prevents dehydration of the sessile bacteria. To this end, it has been shown that acetylated uronic acids increase alginate hydration, demonstrating improved functionality through chemical modification (Boyd and Chakrabarty, 1995). Alginate also has a role in the formation of micro-colonies *in vitro*, and can act as an adhesin, assisting in anchoring the bacteria to surfaces and in cell localisation (Nivens *et al.*, 2001). In particular, mucoid (alginate-producing) *Pseudomonas aeruginosa* has been shown to have a greater attachment to the epithelial cells lining the trachea compared with non-alginate producing *P. aeruginosa*. This confers an advantage to the alginate-producing bacteria, which are the predominant strains of *P. aeruginosa* isolated in the lungs of cystic fibrosis (CF) patients (Doig *et al.*, 1987, Tielen *et al.*, 2005). Finally, alginate is the main constituent of the glycocalyx in alginate-producing bacteria, where it aids bacteria by fixing nutrients through encapsulation in alginate for subsequent growth utilisation (O'Toole *et al.*, 2000). Encapsulation in alginate has been widely exploited in food, textile, and pharmaceutical industries for delivery systems of bioactive agents and probiotics.

The material properties of alginate include the ability to form gel-like structures in the presence of divalent cations, ability to be modified by other biomaterials, and biocompatibility with a number of cells (Hay *et al.*, 2013). Alginate can be modified with other biomaterials such as chitosan, methylcellulose and silk fibroin fibres to form composite matrices that provide additional functionality and improved hydrogel characteristics, such as

resistance to tear in fibroin-alginate composites (de Moraes *et al.*, 2014). Additionally, the ability of alginate films to encapsulate and immobilise whole cells has been extensively exploited allowing alginate to be used as delivery systems for probiotics and antimicrobial agents (Leonard *et al.*, 2013, Ramadas *et al.*, 2000, Shimoyama *et al.*, 2012). Industrial enzymes are frequently immobilised via cross-linking onto solid supports to enhance stability and facilitate repeated use in bioreactors. However, an alginate matrix forms a mechanical barrier that inhibits access of the substrate and release of the product. Enzyme entrapment by alginate is also a non-specific process, requiring separation and purification steps for the desired enzyme prior to immobilisation by alginate. Immobilisation of a recombinant protein specifically to alginate is potentially a more efficient, superior alternative to encapsulation as it eliminates the additional separation and purification steps, and offers specificity for the enzyme to be displayed.

Figure 3. Applications of alginate. Alginate is used as a stabiliser, gelling agent and regulator of viscosity (from top left) in bandaging, ice cream, as well as (from bottom left) beer and pharmaceuticals. Algicare™ is copyright property of Casex.

In an aqueous solution, copolymer blocks of alginate form ionic crosslinks through divalent cations (such as Ca^{++}) to produce gel-like structures, known as hydrogels (Sun *et al.*, 2012). These hydrogels are biocompatible, having a non-toxic effect on humans and mammals and

as such they are utilised extensively in the biomedical and biotechnology fields. Ca^{++}-alginate is a natural haemostat and has thus been employed as an alternative wound dressing to traditional linen and paraffin gauze. In particular alginate dressings provide significant improvement in healing split skin graft donor sites, where the epidermis and part of the dermis have been removed for transplantation. The alginate hydrogel occludes the wound and creates a moist environment, in which scab and scar formation is decreased by the absorbance of ulcer exudates by the dressing. Normally, formation of a scab or scar prolongs the healing process by creating a mechanical barrier to epidermal cell migration. Thus an alginate dressing promotes rapid granulation and re-epithelialisation. When the time comes for removal of the dressing, the gel-forming properties of alginate decreases the likelihood of new trauma, and reduces the pain experienced during dressing changes (Paul and Sharma, 2004). A biocomposite membrane composed of sodium alginate solution reinforced with silk fibroin fibres was tested and found to have improved tensile strength and resistance to tear. As silk fibroin fibres are biocompatible, the silk fibroin-alginate composite has many possible applications in the biomaterial field, including improved wound dressing (Moraes and Beppu, 2013). Alginate hydrogels are also used for whole cell immobilisation and enzyme encapsulation, providing antimicrobial potential. Matrices entrapping bioprotective lactic acid bacteria (LAB), such as *Lactococcus lactis* spp. *lactis*, have been explored to control undesirable microbial growth of *Listeria monocytogenes* in food. LAB whole cells immobilised by an alginate matrix, and especially a composite alginate-caseinate matrix, showed higher antimicrobial activity towards *Listeria* than non-encapsulated LAB whole cells (Leonard *et al.*, 2013). This was attributed to the increased survival rate of LAB cells in the alginate and alginate-caseinate matrices, and from an associated increase in the release of antimicrobial metabolites compared with non-encapsulated cells. Alginate is also used to directly encapsulate antimicrobial agents, such as natamycin. Natamycin is an anti-fungal macrolide naturally produced by *Streptomyces natalensis* during fermentation and inhibits microbial protein biosynthesis. While natamycin and its metabolites have antimicrobial activity at low dosages, it does not have acute toxicity towards mammalian cells, and has not been associated with antimicrobial resistance in fungi, leading to widespread use in the food industry. In a study where potassium sorbate or natamycin was incorporated in an alginate film, alginate films containing potassium sorbate showed no sign of microbial growth inhibition, whereas alginate films with natamycin were able to inhibit growth of *Debaromyces*

hansenii, Penicillium commune and *Penicillium roqueforti* at concentrations as low as 5 µg per gram of biopolymer, and 1 µg per gram of an alginate/chitosan composite film (Silva *et al.*, 2012).The salient difficulty of enzyme entrapment is that accessibility of the substrate and release of the product is inhibited by the mechanical barrier of the alginate structure. Although a study by Léonard *et al*. reported an increased release of antimicrobial metabolites for immobilised LAB cells compared to non-encapsulated cells, this is attributed to the localisation of the cells by the alginate matrix, and it is unlikely that greater antimicrobial activity would be observed for encapsulated LAB metabolites compared to non-encapsulated metabolites (Leonard *et al.*, 2013).

Adsorption of enzymes to the surface of alginate beads is another method of immobilising a target compound (Castro *et al.*, 2009, Castro *et al.*, 2005). However, because adsorption is not an enzymatic reaction it lacks specificity and orientation. Adsorption of enzymes to alginate beads is significantly slower than other types of enzyme immobilisation, and the active site may be blocked by the bead, greatly reducing enzymatic activity.

The main disadvantage of both encapsulation and adsorption as methods of enzyme immobilisation by alginate beads is that the enzyme must be separated and purified prior to immobilisation. Enzyme entrapment does not have specificity for an alginate matrix, and any impurities will be immobilised by alginate in addition to the desired enzyme. A separation step is therefore necessary between protein production and immobilisation on an alginate matrix.

Immobilisation of a recombinant protein that specifically binds to an alginate bead or matrix is an attractive alternative to both enzyme encapsulation and adsorption. Unlike adsorption, a recombinant protein that binds to alginate will possess both specificity and orientation. Specific binding will occur more efficiently than adsorption as the rate of alginate binding is dependent on enzyme kinetics, whereas adsorption is governed by non-specific factors, such as the rate of arrival of molecules at the alginate surface and the proportion of incident molecules which undergo adsorption. Similarly, because alginate binding is specific the recombinant protein will be orientated correctly, ensuring that the active site of the fusion partner is not blocked by alginate. A recombinant protein that specifically binds to alginate will also be superior to enzyme encapsulation as the protein is displayed on the surface of the alginate. Protein display on the surface of alginate greatly increases the accessibility of both

substrate and enzyme compared with an enzyme that is encapsulated by an alginate matrix. Finally, the advantage of immobilisation of an alginate-binding recombinant protein on alginate beads is that there is no requirement for an additional separation step as there is for non-specific methods of immobilisation.

1.3 AlgX, an alginate-binding protein essential to alginate production

AlgX was first characterised in *P. aeruginosa* as a strict periplasmic protein between 49 and 52kDa essential to alginate biosynthesis (Robles-Price *et al.*, 2004, Weadge *et al.*, 2010). A part of the *algX* gene in *P. aeruginosa* strain FRD1::pJLS3 was replaced with a non-polar gentamycin resistance cassette to form an *algX* knockout, where the resulting *algXΔ::Gm* mutant was phenotypically non-mucoid (non-alginate producing). Mucoid phenotype was subsequently restored by the addition of wild-type *P. aeruginosa algX*. Mass spectroscopy and Dionex chromatography analysis of the oligouronic acid produced by the *algXΔ::Gm* mutant indicated it was comprised mainly of mannuronic acid dimers, where the dimers were a result of AlgL degradation of polyM blocks. These results indicated that AlgX is part of a protein scaffold including AlgG and AlgK that surrounds and protects the newly formed polymers from AlgL activity prior to a series of modification steps that the polymer undergoes as it is transported across the periplasm (Robles-Price *et al.*, 2004). Similar results are seen when either *algG* or *algK* is removed, indicating a similar function. What is interesting is the function of AlgX before the modification steps, as the absence of guluronic acid dimers in the *algX* knockout indicates that AlgX functions after polymerisation, but before epimerisation, and that its protective function is possibly M-block specific. AlgX binds the M-blocks of alginate and may align it properly so that AlgG can epimerise some of the mannuronic acid residues, followed by acetylation.

The structure and function of AlgX as an acetyltransferase was further elucidated in recent studies (Figure 4). Sequence analysis of the N-terminal region (residues 50-200) of AlgX from *P. aeruginosa* suggested structural homology to members of the SGNH hydrolase superfamily of enzymes with 9% sequence identity to *Enterococcus faecalis* hydrolase (Weadge *et al.*, 2010). The active sites of this hydrolase superfamily contain four strictly conserved residues, serine, glycine, asparagine, and histidine, hence the SGNH acronym. Asp174, His176 and

Ser269 of AlgX have been suggested to form part of the signature Ser-His-Asn catalytic triad characteristic of SGNH hydrolase superfamily members. The N-terminal region of AlgX also shares 69% similarity and 30% identity with AlgJ from *P. aeruginosa* (the putative alginate acetyltransferase), indicating AlgX may have similar function. Site-specific mutagenesis of the Ser-His-Asp triad or other key residues in the putative active site resulted in either non-acetylated alginate polymer or polymer with reduced acetylation (Riley *et al.*, 2013). The C-terminal region (residues 346-474) functions as a carbohydrate binding module (CBM), with Trp-400, amongst other residues, forming a substrate recognition "pinch-point" that is proposed to aid in binding alginate and substrate orientation. The pinch-point is formed by the presence of aromatic amino acids, such as tryptophan, and conserved polar residues in a groove on the surface of the protein, which assists in passing the polysaccharide through this groove. Aromatic residues have been shown to stack with the rings of the sugar in polysaccharides, which stabilise the polysaccharide-protein complex, and are important in determining specificity to a particular polysaccharide. The polar residues of the pinch point form hydrogen bonds directly with the polymer to increase stability of the complex.

Conservation of the CBM domain is high, with 57% similarity and 18% identity of the CBM in AlgX across all eight *Pseudomonas* spp. and their *A. vinelandii* homologue. Trp-400 is 100% conserved in all alginate-producing *Pseudomonas* spp. and *A. vinelandii*, strongly suggesting a conserved function of this residue in AlgX (Riley *et al.*, 2013). Overall AlgX from *Pseudomonas* spp. has 49% identity with AlgX from *A. vinelandii* (Robles-Price *et al.*, 2004). A C-terminal fusion of AlgX with Strep-tag II was subjected to ^{1}H-NMR analysis, which showed that the C-terminal region does not alter alginate composition and therefore it is not involved with acetyltransferase activity of AlgX (Gutsche *et al.*, 2006).

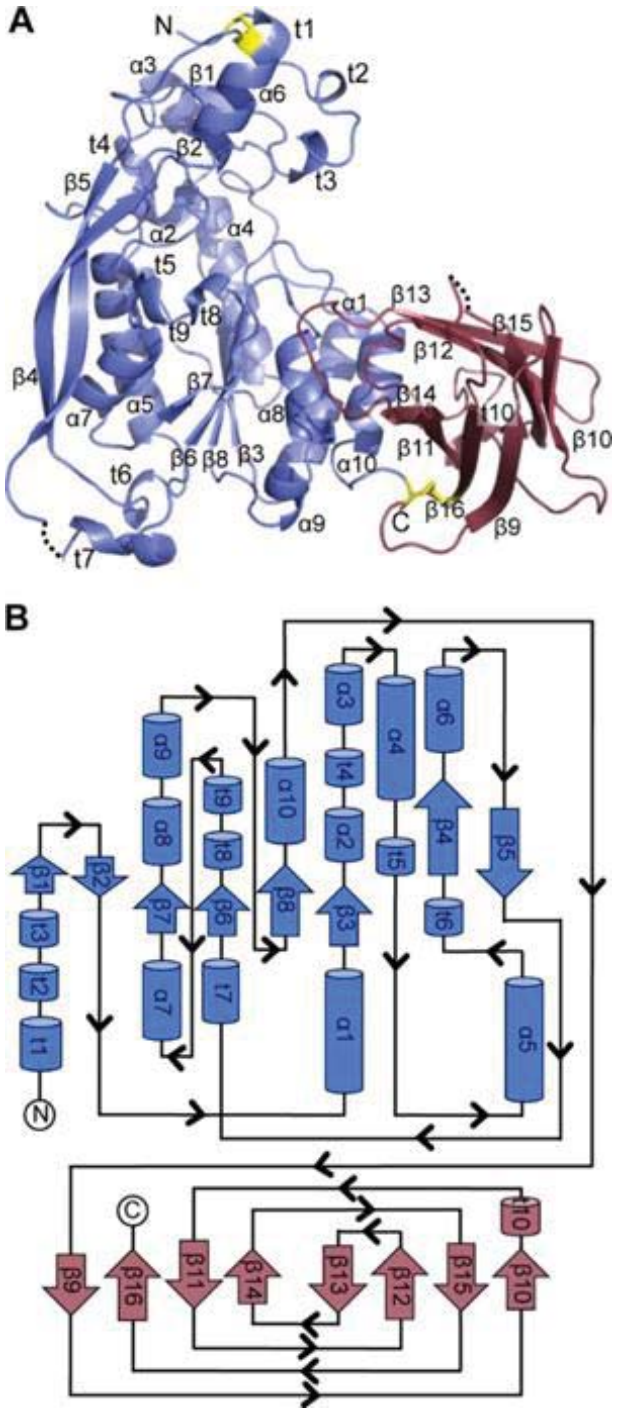

Figure 4. Structure of AlgX. *A.* Three-dimensional schematic representation of AlgX from *P. aeruginosa* with secondary structure elements labelled as follows: α-helix (α), β-strand (β), 3_{10} helix (*t*). The N-terminal and C-terminal domains are represented in *blue* and *red*, respectively; the two disulfide bonds are represented in *yellow*. *B.* Topology representation of AlgX with the secondary structural elements labelled and coloured as in *A.* N and C in both *A* and *B* represent the N and C termini of the protein, respectively (Riley *et al.*, 2013).

The C-terminal region of AlgX is an excellent candidate for the alginate-binding domain of a recombinant protein. AlgX has several advantages over the other alginate biosynthesis proteins. AlgA, AlgC and AlgD are cytoplasmic proteins that recognise and bind intermediates during the conversion of fructose-6-phosphate into GDP-mannuronic acid, and therefore do not bind to mature alginate polymer (Franklin *et al.*, 2011). Alg8 and Alg44 bind oligouronic acid; however, both are membrane proteins, making them difficult to utilise due to the inability to overproduce membrane proteins in functional form. Overproduction of membrane proteins typically results in cytoplasmic accumulation of inactive aggregated protein (Luo *et al.*, 2009). AlgE is also unsuitable as it is an outer membrane protein, which functions as a porin, and thus interaction with alginate polymer is due to AlgE being strongly anion selective, rather than undergoing specific binding (Rehm *et al.*, 1994). Of the periplasmic proteins, AlgG epimerase specifically binds polyM blocks. However, the conserved electropositive groove that facilitates alginate binding contains at least nine substrate binding subsites, which align the polymer in the correct fashion for catalysis to occur (Wolfram *et al.*, 2014). In this way, there is a great deal of crossover between substrate binding sites and the catalytic site, whereas AlgX has a clear delineation between the two functional domains. Interestingly, the other acetyltransferases AlgF, AlgI and AlgJ have either weak or no detectable polymer binding capacity, despite AlgI and AlgJ having similar SGNH hydrolase-like N-terminal regions as AlgX (Baker *et al.*, 2014, Franklin and Ohman, 1993, Franklin and Ohman, 1996). AlgK has no alginate-binding function, and instead has a role in the assembly and stabilisation of functional alginate biosynthesis machinery. AlgL, an alginate lyase, is on par with AlgX as a suitable alginate-binding domain donor. AlgL has a two-domain structure, with an exolytic region and a substrate recognition region (Park *et al.*, 2014). Depending on the active site residues, AlgL can specifically bind either polyM or polyG blocks, whereas AlgX will only bind polyM blocks (Zhu and Yin, 2015). This ambiguity of substrate type in AlgL is a minor disadvantage as a potential donor, although it is controllable. The active site residues for substrate recognition in the selected alginate lyase would require confirmation to determine whether a recombinant protein would be polyM- or polyG-specific, whereas there is no such requirement for AlgX. In practical terms, however, AlgL and AlgX are both highly suitable candidates to provide the alginate-binding domain for the recombinant protein, but one has to be selected.

Taken together, AlgX is a suitable choice as an alginate-binding protein. AlgX is a periplasmic protein and therefore it may have better viability than a cytoplasmic protein when produced as an extracellular recombinant protein. The three-dimensional structure of AlgX has been elucidated and the two functional domains are segregated between the N- and C-terminal in such a way that substrate recognition and binding is carried out by the C-terminal, and is independent of the acetyltransferase activity of the N-terminal (Riley *et al.*, 2013). The C-terminal region of interest is small (17 kDa), allowing for a wider molecular weight range when considering potential fusion partners, as larger recombinant proteins typically encounter difficulties and increased costs in downstream processing compared with low molecular weight proteins.

1.4 Alpha-amylase as a potential fusion partner

Alpha-amylase is an extracellular endo-acting enzyme that hydrolyses 1,4-α-D-glucosidic linkages in starch and glycogen in a random fashion to yield glucose and maltose (Haki and Rakshit, 2003). *Bacillus licheniformis* α-amylase (BLA) is a heat-stable α-amylase widely used in the starch, brewing, food and textile industries, and is an important component in biofuel production (Liu *et al.*, 2014, Qin *et al.*, 2012).The unique characteristics of BLA, including chemical, temperature and pH stability make the enzyme ideal for high temperature enzymatic applications.

The overall structure of BLA is typical of α-amylases and contains three domains, referred to as A, B, and C (Figure 5). The central B domain contains an α/β barrel (TIM barrel), which forms the core of the enzyme, containing the active sites and the N-terminus. Interaction between BLA and polymeric substrate (starch) occurs via multiple binding sites, the catalytically active site (comprising Asp231, Glu261 and Asp328), and two substrate binding sites (His105, His235, and His289). The stability of BLA and the ionisation state of the catalytically active residues have an important role in maintaining enzymatic activity in acidic conditions (Liu *et al.*, 2014).

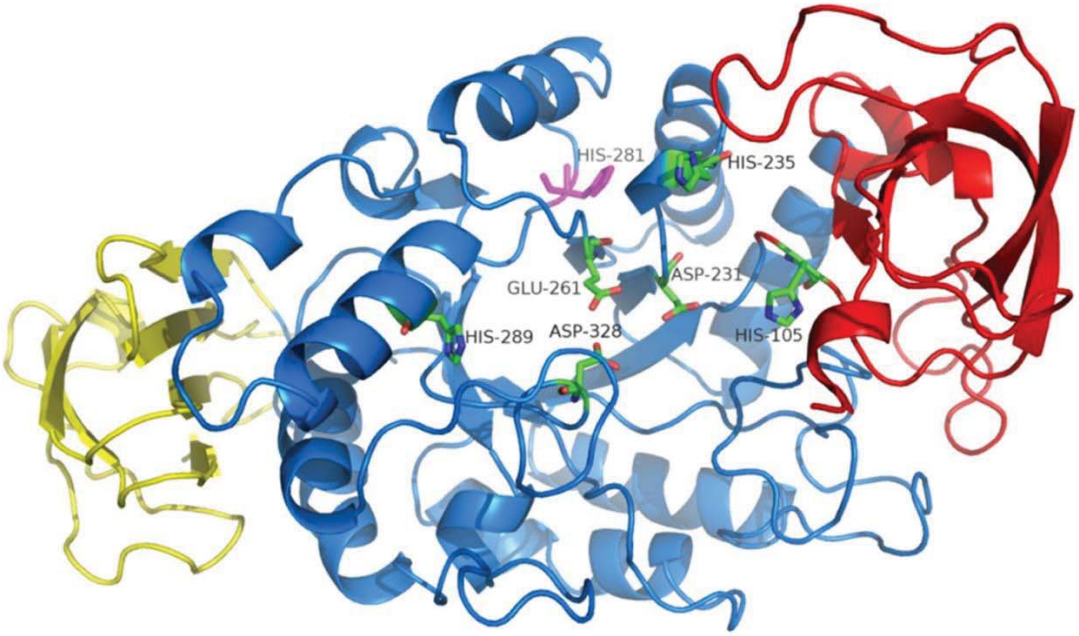

Figure 5. Structure of α-amylase. Three-dimensional schematic representation of *Bacillus licheniformis* α-amylase (BLA). The three domains A, B, C, are represented by *red*, *blue*, and *green*, respectively. The multiple binding sites of BLA located in the central B domain include His105, Asp231, His235, Glu261, His289, and Asp328 (Liu *et al.*, 2014).

In a study by Rasiah and Rehm (2009), BLA was successfully fused with PhaC in *E. coli* to produce a PHA-bound recombinant protein. The N-terminal fusion protein allowed for immobilisation and display of α-amylase on the surface of PHA beads without negatively impacting on the activity of BLA. Analysis of the immobilised α-amylase determined that activity was equivalent to the activity of free α-amylase. The recombinant protein was also demonstrated to have stability at 85˚C (with optimal activity at 75˚C) after no loss of BLA activity was detected in BLA-beads incubated at 85˚C for 1 h. BLA-beads also have the capacity for repeated usage, with two additional assay cycles retaining 72-78% of the initial α-amylase activity (Rasiah and Rehm, 2009).

Assessment of α-amylase activity can be done both qualitatively and quantitatively with ease. Starch degradation by bacterial culture can be detected using Lugol's iodine in a simple screen for α-amylase activity, whereas a more comprehensive 3,5-dinitrosalicylic acid colorimetric

assay measures the rate of maltose liberation from starch to give a quantitative analysis of α-amylase activity (Sigma-Aldrich MAK019) (Rasiah and Rehm, 2009).

BLA is an excellent candidate for inclusion as an alginate-binding recombinant protein. The chemical, pH, and temperature stability of BLA make it advantageous compared to proteins that are susceptible to degradation in extreme conditions, and therefore increase the probability of a functional product. BLA has been widely used as a recombinant protein fusion partner, and of particular significance, BLA was fused with another polymer-binding protein (PhaC) to great success. Saliently, immobilisation by polymer beads has been shown to have no negative impact on the activity of α-amylase. Several commercial kits exist to analyse α-amylase activity, and starch degradation is a useful, visual confirmation of recombinant protein production. BLA is also of significant commercial value, and successful display of α-amylase on the surface of alginate beads could lead to an attractive separation alternative. The inclusion of a self-cleaving module or enzyme cleavage site between BLA and the alginate-binding domain would allow for recovery of α-amylase following display on the surface of alginate, and could lead to an enrichment process for BLA.

1.5 Intein, the protein intron

Intein is a segment of some proteins that is able to undergo auto-cleavage and link the remaining regions, the exteins, with a peptide bond in a process known as protein splicing (Anraku *et al.*, 2005). Due to its splicing mechanism and role in the maturation of the final protein, inteins have been likened to their transcriptional splicing analogues, leading to the epithet “protein introns”.

Inteins catalyse protein splicing through a four-step mechanism. The process begins when an induced N-S or N-O acyl shift breaks the peptide bond between the N-terminal extein (N-extein) and the intein, and the N-extein forms an ester bond to the side chain of the intein’s first residue. In the second step, transesterification links the N-extein to the side chain of the C-extein’s first residue through an ester bond. Next, the peptide bond between intein and the C-extein is broken through cyclisation of the intein’s last residue (usually asparagine). Finally, the ester bond between the two exteins is altered to a peptide bond through an S-N or O-N acyl shift (Figure 6) (Miraula *et al.*, 2015, Volkmann *et al.*, 2009).

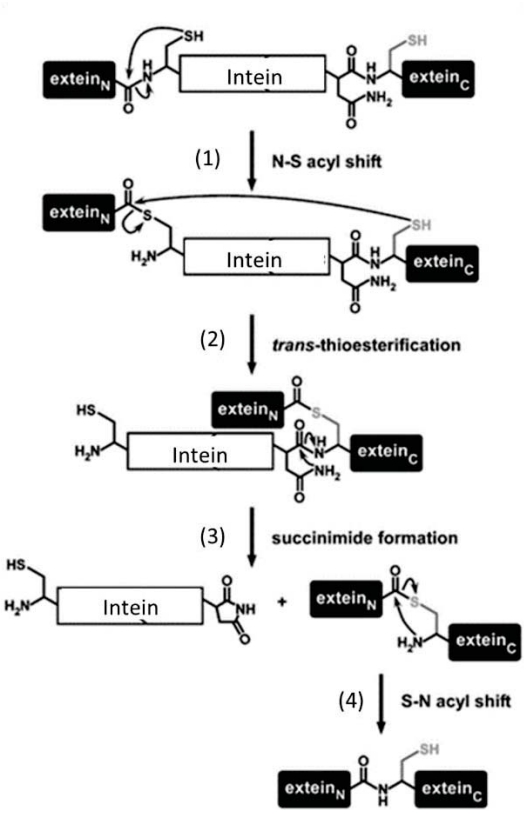

Figure 6. Protein trans-splicing by intein. Schematic representation of the intein trans-splicing mechanism, adapted from Volkmann and Iwai (2010). An induced N-S or N-O acyl shift breaks the peptide bond between the N-terminal extein (extein$_N$) and intein, replaced by an ester bond between extein$_N$ and intein (1). Transesterification links extein$_N$ with the side-chain of the first residue of the C-terminal extein (extein$_C$) (2). The peptide bond between extein$_C$ and intein is broken through cyclisation of the last residue of extein$_C$ (3). Finally, an N-S or N-O acyl shift alters the ester bond between extein$_N$ and extein$_C$ into a peptide bond (4).

The final step in the splicing process can be abolished through alteration of the splicing reaction, which prevents linkage of the two exteins, resulting in site-specific cleavage of the N- or C-terminus of an intein. To achieve N-terminal cleavage, the intein's final residue is mutated to prevent the cyclisation step (Step 3), which in turn prevents the formation of a peptide bond between the two exteins (Step 4). The first step of the splicing mechanism can still happen, and the resulting ester bond between the N-extein and the side-chain of the intein's first residue can spontaneously hydrolyse to separate the N-extein from the intein. To achieve C-terminal cleavage, the intein's first residue is mutated to abolish Step 1, and

consequently Steps 2 and 4. Step 3 can, however, still occur to break the peptide bond between the C-extein and the intein (Volkmann *et al.*, 2009).

Intein cleavage activity can be controlled by an inducer. For N-terminal cleavage, many commercially available inteins are induced by a strong nucleophile such as dithiothreitol (DTT), β-mercaptoethanol (β-ME), or cysteine at low temperatures over a broad pH range. Methods of C-terminal cleavage of an intein are commonly induced by a temperature or pH shift (Chong *et al.*, 1997). However, it remains a challenge to achieve completely controllable cleavages, as unwanted spontaneous cleavages have been encountered when employing contiguous inteins (Volkmann and Iwai, 2010).

Intein can be further modified to minimise its molecular weight. In addition to the splicing domains, inteins can contain a homing endonuclease domain (HEN), a double-stranded DNA-specific endonuclease. This domain is thought to have a role in the transfer of inteins within a species. The HEN domain is not necessary, however, for intein splicing, and therefore it can be removed, forming a 'minimal' or 'mini' intein (Miraula *et al.*, 2015).

Intein-based controllable cleavages have been adapted to an increasing number of useful applications, including single-step purification of affinity-tagged proteins (Volkmann and Mootz, 2013). Affinity tags are frequently used to purify recombinant proteins, as the binding specificity allows for the collection of recombinant protein with few impurities. However, it is typically necessary or desirable to remove the affinity tag through proteolysis during the final purification step. The proteolysis step requires protease specificity in removing affinity tags from the recombinant protein, and the removal of the digestion product. This extra step can be avoided, however, by including a self-cleaving intein linker between the recombinant protein and the affinity tag. The first use of inteins as a tool for protein purification began with a modified *Saccharomyces cerevisiae* VMA (Sce VMA) intein, in which a chitin-binding domain (CBD) from *Bacillus circulans* was used as an affinity tag and fused with a modified Sce VMA intein (Chong *et al.*, 1997). After expressing the CBD recombinant protein, the cell homogenate was passed through a chitin-packed column, allowing for CBD binding. After all impurities had passed through the column, the Sce VMA was then induced to self-cleave by a temperature shift, which allowed for the elution of only the target protein (Chong *et al.*, 1997). This technique has since been adapted into the Intein Mediated Purification with an

Affinity Chitin-binding Tag (IMPACT) method of recombinant protein purification (New England BioLabs).

Inclusion of an intein segment between the alginate-binding domain and fusion partner of a recombinant protein could serve as a modified IMPACT method of purification. After the recombinant protein has been purified by immobilisation on alginate, it may be necessary or desirable to elute the fusion partner from the alginate bead. Ssp DnaB mini-intein is an excellent candidate for the intein segment of the recombinant protein design. It is a smaller intein (18kDa) that undergoes N-terminal cleavage when induced by a pH shift to 6.0 at 20-25˚C. The use of a pH-induced intein has certain advantages over the more commonly used DTT-induced inteins, including reduced production costs. Additionally, DTT has the potential to cause undesirable alterations in the native structure of the recombinant protein, such as the removal of disulfide bridges.

1.6 *Bacillus megaterium* protein production system

Bacillus megaterium is a Gram-positive, chiefly aerobic, spore-forming bacteria found in highly diverse environments. Due to the large size, spore-forming trait, and wide range of pH, temperature and saline tolerances, *B. megaterium* was the major model organism among Gram-positive bacteria for research in biochemistry, sporulation and bacteriophages, prior to the discovery of *Bacillus subtilis* (Bunk *et al.*, 2010). Recently, *B. megaterium* has had renewed prominence in biotechnology for its recombinant protein production capacity, especially for extracellular proteins.

B. megaterium grows at temperatures from 3˚C to 45˚C, with an optimum of around 30˚C, and at pH ranging from 3 to 11, with an optimum of 7. It is an important industrial organism in the production of penicillin amidase, an enzyme used to make synthetic penicillin, glucose dehydrogenase for glucose blood test kits, and amylase for the baking industry. *B. megaterium* amylases (BMA) are predominantly β-amylase, although some strains do produce α-amylase (David *et al.*, 1987, Vary *et al.*, 2007).

After *Escherichia coli*, *Bacillus* species and strains have the greatest popularity for heterologous protein production, with increasing interest in *B. megaterium* since the 1990s (Terpe, 2006). In contrast to *E. coli*, *B. megaterium* lacks an outer membrane and

lipopolysaccharides (LPS). LPS are a major component of the outer membrane of Gram-negative bacteria and are well-known endotoxins, which are pyrogenic to humans and mammals. *B. megaterium* also offers the advantages of a naturally high secretion capacity, in which protein is exported directly into the extracellular medium, structural and segregational stability of plasmids, and the ability to grow on a wide variety of substrates (Demain and Vaishnav, 2009, Terpe, 2006). Additionally, *B. megaterium* has low protease activity, especially compared to other *Bacillus* species, such as *B. subtilis,* and has shown highly efficient expression of homologous and heterologous genes. In contrast to *E. coli*, there is little known about disulfide bond formation and isomerisation of recombinant proteins being produced in *B. megaterium*, and transformation seems to be more difficult than in *E. coli*. Due to the thick peptidoglycan layer, polyethylene glycol-mediated protoplasting is necessary for the efficient transformation of *B. megaterium*. Plasmids typically utilise the xylose-operon for inducing efficient, high-level expression of heterologous genes, with a 130- to 350-fold induction of genes with the addition of 0.5% xylose to the growth medium. Induction is strongly inhibited by the presence of glucose. Due to the high secretion capacity, *B.megaterium* has been used for the production of exoenzymes such as various amylases, penicillin amidase, steroid hydrolases and dextrotransucrase. These exoenzymes are guided by signal peptides to the secretion machinery of the Sec pathway in the cell membrane. Prior to translocation across the cell membrane, these proteins remain unfolded in the cell and fold extracellularly after proteolytic removal of the signal peptide (Terpe, 2006).

B. megaterium strain YYBm1 is a customised deletion mutant of wild type strain DSM319, defined as *ΔnprM* and *ΔxylA* (MoBiTec). The two deletions contain a knockout for a major extracellular protease, and for xylose utilisation by YYBm1. The *ΔnprM* deletion reduces the potential for the recombinant protein product to be degraded after production, and in turn increases product yield. The latter knockout is optimal for expression of plasmids with the xylose promoter as the cells do not metabolise xylose. This enables sustained induction of the xylose promoter, without the need to periodically replenish inducer in the medium.

The production of various amylases by *B. megaterium* poses a potential problem when attempting to screen for recombinant protein expression based on activity of the α-amylase domain of the recombinant protein. However, the production of these native amylases is very low without induction, and their contribution to starch hydrolysis is likely to be minimal,

especially when compared to the functional recombinant protein, in which overproduction is induced (Vary *et al.*, 2007).

1.7 Aim and objectives of this study

On the basis of the current knowledge presented in previous sections, the overall aim of this study was to generate a functionalised recombinant protein-displaying alginate with five objectives:

(1) To generate a hybrid gene of the alginate-binding domain encoding sequence (*ABDx*) of the acetyltransferase AlgX from *Azotobacter vinelandii*, and the α-amylase domain encoding sequence (*amyS*) from *Bacillus licheniformis,* with a mini-intein encoding sequence (*Ssp dnaB*) from *Synechocystis* sp. PCC6803 as a linker.
(2) To overproduce the recombinant AmyS:DnaB:ABDx fusion protein in *Bacillus megaterium* strain YYBm1.
(3) To identify and isolate the recombinant AmyS:DnaB:ABDx fusion protein.
(4) To qualitatively and quantitatively assess the functionality of the alginate-binding domain, α-amylase domain, and the Ssp DnaB mini-intein.
(5) To assess the ability of alginate to separate and purify the recombinant alginate-binding protein.

1.8 Hypothesis statement

This study tested four hypotheses:

(1) A hybrid gene of *ABDx*, *amyS* and *Ssp dnaB* can be generated.
(2) AmyS:DnaB:ABDx recombinant protein can be overproduced and isolated.
(3) The recombinant AmyS:DnaB:ABDx fusion protein is fully functional, demonstrating α-amylase and alginate-binding activity, and that the α-amylase domain can be eluted from the recombinant protein by Ssp DnaB mini-intein activity.
(4) Alginate beads can be used to purify and display a recombinant protein.

CHAPTER TWO
MATERIALS AND METHODS

Unless otherwise stated, all reagents were purchased from Sigma, Ajax Finechem or Merck; all centrifugation events were carried out at room temperature (22 ± 4˚C), and 'water' or 'H_2O' referred to autoclaved Milli-Q water.

2.1 Strains, plasmids, oligonucleotides and expression vectors

Tables 1, 2 and 3 outline the bacterial strains, plasmids and oligonucleotide primers used in the present study. All oligonucleotide primers were synthesised by Integrated DNA Technologies, Inc., USA. Figure 7 shows the hybrid gene design, and Appendix I contains the plasmid maps of the expression vectors used in this study. All DNA sequence maps were generated by SnapGene® Version 2.7.2 (GSL Biotech LLC, USA).

Table 1. Bacterial strains used in this study

Strains	Description	Sources or Reference
Bacillus megaterium MS941	*Δnpr* variant of DSM319	MoBiTec
Bacillus megaterium YYBm1	*Δnpr ΔxylA* variant of DSM319	MoBiTec
Escherichia coli TOP10	Cloning strain	Invitrogen

Table 2. Plasmids used in this study

Plasmids	Description	Sources or Reference
p3stop1623hp	Ap^R, Tet^R, P_{xylA}, *RepU* (referred to as p1623 in text) expression vector	MoBiTec
pUC57-Simple	Ap^R cloning plasmid	GenScript

Table 3. Oligonucleotide primers used in this study

Name	Oligonucleotide sequence (5' to 3')	Sources or reference
Forward pnn	ACTCCTTTGTTTATCCACCG	Katrin Grage
Rev_{10} p1623hp	CGATGGATATGTTCTGCCAA	Katrin Grage
A (*Sfc*I-*Kpn*I) 5Phos	TGTAGCAGGACGACATCATCACCATCACCACTAAGGTAC	This study
B (*Sfc*I-*Kpn*I) 5Phos	CTTAGTGGTGATGGTGATGATGTCGTCCTG	This study
AmySFwd	CATTTAATTAACCAAGGAGGAGGTAGGAAAATGAAAAAGAC	This study
AmySRvr	CCGGATCCACCTCCACCTCCACCTCTTTGCACATAAAT	This study
ABDxFwd	CCGGATCCAGCGGACGTAAAACGGTGTTATCTCGTAAAGTAA	This study
ABDxRvr	CCGGTACCTTAGTGGTGATGGTGATGATGTCGTC	This study

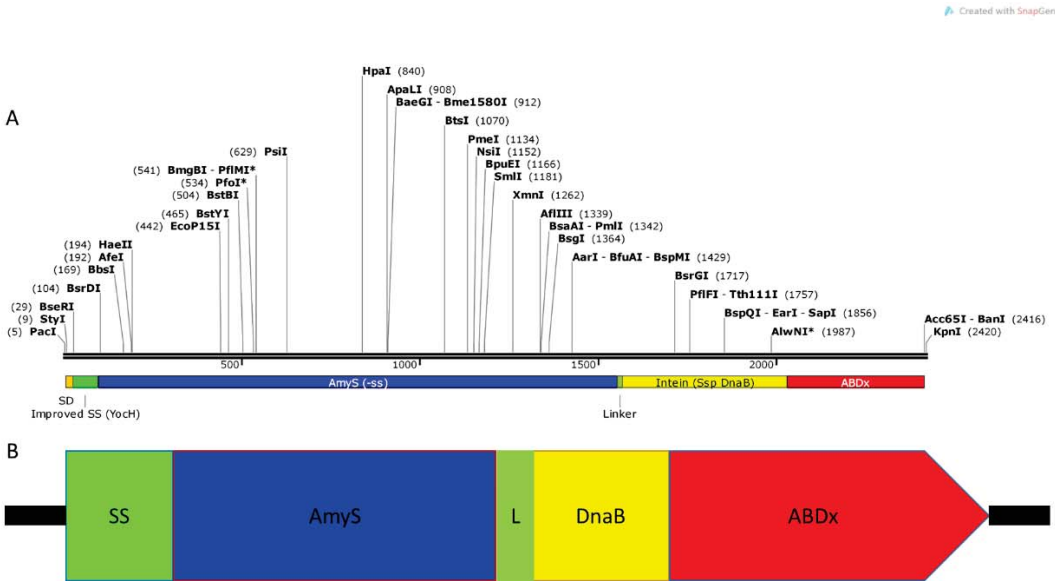

Figure 7. Hybrid gene design. *A.* Sequence map of 2420 bp *amyS-dnaB-ABDx* hybrid gene, including unique restriction sites, Shine-Dalgarno sequence (SD), signal sequence (SS), α-amylase gene without signal sequence (AmyS (-ss)), linker (L), Ssp DnaB mini-intein gene (Intein SSp DnaB), and the alginate-binding domain gene of AlgX (ABDx). *B.* Basic representation of the translated AmyS:DnaB:ABDx recombinant protein design, labelled as in *A*.

2.2 Media

The following liquid and solid media were used in this study. Solid media were prepared by adding agar (Neogen, USA) to 1.5% (w/v) prior to autoclaving. All media were autoclaved at 121˚C for 20min. When required, antibiotics (Section 2.3) were added (Table 4), and cOmplete™ EDTA-free protease inhibitor cocktail (Sigma Aldrich, USA) was added according to the manufacturer's instructions after autoclaving.

2.2.1 Luria-Bertani (LB) medium

Luria-Bertani (LB) medium (Invitrogen Corporation, USA) was prepared according to the manufacturer's instructions. Twenty grams of dry media was dissolved in 1 litre of water, and then autoclaved.

2.2.2 Trace metal mix A5 medium

Trace metal mix A5 medium was prepared according to the Handbook of Microbiological Media, 4th Edition, pg 212-213, and customised for bacterial culture.

A5 medium:

$(NH_4)_2SO_4$	2.0	g
KH_2PO_4	3.5	g
Na_2HPO_4	5.7	g
$MgSO_4$ x $7H_2O$	0.3	g
Yeast extract	1.0	g
H_2O	900.0	ml

The following reagents were filter sterilised and added to A5 medium after autoclaving:

20% (w/v) Glucose	100.0	ml
Trace metal A5 mix	1.0	ml

The following outlines the composition of trace metal A5 mix:

$MnCl_2$ x $4H_2O$	4.0	g
$CaCl_2$ x $2H_2O$	5.3	g
$(NH_4)_6Mo_7O_{24}$ x $4H_2O$	0.2	g
$CoCl_2$ x $6H_2O$	0.2	g
$Fe(II)SO_4$ x $7H_2O$	25.0	mg
H_2O	100	ml

2.2.3 A5-custom medium

A5-custom medium was prepared by combining the protocols for trace metal A5 mix medium (Section 2.2.2) and ZYP-5052 medium (Studier, 2005).

1M Tris-HCl pH 8	100.0	ml
1M $MgSO_4$ x $7H_2O$	2.0	ml
Trace metal mix A5	1.0	ml
ZY	877.0	ml
50 x 5052Xyl	20.0	ml
20 x NPS	50.0	ml

The following outlines the composition of ZY:

Tryptone	10.0	g
Yeast extract	5.0	g
H_2O	1000.0	ml

The following outlines the composition of 50 x 5052Xyl:

Glycerol	25.0	g
Glucose	2.5	g
D-Xylose	10.0	g
H_2O	100.0	ml

The following outlines the composition of 20 x NPS:

$(NH_4)_2SO_4$	6.6	g
KH_2PO_4	13.6	g
Na_2HPO_4	14.2	g
H_2O	100	ml

2.2.4 Terrific Broth (TB) medium

Terrific broth (TB) medium was prepared according to the instructions described by Cold Spring Harbor Protocols 2006. Twelve grams of tryptone and 24 grams of yeast extract were dissolved in 900 millilitres of water.

2.2.5 CR5-top agar medium

CR5-top agar medium was prepared according to the instructions described by MoBiTec for *Bacillus megaterium* protein production system.

CR5-top agar:

Solution A	1.25	ml
8 x CR5 salts	288.0	µl
12% (w/v) proline	125.0	µl
20% (w/v) glucose	125.0	µl
Solution B	713.0	µl

The following outlines the composition of Solution A:

Sucrose	51.5	g
MOPS	3.25	g
NaOH	300.0	mg
H_2O	250.0	ml
pH	7.3	

The following outlines the composition of Solution B:

Agar	2.0	g
Casamino acids	100.0	mg
Yeast extract	5.0	g
H_2O	142.5	ml

The following outlines the composition of 8 x CR5 salts:

K_2SO_4	1.25	g
$MgCl_2$ x $6H_2O$	50.0	g
KH_2PO_4	250.0	mg
$CaCl_2$	11.0	g
H_2O	625.0	ml

LB agar was prepared by dissolving 6 grams of dry media and 1.5% (w/v) agar with 300 millilitres of water prior to autoclaving. To prepare a CR5-top agar plate, 2.5 millilitres of CR5-top agar medium was poured on top of pre-set LB agar.

2.2.6 Starch agar medium

The protocol for starch agar medium was adapted from Rasiah and Rehm (2009). 1% (w/v) soluble starch was combined with 1.5% (w/v) agar with 300 ml of water prior to autoclaving.

2.3 Antibiotic stock solutions and concentrations

Antibiotic stock solutions were prepared as listed in Table 4.

Table 4. Antibiotic stock solutions and concentrations

Antibiotics	Stock concentration (mg/ml)	Final concentration (µg/ml)
	For *E. coli*	
Ampicillin (Na-salt)	100.0 in H_2O	100.0
	For *B. megaterium*	
Tetracycline (hydrochloride)	10.0 in EtOH 70% (w/v)	10.0

2.4 Media pH buffers

For certain experiments, LB (Section 2.2.1) and TB (Section 2.2.4) media were adjusted to pH of 7.4, 8.4, 9.0, or 10.0 through the addition of a pH buffer.

2.4.1 Phosphate-buffered saline (PBS) pH 7.4

A stock 0.2 M phosphate buffer was prepared by mixing sterile Stock A and Stock B Solutions in a ratio of 11:39, respectively. Stock A Solution contains 24 g/L of sodium dihydrogen phosphate (NaH_2PO_4) in 1 L of water. Stock B Solution contains 28.4 g/L of disodium hydrogen phosphate (Na_2HPO_4) in 1 L of water. pH did not require adjusting. 0.2 M PBS pH 7.4 was added to a medium to reach a 1:10 dilution with a final concentration of 20 mM PBS.

2.4.2 Tris-HCl pH 8.4

A stock 1 M Tris-HCl buffer was prepared by adding 121.14 g of Tris to 1 L of water and adjusting pH to 8.4 using 10 M HCl. 1 M Tris-HCl pH 8.4 was added to a medium to reach a 1:10 dilution with a final concentration of 0.1 M Tris-HCl.

2.4.3 Borate buffer pH 9.0

0.2 M borate buffer was prepared according to instructions described by Cold Spring Harbor Protocols:

100 mM boric acid	6.2	g
75 mM NaCl	4.4	g
25 mM sodium tetraborate	9.5	g
H_2O	1000.0	ml
pH	9.0	

2.4.4 Glycine sodium hydroxide buffer pH 10.0

Glycine sodium hydroxide buffer was prepared according to instructions outlined by Cold Spring Harbor Protocols. 75 g of glycine was dissolved in 1 L of water and adjusted to pH 10 using 10 M NaOH before autoclaving.

2.5 Cultivation conditions

All bacterial strains were cultivated at 37˚C, unless otherwise stated. Liquid cultures were grown in Erlenmeyer flasks with shaking at 200 rpm. A ratio of container to culture volume of ≥5:1 was maintained to ensure adequate aeration.

2.6 Long term storage of strains

E. coli TOP10 was grown overnight in LB medium (Section 2.2.1), supplemented with ampicillin (Section 2.3). 1 ml of culture was transferred to a sterile 1.8 ml cryotube vial (Thermo Scientific, USA) and 70 µl of DMSO was added. *B. megaterium* strains were grown to an OD_{600nm} of 0.3 in LB medium, supplemented with tetracycline (Section 2.3). 400 µl of

culture was transferred to a sterile 1.8 ml cryotube vial and 600 µl of 44% (w/v) glycerol was added. Strains were stored at -80˚C and revived when required.

2.7 Competent cell preparation and plasmid DNA uptake

Preparation and transformation of competent *E. coli* TOP10 cells were carried out (Hanahan, 1983). The *B. megaterium* protein production handbook supplied by MoBiTec was followed to prepare and transform protoplasts of *B. megaterium* strains.

2.7.1 Preparation and transformation of competent E. coli

E. coli TOP10 was grown in 50 ml of LB (Section 2.2.1), with ampicillin (Section 2.3), to an optical density at 600nm (OD_{600nm}) of 0.3. The culture was incubated on ice for 10 min before cells were harvested via centrifugation (4,000 g at 4˚C for 20 min). The cell pellet was re-suspended in 18 ml of RF1 solution and incubated on ice for 1 h. The cells were centrifuged as above and re-suspended in 4 ml of RF2 solution. 200 µL aliquots were transferred into clean sterile 1.7 ml microcentrifuge tubes, flash frozen in liquid nitrogen and stored at -80˚C. The composition of RF1 and RF2 solutions, which were sterilised by filtration through separate 0.22 µm filters, are outlined below:

RF1 solution:

RbCl	100.0	mM
$MnCl_2$	50.0	mM
Potassium acetate	30.0	mM
$CaCl_2$ x $6H_2O$	10.0	mM

Adjusted to pH 5.8 with acetic acid

RF2 solution:

RbCl	10.0	mM
MOPS	10.0	mM
$CaCl_2$ x $6H_2O$	75.0	mM
Glycerol	15.0%	(v/v)

Adjusted to pH 5.8 with NaOH

For the transformation of *E. coli*, 50 to 500 ng of plasmid DNA was added to frozen competent cells (as prepared above) and incubated on ice for 1 h. Cells were subjected to heat shock (42˚C for 90 s) and returned to ice for 5 min. 800 µl of LB medium (Section 2.2.1) was added to the cells and incubated for 1 h at 37˚C. Cells were harvested by centrifugation (15,000 g for 2 min) and the cell pellet was re-suspended in 200 µl of LB medium and plated on LB agar containing ampicillin (Section 2.3) to select for colonies containing the plasmid of interest.

2.7.2 Preparation and transformation of competent *Bacillus megaterium* protoplasts

B. megaterium strains were grown in 50 ml LB medium (Section 2.2.1) to an OD_{600nm} of 1.0. Cells were harvested in a 50 ml Falcon® tube via centrifugation (5,000 x g at 4˚C for 15 min). The cell pellet was resuspended in 5 ml freshly prepared SMMP and 50 µl of lysozyme solution (10 mg/ml) was added. The cells were incubated at 37˚C with slight agitation until 80% of cells viewed through a microscope were present as protoplasts. The cells were centrifgued (1,300 x g at 22˚C for 10 min) and the supernatant was carefully removed. The protoplast pellet was resuspended in 5 ml SMMP, and then centrifuged and resuspended again. 750 µl of 87% (v/v) glycerol was carefully mixed with the 5 ml of protoplast suspension and 500 µl aliquots were distributed into clean, sterile Eppendorf® Safe-lock microcentrifuge tubes. *B. megaterium* protoplasts were stored at -80˚C. SMMP is prepared by combining 2 x AB3 and 2 x SMM in a 1:1 ratio. The compositions of 2 x AB3 and 2 x SMM are outlined below:

2 x AB3 (Antibiotic Medium No. 3, Difco)

AB3 (Difco)	7.0	g
H_2O	200.0	ml

2 x SMM

Maleic acid	1.16	g
NaOH	0.8	g
$MgCl_2$ x $6H_2O$	2.03	g
Sucrose	85.58	g
H_2O	Up to 250.0	ml
pH	6.5	
Filter sterilise		

For the transformation of *B. megaterium*, 1-5 µg of plasmid DNA was added to protoplast suspension (as prepared above) and transferred to a 15 ml Falcon® tube containing 1.5 ml of PEG-P and carefully mixed. After incubating the suspension for 2 min at room temperature, 5 ml of SMMP was added and mixed carefully. The cells were centrifuged (1300 x g at 22˚C for 10 min). The supernatant was removed and the cells resuspended in 500 µl SMMP. The cells were incubated at 30˚C for 45 min without agitation, and then 45 min at 300 rpm. After incubation, the cells were transferred to CR5 topagar solution (Section 2.2.5). 2.5 ml of topagar was then poured on top of LB agar containing tetracycline (LBA^{Tet}) (Section 2.3) and spread. After solidification of the topagar (2 h), plates were incubated overnight at 30˚C. Single colonies were then sub-cultured on LBA^{Tet} and incubated overnight at 37˚C for use in protein production (Section 2.9.1). Sub-cultures grown on LBA^{Tet} were stored at 4˚C for a maximum of 10 days.

The composition of PEG-P is outlined below:

PEG-P:

PEG-6000	20.0	g
1 x SMM	Up to 50.0	ml

2.8 DNA isolation, analysis and manipulation

2.8.1 Isolation of plasmid DNA

The GenElute™ Plasmid Miniprep Kit was used for isolation of plasmid DNA from cell cultures according to the manufacturer's instructions (Sigma Aldrich, USA). Cells containing the plasmid of interest were grown at 37˚C for 16 h in LB medium (Section 2.2.1) supplemented with antibiotics (Section 2.3). Cells were harvested and suspended in the Resuspension Solution containing RNase and disrupted by alkaline lysis using the Lysis Solution. Upon lysis, the RNase removed RNA contamination. To the lysed cell suspension, the Neutralisation/Binding Solution was added. After centrifugation (15,000 g for 10 min) to remove the precipitated proteins and chromosomal DNA, the plasmid DNA of the soluble fraction was bound to the GenElute™ Miniprep Binding Columns. After washing with Wash Solution supplemented with 95% (v/v) ethanol to remove contaminants, 80 µl of the provided Elution Solution was used to elute the plasmid DNA.

2.8.2 Isolation of linear dsDNA

To isolate linear dsDNA from polymerase chain reaction (Section 2.8.5) or restriction endonuclease hydrolysis (Section 2.8.6), DNA was first subjected to agarose gel electrophoresis (Section 2.8.4) supplemented with the dsDNA stain SYBR green at 1X concentration (Invitrogen Corporation, USA). Under UV light, the band corresponding to the target dsDNA fragment was excised. Linear dsDNA was purified from the gel fragment using the Zymoclean™ Gel DNA Recovery according to the manufacturer's instructions (Zymo Research, USA). The excised fragment containing the linear dsDNA of interest was solubilised in Agarose Dissolving Buffer at 50˚C for 10 min. After solubilising the gel, DNA from the sample was then bound to a Zymo-Spin™ Column and washed once using the supplied wash buffer to remove contaminants. Finally, the dsDNA was eluted using water.

2.8.3 Determination of DNA concentration

DNA concentration was assessed by spectrophotometry at A_{260nm}. For spectrophotometric analysis, DNA purity can also be analysed as an absorbance ratio at 260/280 nm of 1.8 to 2.0 indicates high purity DNA (Nano-drop ND-1000, USA).

2.8.4 Agarose gel electrophoresis

AGE was used to determine DNA purity and separate DNA fragments after polymerase chain reaction (Section 2.8.5). When required, DNA could be recovered from gels (Section 2.8.2). In general, agarose gels of 1% and 2% (w/v) were used to resolve dsDNA fragments above and below 500 bp, respectively. Agarose (Bioline, USA) was combined with TBE Electrophoresis Buffer (50 mM Tris-HCl, 50 mM Boric acid, 2.5 mM EDTA, pH 8.0) and melted in a microwave oven, poured into a gel chamber and a well comb inserted. After solidification (1 h), the comb was removed and the gel chamber, together with gel, was placed into an electrophoresis apparatus and submerged in TBE buffer. DNA samples supplemented with 0.2 vol of Gel Loading Dye, Purple (6X) (New England Biolabs, USA) were loaded into wells.

A molecular size standard was loaded into a separate well. DNA molecular weight standards in this study were Lambda phage DNA hydrolysed with the restriction endonuclease PstI (Sambrook *et al.*, 1989) and Quick-Load® 100 bp DNA Ladder (New England Biolabs, USA). In general, gels were run in TBE electrophoresis buffer at 6-7 V/cm – distance between anode and cathode – for 60 min. Gels were stained for 30 min in ethidium bromide solution (2 µg/ml)

and de-stained for 1 min in water. DNA bands were visualised using an UV transilluminator (Bio-Rad, Gel Doc, USA) and images were generated.

2.8.5 Polymerase chain reaction

PCR was performed to obtain fragments for cloning and for diagnostic/verification purposes. The high fidelity proofreading Platinum® *Pfx* DNA polymerase (Invitrogen Corporation, USA) was used. The reaction mixture was prepared as outlined below in 0.2 ml clean sterile thin walled PCR tubes (Axygen, USA) on ice:

***Pfx*-DNA-polymerase reaction mixture (A)**

10X *Pfx* Amplification Buffer	20.0	µl
PCR_x Enhancer Solution	22.5	µl
$MgSO_4$ (50 mM)	2.0	µl
DMSO	2.5	µl
Primer 1 (10 pmoles/µl)	3.0	µl
Primer 2 (10 pmoles/µl)	3.0	µl
dNTPs (10 mM each)	3.0	µl
Template DNA	2.0	ng
Platinum® *Pfx* DNA Polymerase (2.5 U/µl)	1.0	µl
H_2O	to 100	µl

For Colony PCR, a scraping of cells from the colony of interest was used as the template DNA, and was added after all other reagents had been mixed.

PCR was performed in a MultiGene™ OptiMax Thermal Cycler (Labnet International, USA) as described below:

1) Primary denature: 94˚C for 300 s
2) Denature: 94˚C for 45 s
3) Anneal: 5˚C below the lowest Tm of the primer pair for 30 s
4) Extend: 68˚C for 60 s per 1 kbp
5) Cycle: steps 2-4 for 30 cycles
6) Hold: 4˚C

2.8.6 DNA hydrolysis with restriction endonucleases

Plasmid DNA (Section 2.8.1) and PCR products (Section 2.8.5) were hydrolysed by restriction endonucleases (REase) for cloning and analysis/verification purposes. Various REase enzymes were used according to the manufacturer's instructions (Invitrogen Corporation, Roche or New England Biolabs). For restriction analysis, 10 U of enzyme was used to hydrolyse 1 µg of DNA in water containing 0.1 vol of 10X recommended buffer. All digestions were performed at 37˚C for 1-3 h and stopped by adding 0.2 vol Gel Loading Dye, Purple (6X) (New England Biolabs, USA). DNA fragments were separated via agarose gel electrophoresis (Section 2.8.4) and fragments of interest could be recovered from gels for subsequent cloning (Section 2.8.2).

2.8.7 DNA ligation

Plasmid DNA and linear dsDNA hydrolysed by restriction endonucleases (Section 2.8.6) were ligated by T4 DNA ligase (New England BioLabs, USA). For ligation, 4000 U of T4 DNA ligase was used to ligate 1 µg of DNA in reaction mixture. The ligation reaction mixture was prepared by combining vector and insert in a ratio of 1:3 and mixed with 0.2 vol 5X reaction buffer. The ligation reaction mixture was incubated overnight at 4˚C.

2.8.8 DNA sequencing

All DNA sequencing of recombinant plasmids was provided by the Massey Genome Service utilising a capillary ABI3730 Genetic Analyser (Applied Biosystems Inc., USA). Results were provided in ABI format and analysed used SnapGene® Version 2.7.2 (GSL Biotech LLC, USA). Four to six hundred nanograms of plasmid DNA purified from cell cultures (Section 2.8.1) or 400 to 600 ng of colony PCR product (Section 2.8.5) were suspended in 14 µl of water and 0.8 µl of each relevant primer (Table 3), and sent for sequencing in 0.2 ml clean sterile thin walled PCR tubes (Axygen, USA).

2.8.9 Addition of a polyhistidine tag

2.8.9.1 Primer dimer synthesis of a polyhistidine tag

Figure 8 outlines the strategy for primer dimer synthesis of a polyhistidine tag genetically fused to the hybrid gene.

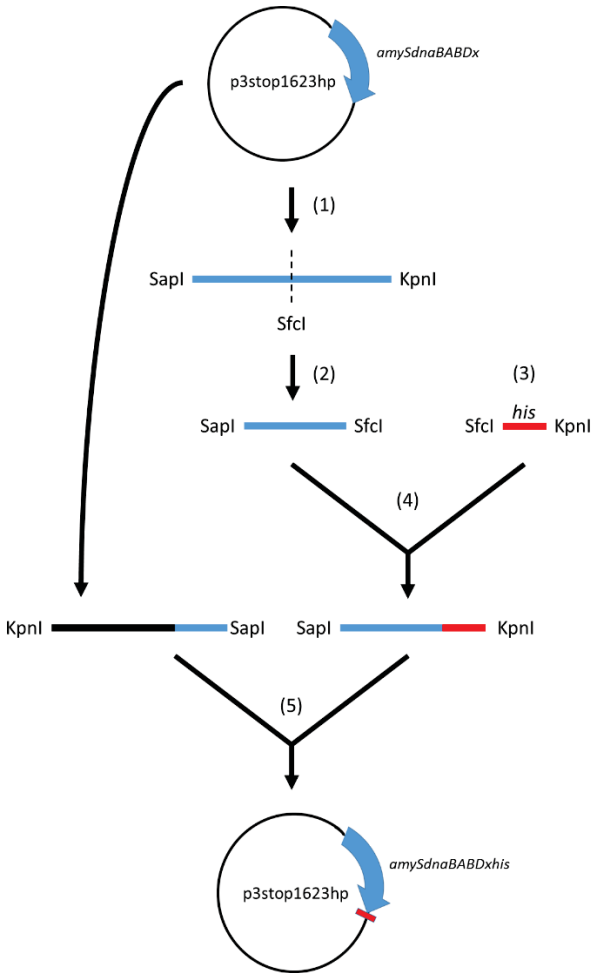

Figure 8. Primer dimer His-tagging. Cloning strategy for His-tagging protein using the primer dimer method. Isolated p1623*amySdnaBABDx* expression vector is hydrolysed by SapI and KpnI restriction endonucleases (REase) (1). The SapI/KpnI-cut gene fragment is hydrolysed by SfcI REase (2). Primers encoding a 6x polyhistidine-tag are annealed to form a primer dimer (3). The Sap/SfcI-cut gene fragment and primer dimer are ligated by T4 DNA ligase (4). The ligated product of (4) and the KpnI/SapI-cut 1623 vector from (1) are ligated by T4 DNA ligase to form p1623*amySdnaBABDxhis* expression vector (5).

Restriction endonuclease digestion of the expression vector was carried out as described in Section 2.8.6 and linear dsDNA was recovered from agarose gel between REase digestions (Section 2.8.2). A non-sequential REase hydrolysis of the expression vector combined the REases of steps (1) and (2) into a single reaction mixture, utilising the shared optimal activity of the restriction enzymes in CutSmart® Buffer (New England BioLabs, USA) (Figure 8). The primers were prepared by adding 0.2 vol of each primer to 0.2 vol 5 M NaCl and 0.2 vol water. Next, primers were annealed (3) by incubating the mixture at 95˚C for 10 mins and cooling to 22˚C. Primer dimers were then added to a ligation reaction mixture (Section 2.8.7) in a 1:200 dilution.

2.8.9.2 Insertion of a polyhistidine-encoding gene fragment

A gene fragment of the hybrid gene was synthesised by GenScript (USA) between *BsrGI* and *KpnI* restriction sites to include a 6xHis-tag (Figure 9).

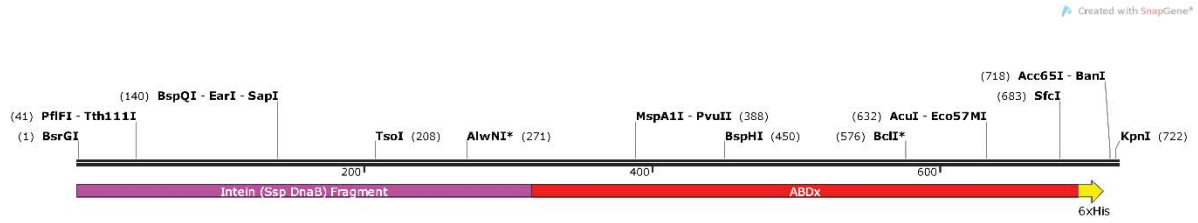

Figure 9. His-tagged gene fragment. Sequence map of the 722 bp *BsrGI-KpnI* His-tagged gene fragment, including unique restriction sites, BsrGI-cut mini-intein gene fragment, alginate-binding domain gene of AlgX (ABDx), and a 6x polyhistidine-tag (6xHis).

The *BsrGI-KpnI* His-tagged gene fragment was synthesised in pUC57-Simple and transferred into TOP10 *E. coli* (Section 2.7.1). Isolated plasmid DNA (Section 2.8.1) was hydrolysed by restriction endonucleases (Section 2.8.6) and linear dsDNA was recovered from agarose gel (Section 2.8.2). The expression vector was hydrolysed by REases and the BsrGI/KpnI digestion of p1623*amySdnaBABDx* was isolated from agarose gel. BsrGI/KpnI-cut vector and insert were ligated (Section 2.8.7)

2.8.10 Excision of a mini-intein encoding gene (*dnaB*)

Figure 10 outlines the strategy for excising the *dnaB* gene.

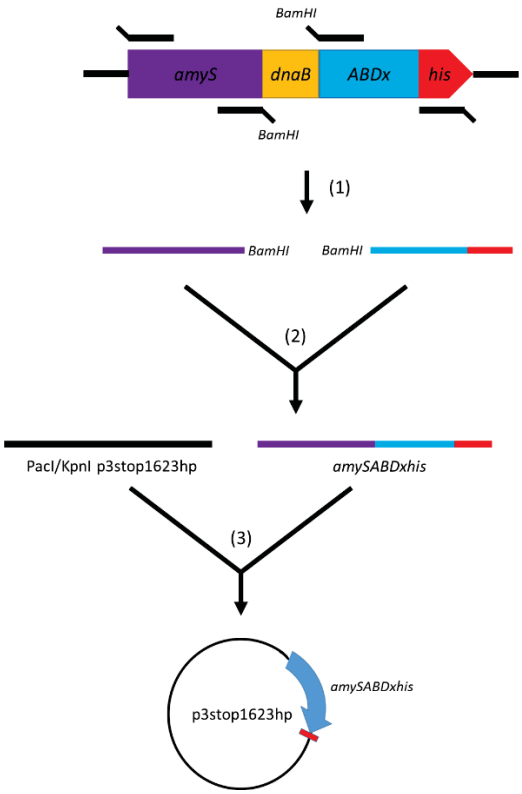

Figure 10. Excision of intein-encoding *dnaB*. PCR amplification and cloning strategy for excising the Ssp DnaB mini-intein gene (*dnaB*). Alpha-amylase gene (*amyS*) and the His-tagged alginate-binding domain gene of AlgX (*ABDx*) are amplified by PCR using primers encoding a *BamHI* restriction site at the 3'-end of *amyS* and 5'-end of *ABDx* (1). The amplified *amyS* and *ABDx* genes are hydrolysed by BamHI restriction endonuclease (REase) and ligated by T4 DNA ligase (2). The ligated product and p1623 vector are hydrolysed by PacI and KpnI REases and ligated by T4 DNA ligase, forming p1623*amySABDXhis* expression vector (3).

2.9 Production of recombinant protein

2.9.1 Protein production in *Bacillus megaterium* strains

Protein production was carried out according to the *B. megaterium* protein production handbook supplied by MoBiTec. *B. megaterium* strains transformed with the hybrid gene were grown in 50 ml of LB medium (LB^{Tet}) (Section 2.2.1) containing tetracycline (Section 2.3) at 37˚C for 14 h. Fresh LB^{Tet} was inoculated with the overnight culture in a 1:100 dilution and

grown until an OD_{600nm} of 0.3-0.4 was reached. To induce *xylA*-mediated production of recombinant protein, sterile 50% (w/v) D-xylose in water was added to the culture to reach a final concentration of 0.5% (w/v) D-xylose in solution. For *B. megaterium* MS941, the concentration of D-xylose in the culture was replenished at OD_{600nm} of 2.0 by adding a second volume of 50% D-xylose to maintain consistent high-level induction of recombinant protein production. *B. megaterium* cultures were grown at 37˚C until an OD_{600nm} of 4-6 was reached. The culture was transferred to a centrifuge container of suitable volume and cells were centrifuged (10,000 x g for 30 min at 4˚C). The cell-free supernatant was transferred to a clean container and stored at 4˚C for extracellular protein collection (Section 2.9.2). The cell pellet was dried and stored at -20˚C.

2.9.2 Extracellular protein collection

The extracellular protein fraction of *B. megaterium* strains was collected and concentrated from the supernatant using ammonium sulfate precipitation (Simpson, 2006) or membrane ultrafiltration with VivaSpin® spin columns (GE Life Sciences, USA).

2.9.2.1 Ammonium sulfate precipitation

The cell-free supernatant (Section 2.9.1) was transferred to a container suitable for centrifugation and with a capacity approximately twice the measured volume of the protein solution. Precipitation of protein with ammonium sulfate was carried out as described by Cold Spring Harbor Protocols (Simpson, 2006). A sufficient amount of solid ammonium sulfate required to give a desired level of saturation (Appendix II) was crushed using a mortar and pestle to ensure a homogenous smooth powder. Ammonium sulfate was added in small batches to the stirring protein solution at 4˚C, allowing each amount to completely dissolve before adding the next. After the addition of ammonium sulfate, the mixture was stirred for another 2 h at 4˚C to ensure complete protein precipitation. The container was then sealed with a cap and centrifuged (10,000 x g for 1 h at 4˚C). Next the supernatant was decanted and the protein pellet was resuspended in 0.1-1.0 ml of 0.1 M Tris-HCl pH 8.4. Residual ammonium sulfate in the resuspension was removed by membrane ultrafiltration using VivaSpin® 500 spin columns (GE Life Sciences, USA) with a molecular weight cut-off (MWCO) of 10kDa. The protein pellet was washed thrice with 0.1 M Tris-HCl pH 8.4 before being collected in a 1.7 ml Eppendorf® Safe-lock microcentrifuge tube for storage at -20˚C.

2.9.2.2 Membrane ultrafiltration

Protein concentration by membrane ultrafiltration used VivaSpin® 20 spin columns with a MWCO of 10 kDa, according to the manufacturer's instructions (GE Life Sciences, USA). The column was prepared for ultrafiltration by first washing with 0.1 M Tris-HCl pH 8.4 at 4˚C to remove trace amounts of glycerine and sodium azide from the membrane. 15 ml of the cell-free supernatant was then loaded into the spin column and centrifuged (6,000 x g for 15 min at 4˚C). This step was repeated until all supernatant had been passed through the spin column. The spin column was then washed thrice before the protein pellet was collected in 0.1-1.0 ml of 0.1 M Tris-HCl pH 8.4. The protein suspension was transferred to a 1.7 ml Eppendorf® Safe-lock microcentrifuge tube for storage at -20˚C.

2.9.3 Determination of protein concentration

The protein concentration of samples was determined using a commercial Bradford assay kit (Biorad, USA). Bovine serum albumin (BSA) at concentrations of 2.0 to 0.016 mg/ml was used to generate a standard curve. Serial two-fold dilutions of samples (up to x128) were made in triplicate. 10 µl of standards and samples were independently mixed with 200 µl of Bradford reagent (Biorad USA) in individual wells of a 96 well plate. After incubation at room temperature for 5 min, the absorbance at 595 nm was measured using a plate reader (ELx808iu Ultramicroplate Reader, Bio-Tek instruments, USA).

2.10 Detection of recombinant protein

2.10.1 Sodium dodecyl sulfate (SDS) gel electrophoresis

Sodium dodecyl sulfate polyacrylamide gel electrophoresis (SDS-PAGE) as outlined by Laemmli (1970) was performed to analyse protein samples. 4X Stacking Gel, 4X Separating Gel, and 10X SDS-PAGE Electrophoresis Buffers were prepared. 4X Stacking Gel Buffer contained 81.7 g/L of Tris and 4 g/L of SDS in 1 litre of water, adjusted to pH 8.9. 4X Separating Gel Buffer contained 60.6 g/L Tris and 4 g/L of SDS in 1 litre of water, adjusted to pH 6.8. 10X SDS-PAGE Electrophoresis Buffer contained 30 g/L of Tris, 10 g/L of SDS and 144 g/L of glycine in 1 litre of water, adjusted to pH 8.5. pH adjustments were made with 10 M NaOH and HCl.

The following describes the preparation of two standard 1.5mm SDS-PAGE gels composed of 10.0 and 3.9% (w/v) acrylamide separating and stacking gels. Unless otherwise stated all

separating gels contained 10% acrylamide. To prepare 20 ml of 10% (w/v) acrylamide separating gel, 5 ml of 4X Separating Gel Buffer, 6.66 ml of 30% (w/v) acrylamide and 8.34 ml of water were thoroughly mixed before a pinch of Na_2SO_3 was added to degas the mixture. Next, 10 µl of 40% (w/v) APS and 10 µl of TEMED were added to the mixture and stirred for 10 s before the mixture was poured into two 1.5 mm mini Novex® Gel Cassettes (Invitrogen, USA), overlaid with isopropanol, and carefully placed on a level surface for 1 h to allow polymerisation.

Upon polymerisation, the isopropanol was removed and the separating gel thoroughly rinsed with water and dried with lint free wipes. To prepare 5 ml of 3.9% (w/v) acrylamide stacking gel, 1.25 ml of 4X Stacking Gel Buffer, 0.65 ml of 30% (w/v) acrylamide and 3.1 ml of water were mixed thoroughly before a pinch of Na_2SO_3 was added to degas the mixture. Then, 2.5 µl of 40% (w/v) APS and 5 µl of TEMED were added to the mixture and stirred for 10 s before the mixture was poured onto the separating gels and well comb inserted. The stacking gel was left to solidify for 1 h.

SDS-PAGE gels were set up in XCell SureLock™ Mini-Cell Electrophoresis Gel Chambers according to the manufacturer's instructions (Invitrogen Corporation, USA). Gels were submerged in 1X SDS-PAGE Electrophoresis Buffer. Protein samples were prepared (Section 2.10.1.1) and loaded into separate wells. For each gel, a protein molecular weight standard (Section 2.10.1.2) was loaded into its own well. SDS-PAGE gels were run at 200 V for 60 min.

Gels were then removed from the 1.5 mm mini Novex® Gel Cassettes and submerged in Coomassie® Brilliant Blue stain for 1 h. Next Coomassie® Brilliant Blue stain was removed and the gels were de-stained with Destaining Solution for 2 h. Destaining Solution was prepared by mixing water, methanol and acetic acid in a ratio of 50/40/10 (v/v/v), respectively. Protein bands were visualised using a Gel Imaging and Doc System (Bio-Rad, Gel Doc, USA) and images were generated.

An isolated protein band of interest was excised from the SDS-PAGE gel and transferred to a sterile 1.7 ml Eppendorf® tube for peptide mass analysis (Section 2.10.4).

Proteins were renatured from some SDS-PAGE gels as outlined by Tabassum *et al.* (2014). After gels were stained with Coomassie® Brilliant Blue and protein bands visualised, SDS-PAGE gels were submerged in 20% (v/v) isopropanol in 0.2 M PBS pH 7.4 for 1 hr at 4˚C. Protein

renaturation was then analysed via the same method as native PAGE gels by incubating in starch solution and staining with Lugol's iodine solution (Section 2.10.3).

2.10.1.1 Preparation of protein samples for SDS-PAGE

Generally for extracellular protein, 25 µl of protein sample was mixed with 5 µl 6X SDS-PAGE loading buffer and held at 95˚C for 5 min. Approximately 25 µg of protein was loaded into each well. For analysis of protein from the bacterial cell lysate, a 50 µl aliquot of cells resuspended in 0.1 M of Tris-HCl pH 8.4 was mixed with 12.5 µl of 8 M urea in 50 mM Tris-HCl pH 7.5, and 12.5 µl of 6X SDS-PAGE loading buffer, prior to incubation at 95˚C for 10 min. The cell debris was then pelleted by centrifugation at 10,000 x g for 1 min, and the cell lysate transferred to a fresh tube. 20 µl of cell lysate sample was loaded into each well. 1 ml of 6X SDS-PAGE loading buffer contained 500 µl of 4X Stacking Buffer, 500 µl of glycerol, 120 mg of SDS, 93 mg of DTT, and 0.2 mg of bromophenol blue.

For analysis of proteins sensitive to strong nucleophiles, a 6X SDS-PAGE loading buffer was made without DTT being added.

2.10.1.2 Protein molecular weight standard for SDS-PAGE

Initially, two stained molecular weight standards, BenchMark™ Pre-stained Protein Ladder (Invitrogen, USA) and Mark12™ Unstained Standard (Novex, USA) were used for estimation of protein molecular weight in SDS-PAGE (Section 2.10.1) and immunoblot experiments (Section 2.10.2). These molecular weight standards were later replaced by GangNam-STAIN™ Pre-stained Protein Ladder (INtRON Biotechnology, South Korea).

2.10.2 Immunoblot analysis

For the identification of recombinant proteins (AmyS:DnaB:ABDx, AmyS:DnaB:ABDx:His, AmyS:ABDx:His) samples were run on SDS-PAGE (Section 2.10.1), transferred to a nitrocellulose membrane (Section 2.10.2.1), subjected to the relevant primary and secondary antibodies, and visualised via chemiluminescence upon exposure and development of X-ray film (Section 2.10.2.2).

2.10.2.1 Transfer to a nitrocellulose membrane

Proteins were transferred to a nitrocellulose membrane from an SDS-PAGE gel (Section 2.10.1) utilising a semi-dry transfer system (iBlot® Gel Transfer Mini-stacks Nitrocellulose and iBlot® Gel Transfer System, Invitrogen Corporation, USA) according to the manufacturer's

instructions using preset program No. 3. The anode (bottom) and cathode (top) consist of copper sheets amalgamated to matrices infused with relevant buffers. The SDS-PAGE gel was carefully placed on the 0.2 µm nitrocellulose membrane, which rests on the anode matrix. After removal of air bubbles by using a roller, a sheet of filter paper moistened with de-ionised water followed by the cathode was placed on the top of the gel. The sponge designed to ensure application of even pressure was placed on the top of the cathode, the lid securely fastened, and the transfer programme initiated.

2.10.2.2 Blocking, antibody application, and visualisation

For identification of the alginate-binding domain (ABDx) from AlgX, polyclonal antibody raised against *P. aeruginosa* AlgX whole protein was used. After transfer, the nitrocellulose membrane (Section 2.10.2.1) was washed thrice with Tris buffered saline supplemented with Tween 20 (TBST: 150 mM NaCl, 10 mM Tris-HCl and 0.1% (v/v) Tween 20 at pH 7.8) for 5 min and blocked for 1 hr in TBST with 2.5% (w/v) skim milk at 22˚C. The membrane was washed thrice and incubated for 1 hr with rabbit anti-AlgX antibody at a 1:5,000 (v/v) ratio in TBST supplemented with 2.5% (w/v) skim milk. After another three washes with TBST, the membrane was incubated for 1 hr with secondary antibody at a 1:10,000 (v/v) ratio with TBST supplemented with 2.5% skim milk. Following a final three TBST washes, the membrane was incubated with 2.5 ml of Super Signal West Pico Stable Peroxide and 2.5 ml of Luminol (Thermo Scientific, USA) for 5 min. All incubation and wash steps were carried out with gentle agitation. Incubations with light sensitive antibodies and substrates were carried out in the dark. For visualisation of bands, the membranes were exposed to BioMax XAR film (Kodak, USA) and images were developed using a developer (Kodax X-Omat-100, USA).

For detection of His-tagged proteins a commercial anti-His antibody conjugated to horse radish peroxidase (HisProbe-HRP Kit, Thermo Scientific, USA) was employed according to the manufacturer's instructions. After the proteins were transferred to the nitrocellulose membrane (Section 2.10.2.1), the membrane was washed thrice with TBST for 5 min and then blocked overnight in TBST supplemented with 1% (w/v) BSA. After washing twice in 15 ml of TBST for 10 min, the membrane was incubated with the antibody at a 1:5,000 (v/v) ratio in TBST for 1 h at 22˚C in the dark. Following another 4 washes with TBST, the membrane was incubated with 2.5 ml of Super Signal West Pico Stable Peroxide and 2.5 ml of Luminol for 5 min. Bands of interest were visualised as described above.

2.10.3 Native gel electrophoresis

Native polyacrylamide gel electrophoresis (native PAGE) was used to analyse protein samples in native (non-denatured) form. Stacking Gel, Separating Gel, and 10X Running Buffers were prepared. Stacking Gel Buffer contained 121.1 g of Tris in 1 L of water, adjusted to pH 6.8. Separating Gel Buffer contained 181.7 g of Tris in 1 L of water, adjusted to pH 8.8. 10X Running Buffer contained 144 g of glycine in 1 L of water and 30 g/L Tris-HCl, adjusted to pH 8.5 using 10 M HCl.

The following describes the preparation of two standard 1.5mm native gels composed of 10.0 and 5.0% (w/v) acrylamide separating and stacking gels. Unless otherwise stated all separating gels contained 10% acrylamide. To prepare 20 ml of 10% (w/v) acrylamide separating gel, 5 ml of Separating Buffer, 6.66 ml of 30% (w/v) acrylamide and 8.13 ml of water were thoroughly mixed. Next, 200 µl of 10% (w/v) APS and 8 µl of TEMED were added to the mixture and stirred for 10 s before the mixture was poured into two 1.5 mm mini Novex® Gel Cassettes (Invitrogen, USA), overlaid with isopropanol, and carefully placed on a level surface for 1 h to allow polymerisation.

Upon polymerisation, the isopropanol was removed and the separating gel thoroughly rinsed with water and dried with lint free wipes. To prepare 5 ml of 5.0% (w/v) acrylamide stacking gel, 0.63 ml of Stacking Gel Buffer, 0.83 ml of 30% (w/v) acrylamide and 3.4 ml of water were mixed thoroughly. Then, 50 µl of 10% (w/v) APS and 5 µl of TEMED were added to the mixture and stirred for 10 s before the mixture was poured onto the separating gels and well comb inserted. The stacking gel was left to solidify for 1 h.

Native gels were set up in XCell SureLock™ Mini-Cell Electrophoresis Gel Chambers according to the manufacturer's instructions (Invitrogen Corporation, USA). Gels were submerged in 1X Running Buffer. Protein samples were prepared (Section 2.10.3.1) and loaded into separate wells. For each gel, a protein molecular weight standard (Section 2.10.3.2) was loaded into its own well. Native gels were run at 120 V for 120 min on ice with slow stirring of the Native Electrophoresis Buffer.

The gel was then removed from the 1.5 mm mini Novex® Gel Cassette and washed with 20 mM PBS pH 7.4 for 1 h at 4˚C. Wash buffer was exchanged for a 1% starch solution, containing 1% (w/v) soluble starch in 20 mM PBS pH 7.4 and 1 mM Ca^{++}, and incubated for 1 h at 4˚C

(Tabassum *et al.*, 2014). Gels were washed a final time with 20 mM PBS pH 7.4 for 5 min at 4˚C. The wash buffer was then removed and the gel sealed in a container, containing a damp lint free wipe to humidify the container and prevent the gel from drying out. The gel was then incubated overnight at 30˚C. Next, the gel was stained with Lugol's iodine solution for 5 min at 22˚C. Lugol's iodine was drained and excess stain washed off with water. Protein bands were visualised using a Gel Imaging and Doc System (Bio-Rad, Gel Doc, USA) and images were generated.

A native PAGE gel run in parallel was stained with Coomassie® Brilliant Blue, following the same staining protocol as used for SDS-PAGE gels (Section 2.10.1).

2.10.3.1 Preparation of protein samples for native PAGE

Protein samples for native PAGE were prepared as outlined below and 20 µl of protein sample was loaded into a native gel well.

Protein sample	10.0	µl
50 mM Tris-HCl	2.0	µl
36 mM Glycine pH 8.8	2.0	µl
0.1% (w/v) Bromophenol blue	2.0	µl
30% (v/v) Glycerol	4.0	µl

2.10.3.2 Protein molecular weight standard for native PAGE

NativeMark™ Unstained Protein Standard (Invitrogen Corporation, USA) was used for the estimation of protein molecular weight in native PAGE (Section 2.10.3).

2.10.4 MALDI-TOF peptide mass analysis

Matrix-assisted laser desorption/ionisation time-of-flight (MALDI-TOF) mass spectrometry of protein samples isolated from SDS-PAGE (Section 2.10.1) were performed by the Centre for Protein Research (CPR), University of Otago, New Zealand, using a protein trypsin digest.

2.11 Purification of recombinant protein

2.11.1 Protein solubility fractionation by ammonium sulfate

Following protein production (Section 2.9.1), solid ammonium sulfate was added to the cell-free supernatant as described in Section 2.9.2.1 to sequentially achieve a saturation level of 12%, 55% and 80% in the protein solution. Proteins that were insoluble at a given concentration of ammonium sulfate were precipitated out of the solution and collected (Section 2.9.2.1). Each protein fraction was analysed by SDS-PAGE (Section 2.10.1) and by a starch degradation screen for α-amylase activity (Section 2.12.1). Based on detection of the recombinant protein in a given fraction, fractionation was repeated with an ammonium sulfate saturation range of greater specificity (target saturation % ± 5). Protein fractionation was repeated until the bulk of extraneous proteins were removed and the recombinant protein isolated.

2.11.2 Size exclusion chromatography

All gel filtration chromatography of protein samples was provided by Trevor Loo, Massey University, utilising an ÄKTA™ Explorer Fast Protein Liquid Chromatography (FPLC) System with a P-900 series pump system (Amersham Biosciences). Protein samples were centrifuged to remove any insoluble parts, such as denatured protein, prior to gel filtration chromatography. 0.1 M PBS pH 7.4 was used as wash buffer for the gel filtration system. 100 µl of protein sample was loaded into the needle port and pumped through a Superdex™ 200 Increase 10/300 GL column (GE Life Sciences). The eluate was collected in 500 µl fractions to max elution volume of 30 ml.

2.11.3 Affinity purification of polyhistidine-tagged protein

Polyhistidine-tagged (His-tagged) protein was produced (Section 2.9.1), concentrated (Section 2.9.2) and then purified using His-Spin™ Protein Miniprep Kit (Zymo Research) according to the manufacturer's instructions. A Zymo-Spin™ P1 Fast-spin column was loaded with His-Affinity Gel and prepared by adding His-Binding Buffer (Zymo Research). 300 µl of protein sample was loaded into the column and used to resuspend the His-Affinity Gel. The column was incubated for 30 min at 22˚C with agitation. Next, the column was centrifuged (10,000 x g for 13 s at 22˚C) and washed twice with His-Wash Buffer. The protein was incubated for 5 min at 22˚C with 150 µl His-Elution Buffer. His-purified protein was eluted

from the column and stored at -20˚C for later use in SDS-PAGE (Section 2.10.1) and immunoblot analysis (Section 2.10.2).

2.11.4 Affinity purification of alginate-binding protein

The protocol for purification of alginate-binding protein was adapted from the method used for affinity purification of His-tagged protein (Section 2.11.3). Protein was first produced (Section 2.9.1) and concentrated (Section 2.9.2). 200 µl of polymannuronate alginate bead solution (20110001-3, bio-WORLD) was loaded into a Zymo-Spin™ P1 Fast-spin column (Zymo Research). The alginate beads were then washed with 0.1 M Tris-HCl (pH 8.4). 250 µl of protein sample was mixed with the alginate beads and incubated for 2 h at 4˚C with agitation. The column was washed thrice with 0.1 M Tris-HCl pH 8.4. The protein-alginate bead solution was collected in 200 µl 0.1 M Tris-HCl pH 8.4 and stored at -20˚C for later use in SDS-PAGE (Section 2.10.1) and immunoblot analysis (Section 2.10.2).

2.12 Functional analysis of the recombinant protein

2.12.1 Starch degradation screen for α-amylase activity

A starch degradation screen for α-amylase activity was adapted from Rasiah and Rehm (2009). Protein was produced (Section 2.9.1) and concentrated (Section 2.9.2). Typically, 20 µg of protein sample and 80 µg of *B. licheniformis* α-amylase (Sigma Aldrich, A3403) (positive control) were placed onto starch agar medium (Section 2.2.6). The medium was incubated overnight at 30˚C and clear zones (areas of starch degradation) around the protein sample were recorded. Photographs of the starch agar plates were taken against a sheet of black paper.

2.12.2 Maltose assay for α-amylase activity

A Maltose Assay Kit (MAK019 Sigma Aldrich) was used to quantitatively analyse α-amylase activity in a protein sample according to the manufacturer's instructions. Table 5 outlines the steps for assaying a protein sample. Maltose at concentrations of 0.2% to 0.005% were used to generate a standard curve. Colorimetric assay of all standards and samples was measured at absorbance 540 nm (A_{540nm}) at 22˚C using a spectrophotometer (UV-1800 UV-VIS Spectrophotometer Shimadzu). 1% soluble starch solution (Starch) contained 250 mg soluble starch in 25 ml Buffer. Solution A contained 12 g of sodium potassium tartrate tetrahydrate

in 8 ml of 2 M sodium hydroxide. Solution B contained 438 mg of 3,5-dinitrosalicylic acid in 20 ml of water. Colour reagent solution was prepared by mixing 18 ml of Solution A with 20 ml of Solution B in 40 ml of water. 0.2% maltose standard contained 20 mg of maltose monohydrate in 10 ml of water. Buffer was prepared as follows:

20 mM Sodium Phosphate Buffer with 6.7 mM NaCl pH 6.9 (Buffer):

20 mM NaH_2PO_4	22.0 ml
20 mM Na_2HPO_4	78.0 ml
NaCl	39.2 mg
	Adjust pH to 6.9 using 10 M NaOH

Table 5. Maltose assay for α-amylase activity

	Test 1	**Test 2**	**Test 3**	**Blank**
Reagent	**Volume (ml)**	**Volume (ml)**	**Volume (ml)**	**Volume (ml)**
Starch	1	1	1	1
Enzyme (sample)	0.5	0.7	1	–
Mix and incubate for three minutes at room temperature (22 ± 4˚C).				
Colour reagent solution	1	1	1	1
Enzyme (sample)	0.5	0.3	–	1
Mix and incubate for 15 minutes in boiling water. Cool on ice for three minutes.				
H_2O	9	9	9	9

CHAPTER THREE
RESULTS

3.1 Molecular Cloning

To address the aim of this study, a hybrid gene was designed with the alginate-binding domain of *Pseudomonas aeruginosa* alginate acetyltransferase, AlgX (*ABDx*), and the α-amylase domain of *Bacillus licheniformis* amylase (*amyS*). A Ssp DnaB mini-intein (*dnaB*) was included in the hybrid gene design between *amyS* and *ABDx* to allow for the recovery of the target protein (α-amylase), following display on alginate beads.

3.1.2 Construction of plasmid p1623*amySdnaBABDx*

A restriction digest of plasmid p1623 with PacI and KpnI resulted in a 6.4 kbp fragment consistent with PacI/KpnI-cut p1623 backbone. Following the strategy outlined in Section 2.8.2, p1623 PacI/KpnI-cut backbone was purified by gel electrophoresis.

Concurrent with p1623 vector, a restriction endonuclease digest of pUC57-Simple*amySdnaBABDx* with PacI and KpnI generated a 2.4 kbp fragment, which is consistent with PacI/KpnI-cut *amySdnaBABDx*. Subsequently, this fragment was purified by gel electrophoresis (Section 2.8.2).

PacI/KpnI-cut p1623 vector and the *amySdnaBABDx* insert were ligated (Section 2.8.7) and transferred into *Escherichia coli* TOP10 cells (Section 2.7.1). Restriction fragment analysis of p1623*amySdnaBABDx* revealed two fragments: (1) 6.4 kbp fragment consistent with PacI/KpnI-cut p1623; and (2) 2.4 kbp fragment consistent with PacI/KpnI-cut *amySdnaBABDx* (Figure 11). The integrity of the construct within *E. coli* Top10 was analysed by DNA sequencing (Section 2.8.8), which showed there were no mutations or frame shifts present in either p1623 or *amySdnaBABDx*.

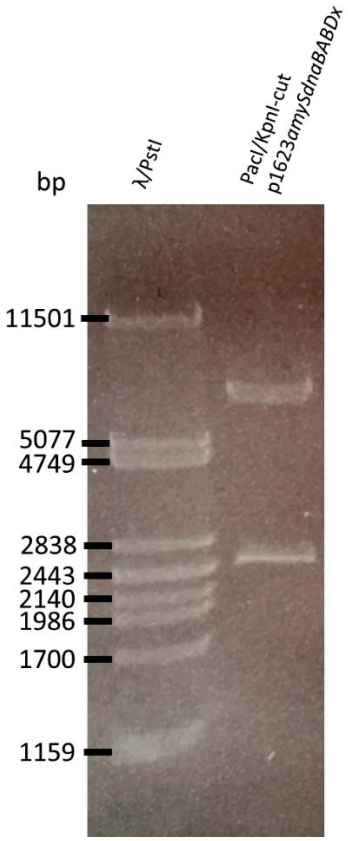

Figure 11. Confirmation of *E. coli* transformed with p1623*amySdnaBABDx*. 1% agarose gel electrophoresis of restriction p1623*amySdnaBABDx* fragment analysis. Lane labelled PacI/KpnI-cut p1623*amySdnaBABDx* contains isolated p1623*amySdnaBABDx* DNA hydrolysed by restriction endonucleases (REase) PacI and KpnI. Lane labelled λ/PstI represents a DNA molecular size standard of Lambda phage DNA hydrolysed by REase PstI. Molecular size is given in base pairs (bp).

3.1.3 Transformation of *Bacillus megaterium*

Following the protocol outlined in Section 2.7.2, p1623*amySdnaBABDx* expression vector was transformed into *B. megaterium* strains YYBm1 and MS941. Colony growth of YYBm1 and MS941 on tetracycline selective CR5-topagar (Section 2.2.5) indicated successful transformation of both strains with p1623*amySdnaBABDx*. Five colonies from each strain were screened by colony PCR, using primers targeting *amySdnaBABDx* sequence (Section 2.8.5). Colony PCR of YYBm1 and MS941 colonies resulted in a 2.5 kbp PCR product, which is consistent with *amySdnaBABDx* (Figure 12).

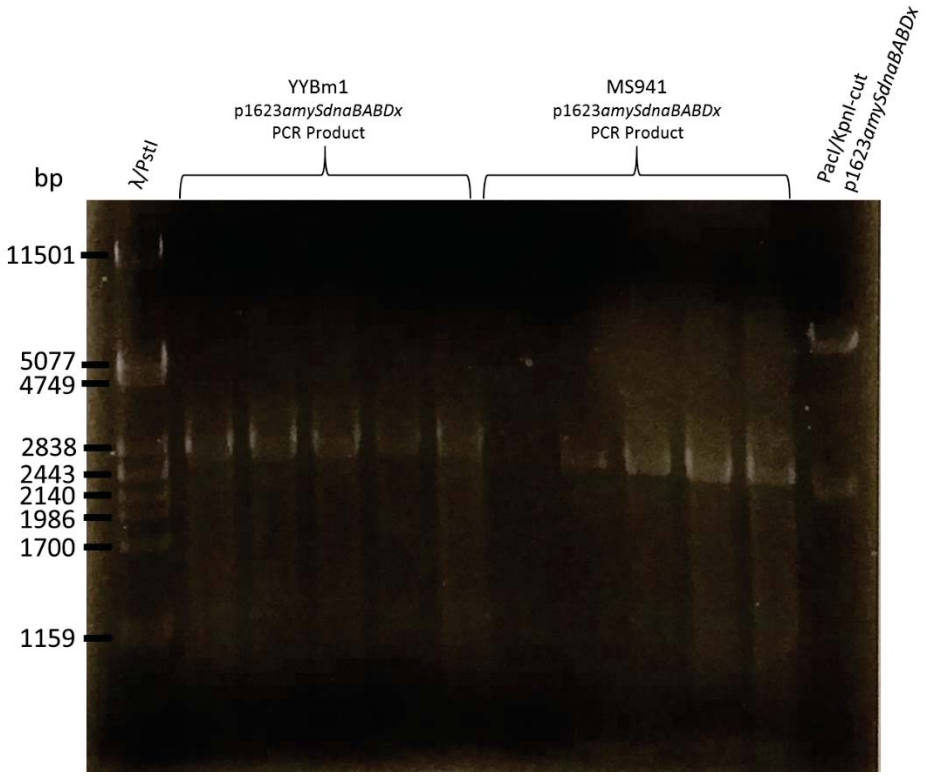

Figure 12. Confirmation of *B. megaterium* transformed with p1623*amySdnaBABDx*. Colony PCR products of *B. megaterium* strains YYBm1 and MS941 transformed with p1623*amySdnaBABDx* analysed by 1% agarose gel electrophoresis. Colony PCR products of *B. megaterium* YYBm1 transformed with p1623*amySdnaBABDx* are labelled YYBm1 p1623*amySdnaBABDx* PCR product. Colony PCR products of *B. megaterium* MS941 transformed with p1623*amySdnaBABDx* are labelled MS941 p1623*amySdnaBABDx* PCR product. Lane labelled PacI/KpnI-cut p1623*amySdnaBABDx* contains isolated p1623*amySdnaBABDx* DNA hydrolysed by restriction endonucleases (REase) PacI and KpnI. Lane labelled λ/PstI represents a DNA molecular size standard of Lambda phage DNA hydrolysed by REase PstI. Molecular size is given in base pairs (bp).

3.2 Production of AmyS:DnaB:ABDx

B. megaterium YYBm1 and MS941 p1623*amySdnaBABDx* transformants were used for protein production, in which D-xylose was added to the growth media to a final concentration of 0.5% to induce production of AmyS:DnaB:ABDx (Section 2.9.1). The same protocol was used for a YYBm1 p1623empty (empty vector) transformant to be used as a negative control for AmyS:DnaB:ABDx production. Bacterial growth was monitored periodically until an optical density at 600 nm (OD_{600nm}) of 6 was reached in all cultures, at which point the culture was

harvested. Following Section 2.9.2.1 for the collection of extracellular protein, ammonium sulfate at a saturation level of 55% was used to precipitate proteins from the cell-free supernatant. The pellet was collected and resuspended in 0.02 M PBS pH 7.4 (Section 2.4.1), and stored at -20˚C.

The bulk extracellular protein was quantified by a Bradford assay against a bovine serum albumin standard, which resulted in a bulk protein concentration of 3 mg/ml for YYBm1 p1623*amySdnaBABDx*, and 1 mg/ml for YYBm1 p1623empty, MS941 p1623*amySdnaBABDx* and p1623empty (Section 2.9.3).

Figure 13 shows the results of SDS-PAGE analysis (Section 2.10.1) of the extracellular protein profile of YYBm1 and MS941 p1623*amySdnaBABDx* and p1623empty transformants. In the profile of YYBm1 p1623*amySdnaBABDx*, a distinct band representing a protein with apparent molecular weight (MW) of 85 kDa is indicated by a black arrow, which corresponds with the expected MW of AmyS:DnaB:ABDx (87.2 kDa). Additionally, in the YYBm1 p1623*amySdnaBABDx* profile, a white arrow is used to indicate a protein with an apparent MW of 56 kDa, and a red arrow indicates a protein with a MW of 40 kDa. These bands appear to be unique to the YYBm1 p1623*amySdnaBABDx* profile when compared to the extracellular protein profile of YYBm1 p1623empty. The 56 kDa and 40 kDa bands are close to the expected size of AmyS (55.8 kDa) and DnaB:ABDx (31.4 kDa) protein regions, respectively. These regions form following N-terminus intein cleavage. A blue arrow is used to indicate a protein with an apparent MW of 67kDa, which appears to be unique to the MS941 p1623*amySdnaBABDx* profile.

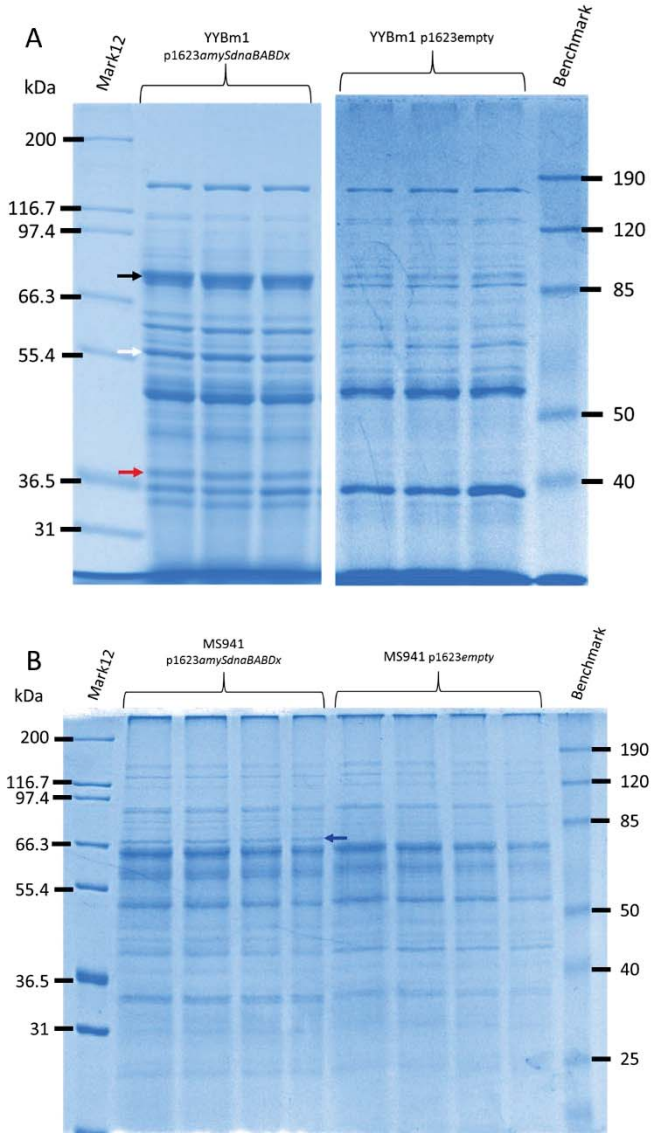

Figure 13. Protein analysis of *B. megaterium* transformed with p1623*amySdnaBABDx*. 10% SDS-PAGE analysis of the extracellular protein profiles of *B. megaterium* YYBm1 and MS941 transformed with p1623*amySdnaBABDx* or p1623 empty vector. Lane labelled Mark12 and Benchmark are protein molecular weight (MW) standards Mark12™ Unstained Standard and BenchMark™ Pre-stained Protein Ladder, respectively. MW is given in kilodaltons (kDa). *A.* Protein from *B. megaterium* YYBm1 transformed with p1623*amySdnaBABDx* is labelled YYBm1 p1623*amySdnaBABDx*. Protein from YYBm1 transformed with p1623 empty vector is labelled YYBm1 p1623empty. Protein bands unique to YYBm1 p1623*amySdnaBABDx* with MW of 85, 56, and 40 kDa are labelled with *black*, *white*, and *red* coloured arrows, respectively. *B.* Protein from *B. megaterium* MS941 transformed with p1623*amySdnaBABDx* is labelled MS941 p1623*amySdnaBABDx*. Protein from MS941 transformed with p1623 empty vector is labelled MS941 p1623empty. A protein band unique to MS941 p1623*amySdnaBABDx* with MW of 67 kDa is labelled with a *blue* coloured arrow.

3.3 Functional analysis of AmyS:DnaB:ABDx

The first part of this section focusses on the results of a starch degradation screen to detect α-amylase activity, and hence assesses the functionality of the recombinant protein amylase domain (AmyS). The second part of this section shows the results of alginate-binding purification as a method of analysing the functionality of the recombinant protein alginate-binding domain (ABDx).

3.3.1 AmyS functional analysis

A 30 µg extracellular protein sample was collected from both YYBm1 and MS941 p1623*amySdnaBABDx* and screened for starch degradation (Section 2.12.1). 80 µg of *B. licheniformis* α-amylase (Sigma Aldrich, A3403) was used as a positive control. In addition, a 30 µg extracellular protein sample from YYBm1 and MS941 p1623empty was included as a negative control. Figure 14 shows the results of the starch degradation screen for each strain. A clear zone in the starch agar where protein from YYBm1 p1623*amySdnaBABDx* was added indicates starch degradation, corresponding to α-amylase activity. The protein sample from MS941 p1623*amySdnaBABDx* resulted in less starch degradation when compared to YYBm1, and has been highlighted by a red circle for easier visualisation. The extracellular protein collected from the YYBm1 and MS941 empty vector negative controls both tested negative for starch degradation.

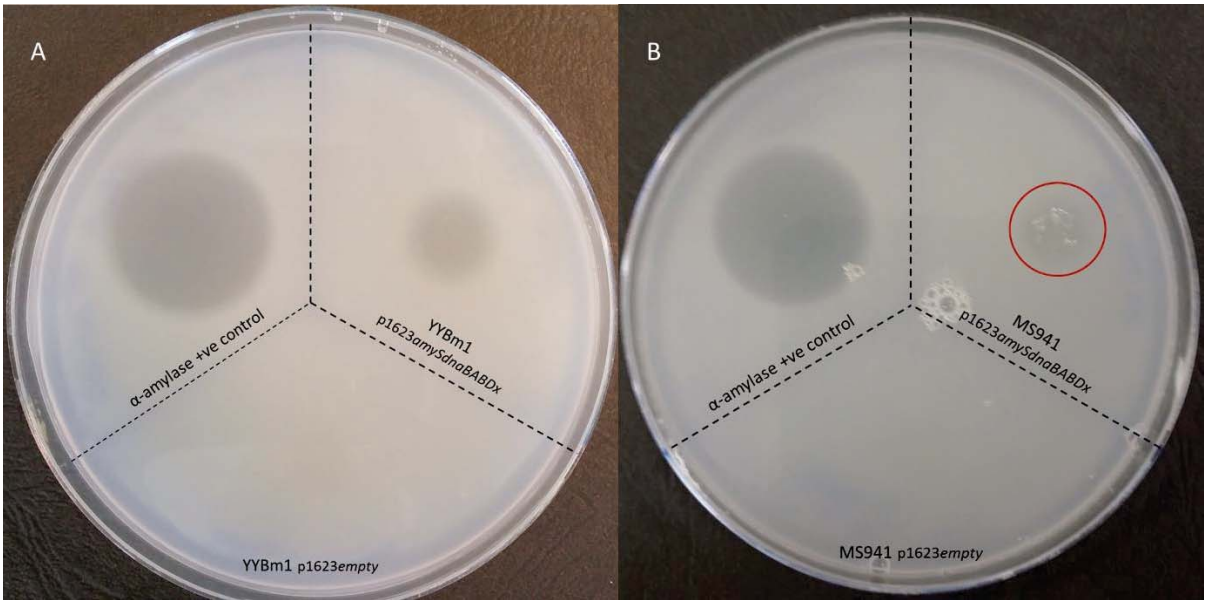

Figure 14. Confirmation of α-amylase activity by strains transformed with p1623*amySdnaBABDx*. Starch degradation screen of the extracellular protein from *B. megaterium* YYBm1 and MS941 transformed with p1623*amySdnaBABDx* or p1623 empty vector. *B. licheniformis* α-amylase (BLA) is labelled α-amylase +ve control. *A.* YYBm1 p1623*amySdnaBABDx* represents the protein sample from *B. megaterium* YYBm1 transformed with p1623*amySdnaBABDx*. YYBm1 p1623*empty* represents the protein sample from YYBm1 transformed with p1623 empty vector. *B.* MS941 p1623*amySdnaBABDx* represents the protein sample from *B. megaterium* MS941 transformed with p1623*amySdnaBABDx*. MS941 p1623*empty* represents the protein sample from MS941 transformed with p1623 empty vector. A *red* circle highlights a zone of starch degradation.

3.3.2 ABDx functional analysis

An attempt to purify the extracellular protein collected from YYBm1 p1623*amySdnaBABDx* and p1623empty by alginate beads (Section 2.11.4) was analysed by SDS-PAGE (Section 2.10.1). The results of SDS-PAGE analysis of alginate-purified samples shows two distinct bands in the protein profile of alginate-purified YYBm1 p1623*amySdnaBABDx* (Figure 15). The first band is highlighted by a black arrow and corresponds to a protein with an apparent MW of 87 kDa. The second band is indicated by a white arrow and the apparent protein MW is estimated to be about 53 kDa. Due to the MW similarity, the former is a possible match to the full-length recombinant (87.2 kDa), which would be a strong indication of alginate-binding activity of the ABDx domain. No distinct bands were seen in the protein profile of alginate-purified YYBm1 p1623empty (negative control).

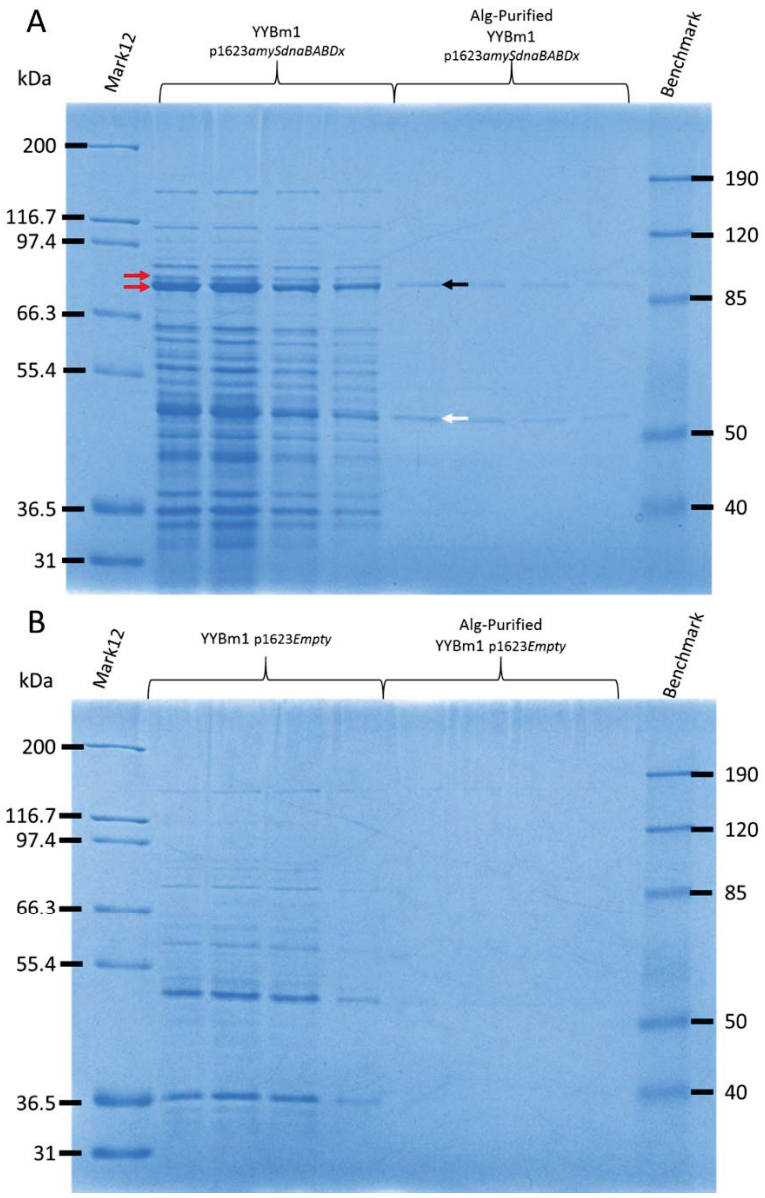

Figure 15. Analysis of alginate protein purification from strains transformed with p1623*amySdnaBABDx*. 10% SDS-PAGE analysis of the extracellular and alginate-purified protein profiles of *B. megaterium* YYBm1 and MS941 transformed with p1623*amySdnaBABDx* or p1623 empty vector. Lane labelled Mark12 and Benchmark are protein molecular weight (MW) standards Mark12™ Unstained Standard and BenchMark™ Pre-stained Protein Ladder, respectively. MW is given in kilodaltons (kDa). *A.* Protein from *B. megaterium* YYBm1 transformed with p1623*amySdnaBABDx* is labelled YYBm1 p1623*amySdnaBABDx*. Protein purified by alginate from YYBm1 transformed with p1623*amySdnaBABDx* is labelled Alg-Purified YYBm1 p1623*amySdnaBABDx*. Protein bands unique to YYBm1 p1623*amySdnaBABDx* with MW of 87 kDa are labelled with *black* and *red* coloured arrows, whereas a *white* arrow indicates a protein with MW of 53 kDa. *B.* Protein from *B. megaterium* YYBm1 transformed with p1623 empty vector is labelled YYBm1 p1623empty. Protein purified by alginate from YYBm1 transformed with p1623 empty vector is labelled Alg-Purified YYBm1 p1623empty.

3.4 Identification of AmyS:DnaB:ABDx

Identification of AmyS:DnaB:ABDx was attempted through protein mass spectrometry of selected proteins from the extracellular protein profile of YYBm1 p1623*amySdnaBABDx*. The 87 kDa protein that was purified by alginate beads (Section 3.3.2) was selected as an optimal candidate for the full-length recombinant protein, in addition to the corresponding 87 kDa protein in the YYBm1 p1623*amySdnaBABDx* extracellular protein profile (Figure 15; black and red arrow, respectively). Due to similar MW of two proteins in the extracellular protein profile (Figure 15, red arrows), in which either protein could be a match to the 87 kDa protein purified by alginate, both bands were excised for protein mass spectrometry (Section 2.10.4). The protein samples were sent to the Centre of Protein Research, University of Otago, for MALDI-TOF peptide mass analysis. The results of protein mass spectrometry reported that the peptide mass for each of these proteins did not match the protein sequence of AmyS:DnaB:ABDx. When matched against proteins in the NCBI database, the sequence was a sufficient match for peptidase S8 [*Bacillus megaterium*] with coverage of 37% for the YYBm1 p1623*amySdnaBABDx* sample and 22% for the alginate-purified YYBm1 p1623*amySdnaBABDx* sample (Appendix III).

3.5 Detection and isolation of AmyS:DnaB:ABDx

Several strategies were undertaken to achieve detection and isolation of AmyS:DnaB:ABDx. An antibody targeting the recombinant protein alginate-binding domain was utilised in an immunoblot to detect AmyS:DnaB:ABDx, and the results are described in Section 3.5.1. Section 3.5.2 shows the results of Native-PAGE analysis of the extracellular protein profile of YYBm1 p1623*amyS-dnaB-ABDx*, which attempted to isolate AmyS:DnaB:ABDx based on activity of the amylase domain (AmyS). Finally, two separate strategies of fractionation were used to isolate AmyS:DnaB:ABDx from an extracellular protein mixture and the results presented in Section 3.5.3.

3.5.1 Anti-AlgX immunoblot

Polyclonal antibodies raised against the alginate acetyltransferase, AlgX, were used in an immunoblot targeting the alginate-binding domain of AmyS:DnaB:ABDx (Section 2.10.2). Figure 16 shows a side-by-side comparison of the results of SDS-PAGE and immunoblot

analysis. In the immunoblot developed film, white arrows indicate two distinct bands that were detected by anti-AlgX antibody, which correspond to a protein with an estimated MW of 34 kDa. These bands were detected in the extracellular protein profile of YYBm1 and MS941 p1623empty. In the SDS-PAGE, black arrows indicate the protein bands that likely correspond to the bands detected in the immunoblot. A red circle highlights a possible band that was detected in the extracellular protein profile of YYBm1 p1623*amySdnaBABDx*, corresponding to a protein with an apparent MW of 34 kDa.

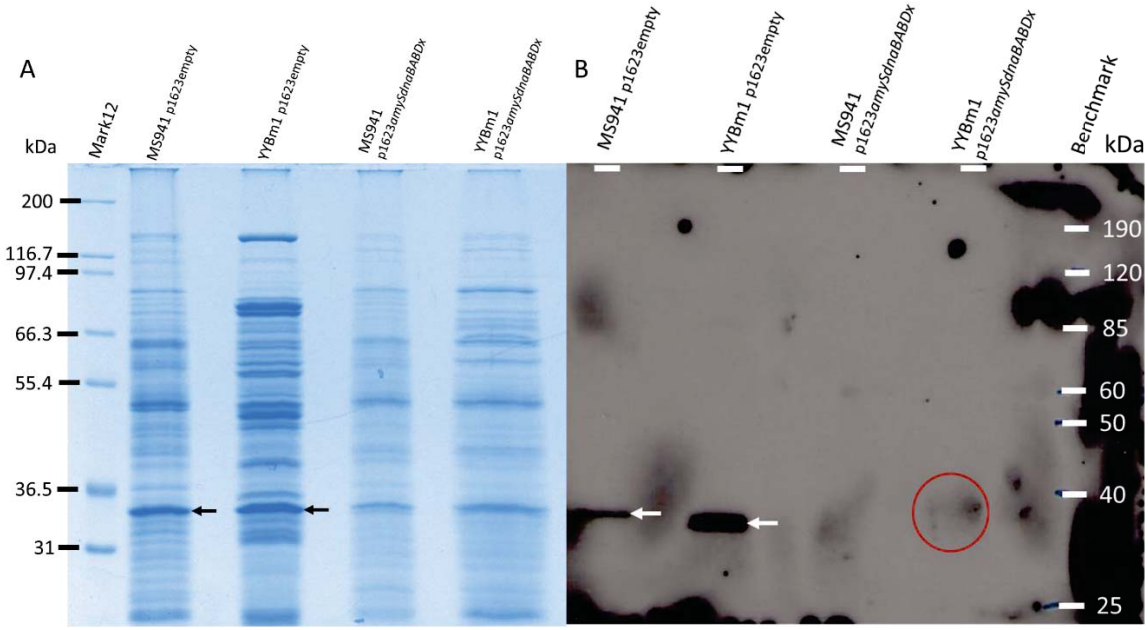

Figure 16. Detection of AlgX alginate-binding domain. *A.* 10% SDS-PAGE analysis of the extracellular protein profiles of *B. megaterium* YYBm1 and MS941 transformed with p1623*amySdnaBABDx* or p1623 empty vector. *Black* arrows indicate proteins with molecular weight (MW) of 34 kDa. *B.* Anti-AlgX immunoblot analysis of the extracellular protein profiles of *B. megaterium* YYBm1 and MS941 transformed with p1623*amySdnaBABDx* or p1623 empty vector. *White* arrows and a *red* circle highlight proteins detected by anti-AlgX antibodies with a MW of 34 kDa. Lanes labelled Mark12 and Benchmark are protein MW standards Mark12™ Unstained Standard and BenchMark™ Pre-stained Protein Ladder, respectively. MW is given in kilodaltons (kDa). Extracellular protein from strains YYBm1 and MS941 transformed with p1623*amySdnaBABDx* are labelled YYBm1 p1623*amySdnaBABDx* and MS941 p1623*amySdnaBABDx*, respectively. Extracellular protein from strains YYBm1 and MS941 transformed with p1623 empty vector are labelled YYBm1 p1623empty and MS941 p1623empty, respectively.

3.5.2 Native protein detection and isolation

The first part of this section shows the results of native PAGE combined with a starch degradation screen as a method of detecting and isolating AmyS:DnaB:ABDx based on the activity of the AmyS domain. The second part focusses on the results of SDS-PAGE protein renaturation followed by an amylase activity screen.

3.5.2.1 Native PAGE analysis

The extracellular protein of YYBm1 p1623*amySdnaBABDx* and p1623empty was analysed by native PAGE using either Coomassie® Brilliant Blue stain or treatment with a 1% starch solution followed by staining with Lugol's reagent (Section 2.10.3). Alpha-amylase (Sigma Aldrich A3403) was used as a positive control. Additionally, a sample of YYBm1 p1623*amySdnaBABDx* was used for alginate protein purification prior to native PAGE analysis. The result of the starch degradation screen shows a clear zone around the α-amylase positive control, indicating degradation of the embedded starch by α-amylase activity (Figure 17). A similar clear zone around a protein band in the profile of YYBm1 p1623*amySdnaBABDx* is highlighted by a black arrow. This clear zone is an indication of amylase activity by the protein band.

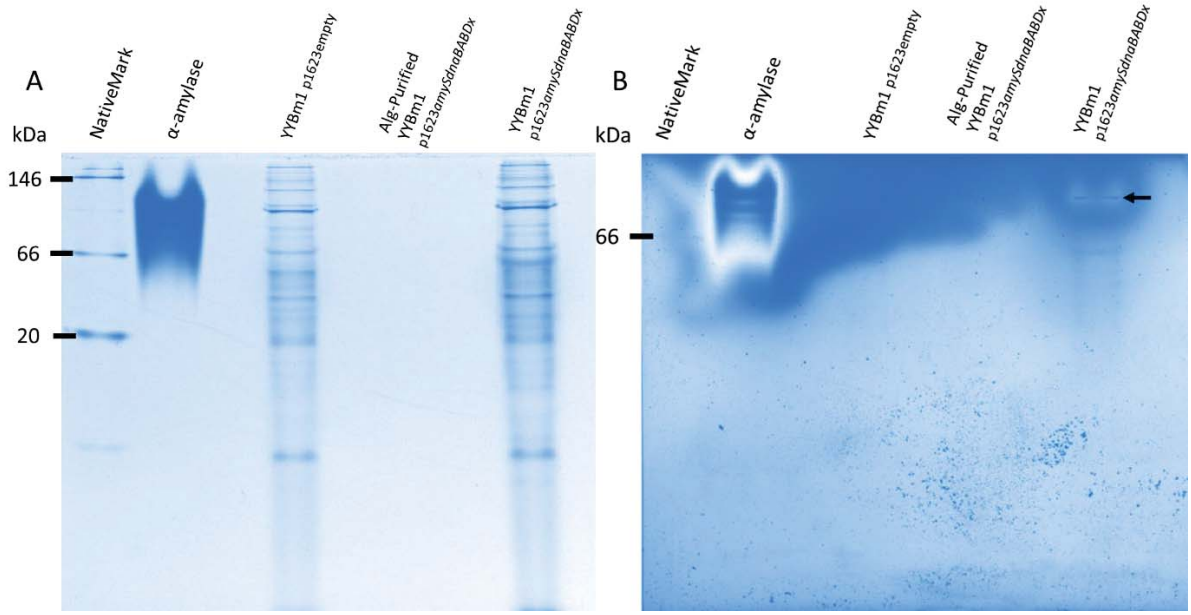

Figure 17. Detection of α-amylase activity by protein isolated by native PAGE. *A.* Coomassie® Brilliant Blue stain; 10% native PAGE analysis of extracellular and alginate purified protein from *B. megaterium* YYBm1 transformed with p1623*amySdnaBABDx* or p1623 empty vector, as well as *B. licheniformis* α-amylase (BLA). *B.* Lugol's iodine solution stain; starch degradation screen of extracellular and alginate purified protein from *B. megaterium* YYBm1 transformed with p1623*amySdnaBABDx* or p1623 empty vector, as well as *B. licheniformis* α-amylase (BLA). *Black* arrow indicates a protein band with a clear zone surrounding it. YYBm1 p1623*amySdnaBABDx* and p1623empty represent protein profiles from YYBm1 transformed with p1623*amySdnaBABDx* and p1623 empty vector, respectively. Alg-Purified YYBm1 p1623*amySdnaBABDx* represents protein from YYBm1 transformed with p1623*amySdnaBABDx* purified by alginate. BLA is labelled α-amylase. NativeMark represents NativeMark™ Unstained Protein Standard. Molecular weight is given in kilodaltons (kDa).

3.5.2.2 SDS-PAGE protein renaturation

An SDS-PAGE was undertaken as in Section 3.5.2.1, with YYBm1 p1623*amySdnaBABDx*, p1623empty, an alginate-purified p1623*amySdnaBABDx* sample, and an α-amylase control. Following SDS-PAGE (Section 2.10.1), proteins were renatured in 20% isopropanol before undergoing the same development process as for Native-PAGE (Section 2.10.3). The results of protein renaturation shows a clear zone around the α-amylase positive control, which indicates α-amylase activity, and therefore successful protein renaturation (Figure 18). Two clear zones were detected in YYBm1 p1623*amySdnaBABDx* and have been marked with a

black arrow and a white arrow. The former corresponds to a protein with an apparent MW of 200 kDa, while the latter corresponds to a protein with an apparent MW of 63 kDa.

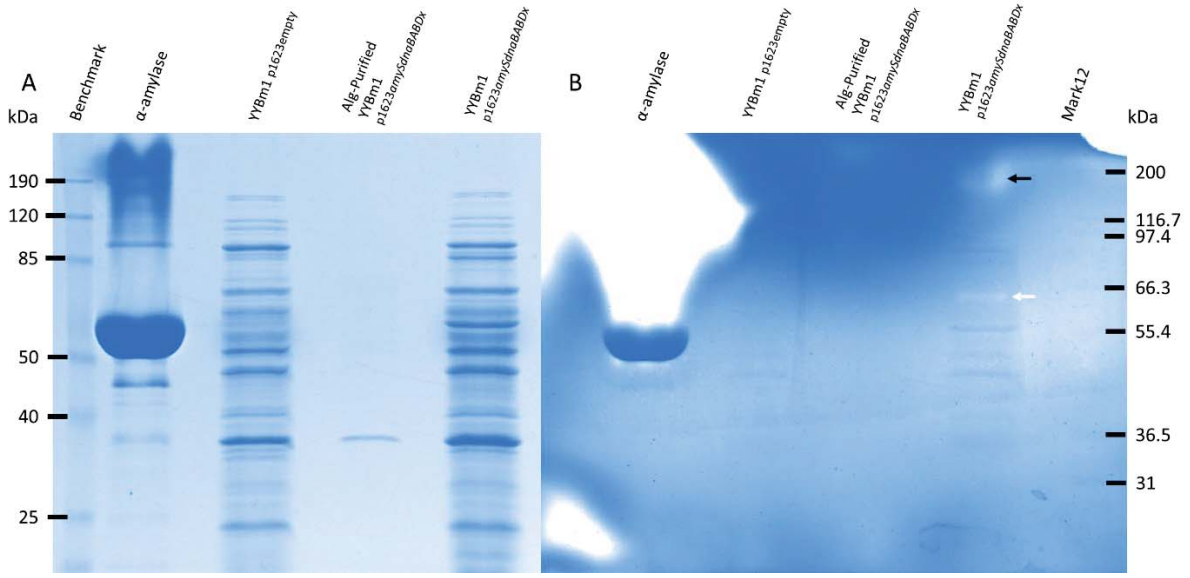

Figure 18. Renaturation of protein isolated by SDS-PAGE. *A.* Coomassie® Brilliant Blue stain; 10% SDS-PAGE analysis of extracellular and alginate purified protein from *B. megaterium* YYBm1 transformed with p1623*amySdnaBABDx* or p1623 empty vector, as well as *B. licheniformis* α-amylase (BLA). *B.* Lugol's iodine solution stain; starch degradation screen of extracellular and alginate purified protein from *B. megaterium* YYBm1 transformed with p1623*amySdnaBABDx* or p1623 empty vector, as well as *B. licheniformis* α-amylase (BLA). A *black* and *white* coloured arrow indicate protein bands with clear zones surrounding them and apparent molecular weights (MW) of 200 kDa and 67 kDa, respectively. YYBm1 p1623*amySdnaBABDx* and p1623empty represent protein profiles from YYBm1 transformed with p1623*amySdnaBABDx* and p1623 empty vector, respectively. Alg-Purified YYBm1 p1623*amySdnaBABDx* represents protein from YYBm1 transformed with p1623*amySdnaBABDx* purified by alginate. BLA is labelled α-amylase. Lanes labelled Mark12 and Benchmark are protein MW standards Mark12™ Unstained Standard and BenchMark™ Pre-stained Protein Ladder, respectively. MW is given in kilodaltons (kDa).

3.5.3 Fractionation

Two separate fractionation strategies were employed. The first part of this section focusses on the results of ammonium sulfate precipitation as a method of fractionating a complex protein mixture based on differential solubility of proteins in a highly ionic solution (Section 2.11.1). The second part shows the results of size exclusion chromatography as a method of fractionating a complex protein mixture based on protein size, as outlined in Section 2.11.2.

3.5.3.1 Protein fractionation by solubility

A preliminary fractionation of proteins in a complex mixture was accomplished using a broad range of ammonium sulfate saturations. A screen for AmyS:DnaB:ABDx precipitation utilised α-amylase activity of AmyS on starch agar (Section 2.12.1). Three saturations, which included a 12%, 55%, and 80%, were serially achieved, with the fractions collected and screened. Alpha-amylase activity was not detected in fractions precipitated from either 12% or 80% ammonium sulfate saturation, whereas α-amylase activity was detected in the fraction precipitated at 55% saturation. The result indicates that the recombinant protein was precipitated at 55%, which allows for narrowing the saturation range with 55% as the upper limit (Section 2.11.1).

A second set of ammonium sulfate saturation ranges, which included 30%, 40%, 45%, and 55%, was used to achieve significantly greater fractionation. Fractions precipitated from 30% and 40% displayed no α-amylase activity, whereas activity was detected in fractions precipitated from 45% and 55%.

Fractionation was further optimised around a narrower range of ammonium sulfate saturations, which included 45%, 50%, 52.5%, and 55%. When 30 µg of total protein from each fraction was placed on a starch agar plate, α-amylase activity was detected in all of them (Figure 19). Fractionation was repeated with variation to technique when adding ammonium sulfate to solution. Ammonium sulfate was added in smaller amounts over a longer period of time to reach a desired saturation level in solution. Additionally, mixing of the ammonium sulfate with solution was closely monitored to ensure each ammonium sulfate amount was fully dissolved before progressing with the next amount. Fractions were collected and screened for starch degradation, with α-amylase activity detected in all fractions.

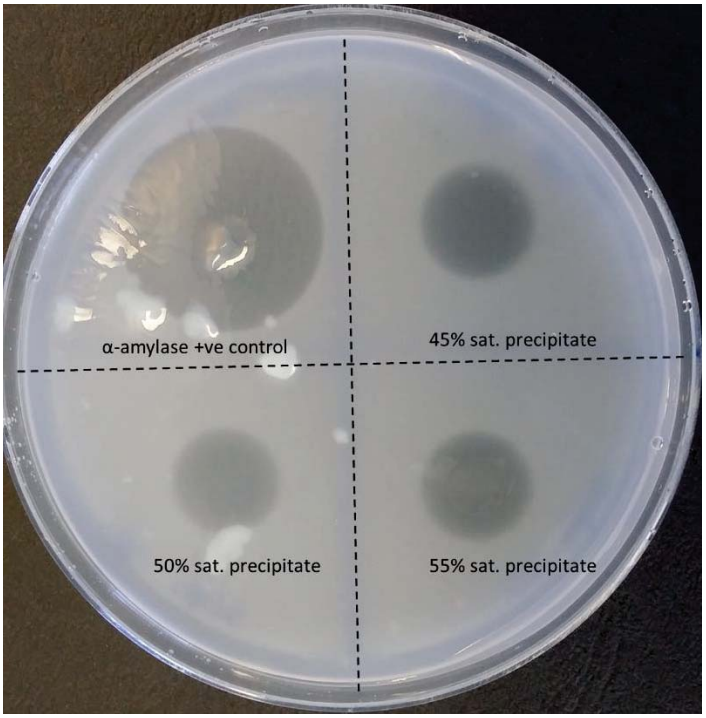

Figure 19. Detection of α-amylase from fractionated protein. Starch degradation screen of the fractionated extracellular protein from *B. megaterium* YYBm1 transformed with p1623*amySdnaBABDx*. *B. licheniformis* α-amylase (BLA) is labelled α-amylase +ve control. Protein precipitated at 45%, 50%, and 55% ammonium sulfate saturation is labelled 45% sat. precipitate, 50% sat. precipitate, and 55% sat. precipitate, respectively.

3.5.3.2 Size exclusion chromatography

The chromatogram results of size exclusion chromatography (SEC) are shown in Appendix IV. Activity peaks corresponding to proteins passing through the column cover a range of 27 fractions, with fractions B1, B2, B3 falling under a narrow peak, and fractions B8 to D1 covered by a broader peak. These 27 fractions were screened for α-amylase activity. Of the 27 fractions, 11 tested positive for starch degradation, which indicates α-amylase activity. The fractions that tested positive for α-amylase activity underwent protein quantification (Section 2.9.3), and were analysed by SDS-PAGE (Section 2.10.1). The protein concentration of the gel filtration fractions was too low to be quantified by a Bradford assay, and no protein bands were detected by SDS-PAGE.

SEC was repeated with a concentrated sample of YYBm1 p1623*amyS-dnaB-ABDx* extracellular protein, in which 7 mg/ml was achieved through membrane ultrafiltration (Section 2.9.2.2).

The second chromatogram result shown in Appendix IV contains a significantly stronger peak in comparison to the first SEC experiment. This peak covers a range of 33 fractions from B1 to D3. All 33 fractions were screened for α-amylase activity. Starch degradation was not detected in any of the fractions. A selection of the fractions was taken for protein quantification and SDS-PAGE analysis. As with the results of the first SEC, the protein concentration was too low to be detected by a Bradford assay. An initial SDS-PAGE analysis of these fractions revealed a band in fractions C4, C6, C8 and C10, corresponding to a protein with an apparent MW of 67 kDa. These fractions were concentrated 10-fold (from 500 µl to 50 µl) by ultrafiltration (Section 2.9.2.2) and screened by SDS-PAGE analysis (Figure 20). The results indicate that these fractions contain protein with MW of less than 70 kDa, which in turn suggests the peak seen in the chromatogram does not correspond to proteins in the desired MW range of 70 – 100 kDa.

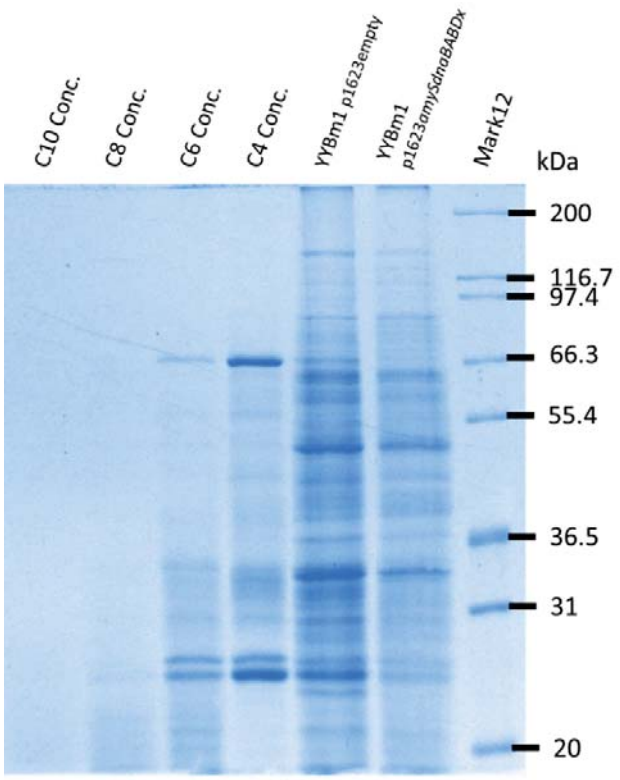

Figure 20. Protein fractionation by size exclusion chromatography. 10% SDS-PAGE analysis of fractionated extracellular protein from *B. megaterium* YYBm1 transformed with p1623*amySdnaBABDx*. The protein profiles of concentrated gel filtration eluate C4, C6, C8, and C10 are labelled C4 Conc., C6 Conc., C8 Conc., and C10 Conc., respectively. YYBm1 p1623*amySdnaBABDx* and YYBm1 p1623empty refers to the protein profiles of YYBm1 transformed with p1623*amySdnaBABDx* and 1623 empty vector, respectively. The lane labelled Mark12 is Mark12™ Unstained Standard. Molecular weight is given in kilodaltons (kDa).

3.6 Construction of *amySdnaBABDxhis*

Several methods of detecting and isolating AmyS:DnaB:ABDx were attempted and the results of these experiments are presented above. Overall, these methods were unsuccessful in achieving AmyS:DnaB:ABDx isolation. Subsequently, a strategy was designed to add a polyhistidine detectable marker (His-tag) to the C-terminus of the recombinant protein alginate-binding domain (ABDx). The first part of this section focusses on the results of a primer dimer method of His-tagging the fusion protein. In Section 3.6.2, a His-tag encoding sequence was synthesised into a BsrGI-KpnI gene fragment as a method of His-tagging the fusion protein.

3.6.1 Primer dimer His-tagging

This method was unable to be progressed to its conclusion due to the failure of the first step in which p1623*amySdnaBABDx* was cut by SapI/KpnI restriction endonucleases (REase) (Section 2.8.9.1) (Figure 8). A SapI/KpnI-cut *amySdnaBABDx* fragment was not detected by gel electrophoresis, which indicates inefficient REase activity by SapI/KpnI. Variations to this step were attempted, which included a non-sequential simultaneous restriction digest (Section 2.8.9.1). Both sequential and simultaneous REase digests were unsuccessful. Further attempts were made to achieve a successful restriction digest by varying the incubation time of the REase. These variations included a 30 min, 1 h and 2 h incubation time. Variation to incubation time was unsuccessful in achieving an efficient REase hydrolysis of p1623*amySdnaBABDx*. Fresh reagents, which included new SapI and CutSmart buffer were used without success. Additionally, the experiment was undertaken independently by Dr. Moradali without success. Restriction fragment analysis of p1623*amySdnaBABDx* using PacI/SapI and PacI/KpnI showed efficient restriction endonuclease activity for PacI/KpnI, and a poor hydrolysis result for PacI/SapI, which indicates an inefficient restriction digest is because of the *SapI* restriction site of *amySdnaBABDx*.

3.6.2 BsrGI-KpnI His-tag insertion

An alternative strategy for His-tagging the recombinant protein was developed following the unsuccessful attempt using the primer dimer method (Section 3.6.1). A BsrGI-KpnI gene fragment of *amySdnaBABDx* was designed to encode a His-tag, and was subsequently synthesised by GenScript into pUC57Simple vector (Figure 9). Following the protocol outlined in Section 2.8.9.2, the BsrGI-KpnI His-tag insert was ligated with BsrGI/KpnI hydrolysed *amySdnaBABDx* and transformed into TOP10 *E. coli* (Section 2.7.1). A restriction fragment analysis of plasmid isolated from TOP10 *E. coli* showed a BsrGI-KpnI fragment that had a comparable molecular size to the BsrGI-KpnI fragment isolated from pUC57Simple*hisBsrGI* (Figure 21, red arrows). The BsrGI-KpnI fragment from TOP10 has a greater molecular size than the BsrGI-KpnI fragment from p1623*amySdnaBABDx* (indicated by the white arrow), which is expected given the additional base pairs encoding the His-tag.

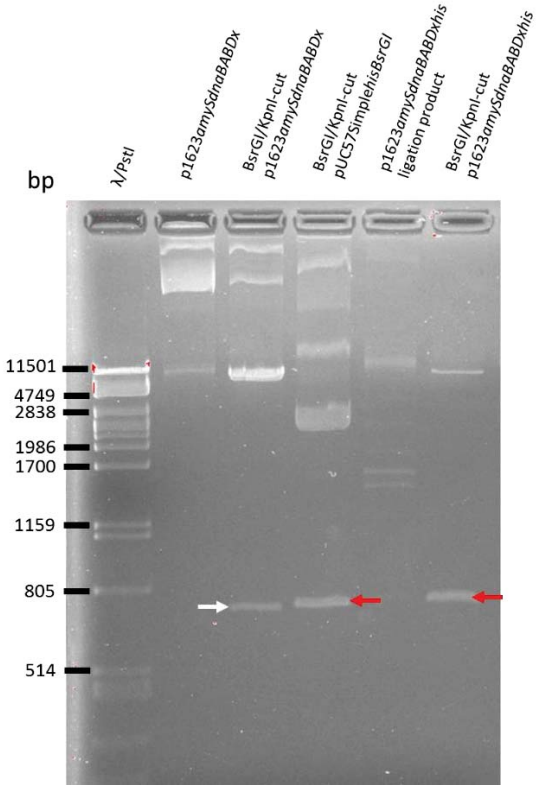

Figure 21. Confirmation of *E. coli* transformed with p1623*amySdnaBABDxhis*. 1% agarose gel electrophoresis of restriction p1623*amySdnaBABDxhis* fragment analysis. The lane p1623*amySdnaBABDx* contains p1623*amySdnaBABDx* vector that has not been hydrolysed by restriction endonucleases (REase). The lanes labelled BsrGI/KpnI-cut p1623*amySdnaBABDx*, BsrGI/KpnI-cut pUC57Simple*hisBsrGI*, and BsrGI/KpnI-cut p1623*amySdnaBABDxhis* contain isolated p1623*amySdnaBABDx*, pUC57Simple*hisBsrGI*, and p1623*amySdnaBABDxhis* DNA hydrolysed by REase BsrGI and KpnI, respectively. The lane p1623*amySdnaBABDxhis* ligation product represents a DNA sample from the ligation reaction of BsrGI/KpnI-cut p1623*amySdnaBABDx* vector and BsrGI-KpnI His-tagged insert. Lane labelled λ/PstI represents a DNA molecular size standard of Lambda phage DNA hydrolysed by REase PstI. Molecular size is given in base pairs (bp). *Red* arrows indicate REase hydrolysed gene fragments with size of 720 bp. A *white* arrow indicates an REase hydrolysed gene fragment with size of 700 bp.

3.7 Transformation and production of AmyS:DnaB:ABDx:His

The p1623*amySdnaBABDxhis* expression vector was transformed into *B. megaterium* strain YYBm1 (Section 2.7.2). Colony growth of YYBm1 on tetracycline selective CR5-topagar (Section 2.2.5) indicated successful transformation of this strain with p1623*amySdnaBABDxhis*.

B. megaterium YYBm1 p1623*amySdnaBABDx* was used for protein production, in which D-xylose was added to the growth media to a final concentration of 0.5% to induce expression of AmyS:DnaB:ABDx (Section 2.9.1). Due to the presence of a pH-sensitive (pH 6) intein in the recombinant protein design, growth was monitored in relation to pH of the media over time. The growth medium was initially buffered to pH 8.4 by 100 mM Tris-HCl buffer (Section 2.4.2), and culture was harvested when pH in the medium dropped to below 8 (pH 7.93). OD_{600nm} was recorded as 1.85 at the time of harvesting. Following Section 2.9.2.1 for the collection of extracellular protein, ammonium sulfate at a saturation of 55% was used to precipitate proteins from the cell-free supernatant. The pH was monitored during ammonium sulfate precipitation and a decrease to pH 7.8 was recorded. The protein pellet was collected and resuspended in 100 mM Tris-HCl pH 8.4, and stored at -20˚C.

3.7.1 Analysis of AmyS:DnaB:ABDx:His

The bulk extracellular protein was quantified by a Bradford assay against a bovine serum albumin standard (Section 2.9.3), which resulted in a bulk protein concentration of 1.1 mg/ml for YYBm1 p1623*amySdnaBABDxhis*.

Figure 22 shows the results of anti-His-tag immunoblot (Section 2.10.2) and SDS-PAGE analysis (Section 2.10.1) of the extracellular protein profile of YYBm1 transformed with p1623*amySdnaBABDxhis* and p1623 empty vector. Additionally, an aliquot of YYBm1 p1623*amySdnaBABDxhis* and p1623empty cells was lysed and the cell lysate prepared for SDS-PAGE analysis (Section 2.10.1.1). The anti-His-antibody detected a band in both the extracellular protein and cell lysate fraction of YYBm1 transformed with p1623*amySdnaBABDxhis*, corresponding to a protein with a MW of 40 kDa, which is close to the expected MW of DnaB:ABDx:His following N-terminus intein cleavage. The corresponding 40 kDa protein in the SDS-PAGE extracellular and lysate protein profiles is indicated by black arrows (Figure 22). Additionally, a band in both SDS-PAGE profiles corresponding to a protein with a MW of 56 kDa has been highlighted by red arrows. This is close to the expected MW of the recombinant protein AmyS domain following N-terminus intein cleavage. The absence of a band that could correspond to the full-length recombinant protein (87.2 kDa) in the anti-His-tag immunoblot indicates that total intein cleavage has occurred.

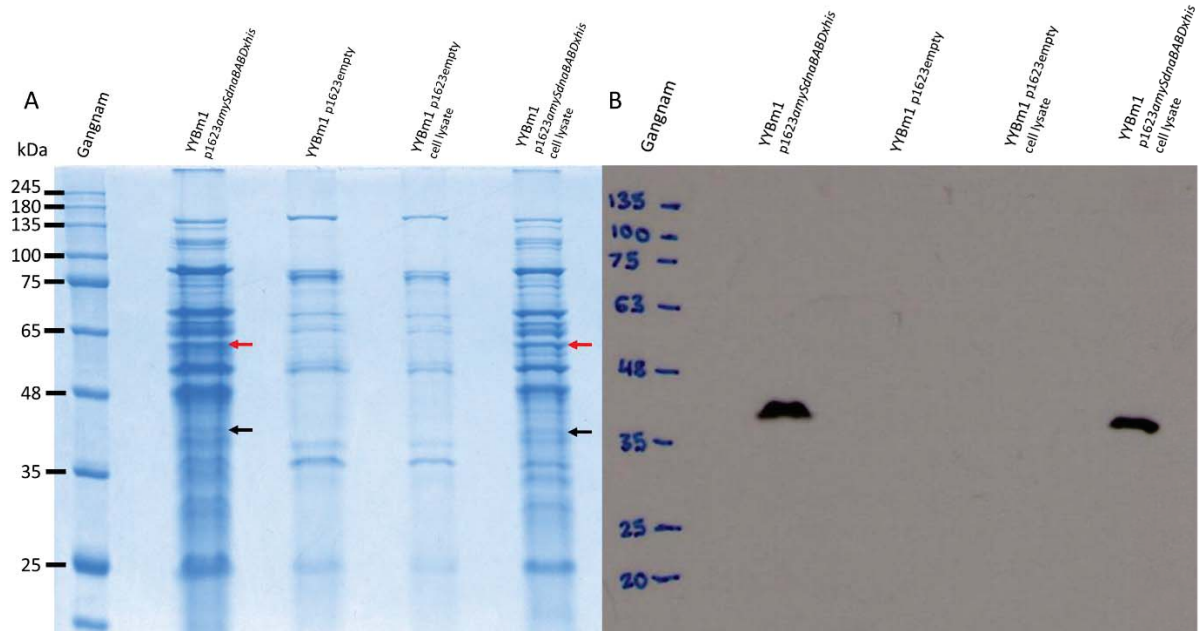

Figure 22. Confirmation of recombinant protein from *B. megaterium* transformed with p1623*amySdnaBABDxhis*. *A.* 10% SDS-PAGE analysis of extracellular and cell lysate protein profiles of *B. megaterium* YYBm1 transformed with p1623*amySdnaBABDxhis* or p1623 empty vector. In the protein profiles of YYBm1 p1623*amySdnaBABDx* proteins with molecular weight (MW) of 56 kDa and 40 kDa are indicated by r*ed* and *black* arrows, respectively. *B.* Anti-His-tag immunoblot analysis of extracellular and cell lysate protein profiles of *B.megaterium* YYBm1 transformed with p1623*amySdnaBABDxhis* or p1623 empty vector. The lane labelled Gangnam contains a MW standard GangNam-STAIN™ Pre-stained Protein Ladder. MW is given in kilodaltons (kDa).

3.7.2 Ssp DnaB intein activity inhibition

The Ssp DnaB mini-intein is designed to self-cleave at pH 6. However, the results in Section 3.7.1 indicate that intein activity is occurring with complete efficiency at pH 8. This spontaneous total cleavage prevents recovery of the full-length recombinant protein, which in turn prevents progression of the project. To inhibit intein cleavage, variations were made to the method of protein production and collection. Alternative growth media were employed, including: trace metal mix A5 medium (Section 2.2.2); a custom A5 medium (Section 2.2.3); and Terrific Broth (TB) medium (Section 2.2.4). All three media had significantly better growth rates for *B. megaterium* YYBm1 compared to Luria-Bertani (LB) medium; however, total intein cleavage still occurred regardless of media. A 0.2 M borate buffer pH 9 (Section 2.4.3) and glycine sodium hydroxide buffer pH 10 (Section 2.4.4) were used to achieve pH 9 and 10 in the media, respectively. Bacterial growth was drastically

impaired in growth media buffered to pH 9 and 10, which prevented protein production from taking place.

Two further strategies were used to investigate whether Ssp DnaB is sensitive to another inducer, in addition to pH-sensitivity. The first strategy looked at ionic strength in the solution containing AmyS:DnaB:ABDx. Ammonium sulfate, which is used to precipitate protein from the supernatant, greatly increases the ionic strength of the solution. Therefore ultrafiltration (Section 2.9.2.2) was used as an alternative method of protein collection and concentration in place of ammonium sulfate precipitation. The results of this experiment indicated that the recombinant protein was undergoing total cleavage regardless of the ionic strength of the solution.

A second experiment tested DnaB for sensitivity to a strong nucleophile inducer, such as 1,4-dithiothreitol (DTT). DTT is a component of the SDS-loading buffer used for SDS-PAGE analysis to reduce disulfide bonds formed between cysteine residues. SDS-loading buffer that did not contain DTT or any other reducing agent was formulated (Section 2.10.1.1). Figure 23 shows the results of an anti-His-tag immunoblot (Section 2.10.2) and SDS-PAGE (Section 2.10.1) analysis of the extracellular protein of YYBm1 p1623*amySdnaBABDxhis* with and without DTT-treatment. The absence of a reducing agent appears to have caused aggregation of protein at the top of the polyacrylamide gel (Figure 23, black arrows). The aggregated protein was strongly detected in the immunoblot, indicating that recombinant protein, in either cleaved or full-length form, is part of this aggregation. Another band was detected by anti-His-antibodies, and is highlighted by a red arrow. This band corresponds to a protein with a MW of 40 kDa, which is comparable to the molecular weight of the protein detected in the DTT-treated YYBm1 p1623*amySdnaBABDxhis* profile, and is likely to be the cleaved DnaB:ABDx:His region of the recombinant protein. Absence of a band corresponding to the full-length recombinant protein, in combination with detection of the cleaved domain, strongly supports that Ssp DnaB is not DTT-sensitive.

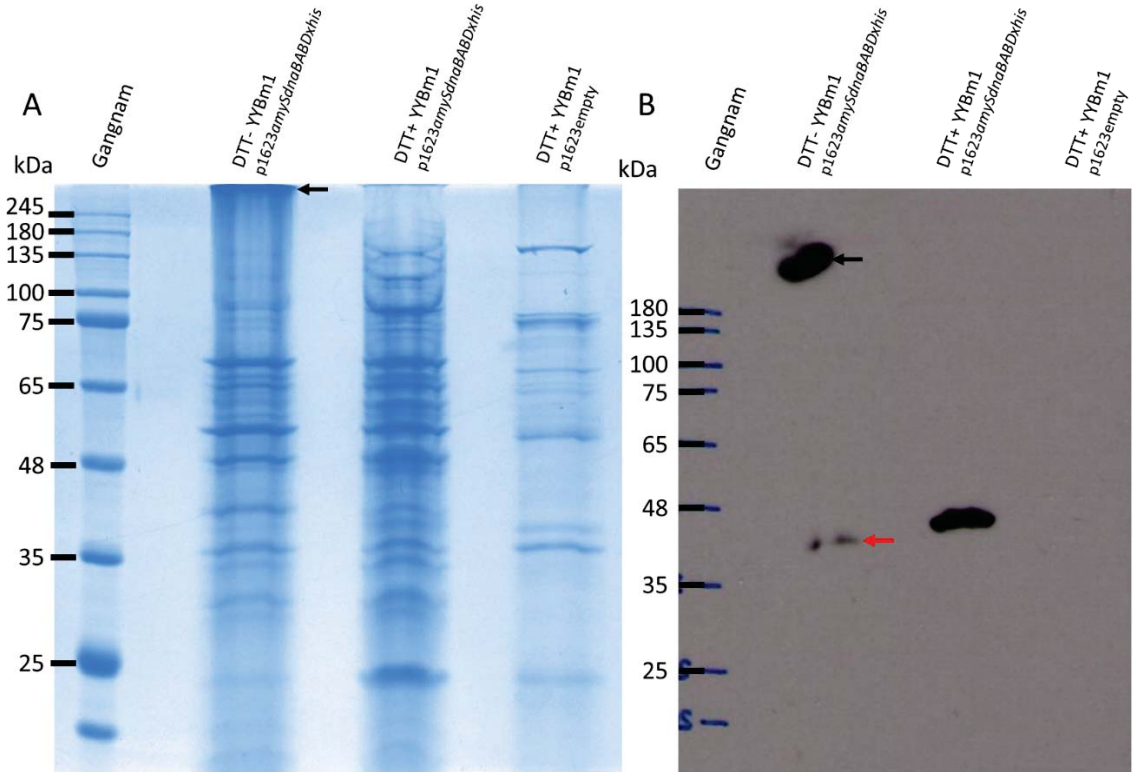

Figure 23. Intein cleavage is DTT-independent. *A*. 10% SDS-PAGE analysis of extracellular protein from *B. megaterium* YYBm1 transformed with p1623*amySdnaBABDxhis* or p1623 empty vector and treated with SDS loading buffer containing or lacking dithiothreitol (DTT). *B*. Anti-His-tag immunoblot analysis of extracellular protein from *B. megaterium* YYBm1 transformed with p1623*amySdnaBABDxhis* or p1623 empty vector and treated with SDS loading buffer containing or lacking DTT. *Black* arrows indicate an aggregation of His-tagged protein at the top of the DTT-free lane. A *red* arrow indicates a small concentration of non-aggregated His-tagged protein detected by anti-His-tag antibodies. The lane labelled Gangnam contains a MW standard GangNam-STAIN™ Pre-stained Protein Ladder. MW is given in kilodaltons (kDa).

3.8 Functional analysis of AmyS:DnaB:ABDx:His

The functionality of the recombinant protein amylase domain (AmyS) was assessed by a starch degradation screen to detect α-amylase activity and a maltose assay to quantify α-amylase activity. These results are described in the first part of this section. The second part of this section shows the results of alginate-binding purification as a method of analysing the functionality of the recombinant protein alginate-binding domain (ABDx).

3.8.1 Functional analysis of AmyS

The results of a starch degradation screen for amylase activity showed a clear zone around the spot where YYBm1 p1623*amySdnaBABDxhis* extracellular protein was applied, which indicates α-amylase activity (Figure 24). No degradation of starch was detected in YYBm1 p1623empty, indicating that α-amylase activity is associated with *amySdnaBABDxhis*.

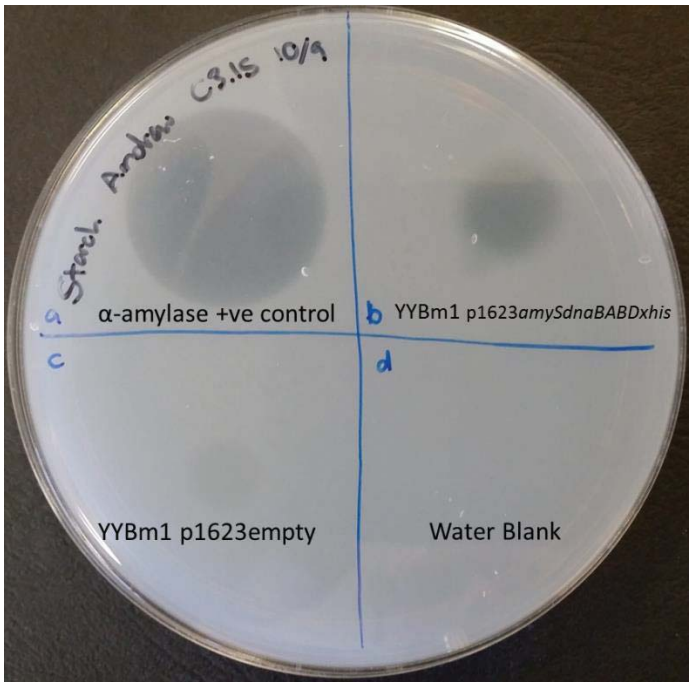

Figure 24. Confirmation of α-amylase activity by *B. megaterium* transformed with p1623*amySdnaBABDxhis*. Starch degradation screen of the extracellular protein from *B. megaterium* YYBm1 transformed with p1623*amySdnaBABDxhis* or p1623 empty vector. *B. licheniformis* α-amylase (BLA) is labelled α-amylase +ve control. YYBm1 p1623*amySdnaBABDxhis* represents the protein sample from *B. megaterium* YYBm1 transformed with p1623*amySdnaBABDxhis*. YYBm1 p1623*empty* represents the protein sample from YYBm1 transformed with p1623 empty vector. Water was applied as a blank.

A maltose assay was undertaken to quantify the α-amylase activity of AmyS:DnaB:ABDx:His (Section 2.12.2). Table 6 outlines the results of the maltose assay. An α-amylase positive control was determined to have enzymatic activity of 10 u/mg of protein, in which one unit will liberate 1 mg of maltose from starch in 3 min at pH 6.9 and room temperate (22 ± 4˚C). YYBm1 transformed with p1613 empty vector was shown to have activity of 0.4 u/mg protein.

From the results of the maltose assay, the recombinant protein AmyS domain was determined to have activity of 1.4 u/mg of protein.

Table 6. Results of a maltose assay for α-amylase activity

	Test	A540nm	ΔA540nm	Maltose (mg)	Enzyme (ml)	Activity (unit/mg protein)	Average (unit/mg protein)
α-amylase Control	1	2.542	2.403	6.622	0.5	13.24	10.17
	2	2.695	2.558	7.039	0.7	10.06	
	3	2.763	2.627	7.225	1	7.23	
	Blank	0.134	-	-	-	-	
AmyS-ABDx-His extracellular protein	1	0.892	0.253	0.830	0.5	1.66	1.37
	2	0.937	0.299	0.954	0.7	1.36	
	3	0.993	0.354	1.102	1	1.10	
	Blank	0.639	-	-	-	-	
Empty vector extracellular protein	1	0.165	0.029	0.226	0.5	0.41	0.37
	2	0.183	0.057	0.302	0.7	0.39	
	3	0.193	0.069	0.334	1	0.304	
	Blank	0.125	-	-	-	-	

3.8.2 Functional analysis of ABDx

Protein purification with alginate beads (Section 2.11.4) using extracellular protein collected from YYBm1 p1623*amySdnaBABDxhis* and p1623empty was attempted and the results analysed by SDS-PAGE and an anti-His-tag immunoblot. SDS-PAGE analysis results showed no bands in the protein samples that had been purified by alginate beads for either YYBm1 p1623*amySdnaBABDxhis* or p1623empty, and His-tag was not detected in these samples. A protein with a MW of 40 kDa was detected by immunoblot in the extracellular protein of YYBm1 p1623*amySdnaBABDxhis*, which indicates the presence of the recombinant protein in this sample. His-tag was not detected in YYBm1 p1623empty, which is expected as detection of His-tag is associated with expression of *amySdnaBABDxhis*.

3.9 Construction of *amySABDxhis* and *dnaB* excision

The aberrant activity of Ssp DnaB mini-intein caused total cleavage of AmyS:DnaB:ABDx:His to form the N-terminal AmyS and C-terminal DnaB:ABDx:His regions, and prevented the collection of full-length recombinant protein (Section 3.7.1). Attempts to inhibit intein activity were unsuccessful (Section 3.7.2). Hence, an alternative strategy to overcome recombinant protein cleavage was developed, which involved PCR amplification of the gene sequences encoding AmyS (*amyS*) and ABDx:His (*ABDxhis*), and construction of a restriction site between these sequences, effectively excising the intein-encoding *dnaB* sequence (Section 2.8.10) (Figure 10).

Primers were designed to amplify *amyS* and construct a BamHI restriction site at the 3' end, and to amplify *ABDxhis* and construct a BamHI restriction site at the 5' end (Section 2.1) (Table 3). The PCR products were analysed by gel electrophoresis (Section 2.8.4) and the results presented in Figure 25.

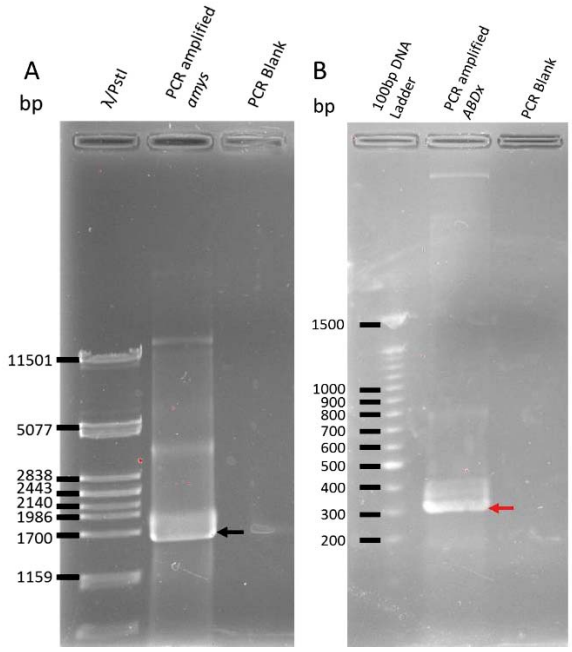

Figure 25. Amplification of *amyS* and *ABDxhis* gene fragments. *A.* 1% agarose gel electrophoresis of PCR amplified *amyS* product. A linear dsDNA band with a molecular size of 1600 bp is indicated by a *black* arrow. *B.* 2% agarose gel electrophoresis of PCR amplified *ABDxhis* product. A *red* arrow indicates a linear dsDNA band with a size of 400 bp. Lane labelled λ/PstI represents a DNA molecular size standard of Lambda phage DNA hydrolysed by REase PstI. Quick-Load® 100 bp DNA Ladder is labelled 100bp DNA ladder. A blank PCR reaction mixture without DNA template is labelled PCR Blank.

The PCR product of *amyS* amplification resulted in a band with a molecular size of 1600 bp, which corresponds to the expected *amyS* fragment size of 1580 bp. Amplification of *ABDxhis* generated a band with size of 400 bp, which is consistent with the expected size of the *ABDxhis* fragment (418 bp).

The PCR products were hydrolysed by restriction endonucleases (REase) (Section 2.8.6) and ligated (Section 2.8.7), prior to ligation into p1623. The expression vector p1623*amySABDxhis* was transferred into TOP10 *E. coli* (Section 2.7.1). Figure 26 shows the results of restriction fragment analysis of p1623*amySABDxhis*.

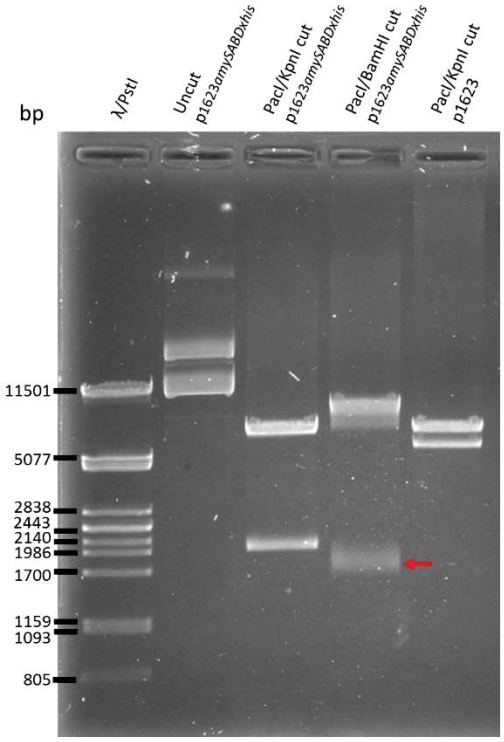

Figure 26. Confirmation of *dnaB* excision. 1% agarose gel electrophoresis of p1623*amySABDxhis* restriction fragment analysis. The lane labelled Uncut p1623*amySABDxhis* contains p1623*amySABDxhis* DNA that has not been hydrolysed by restriction endonucleases (REase). PacI/KpnI cut p1623*amySABDxhis* contains p1623*amySABDxhis* DNA that has been hydrolysed by REase PacI and KpnI. PacI/BamHI cut p1623*amySABDxhis* contains p1623*amySABDxhis* DNA that has been hydrolysed by REase PacI and BamHI. Empty vector p1623 hydrolysed by REase PacI/KpnI was loaded in the lane labelled PacI/KpnI cut p1623. A *red* arrow indicates the gene fragment product of PacI/BamHI hydrolysis, which has a molecular size of 1600 bp. The lane labelled λ/PstI represents a DNA molecular size standard of Lambda phage DNA hydrolysed by REase PstI.

REase PacI/KpnI hydrolysis of the expression vector resulted in a band with a molecular size of 2000 bp, which is consistent with the expected size of 2008 bp for the *amySABDxhis* construct. Additionally, a restriction digest of p1623*amySABDxhis* with REase BamHI was successful, which indicates that the BamHI restriction site is present in the construct, whereas the previous p1623*amySdnaBABDxhis* construct lacked a BamHI restriction site (Appendix I). REase PacI/BamHI hydrolysis of p1623*amySABDxhis* generated a band with size of 1600 bp, which is consistent with the expected size of 1580 bp for the PacI/BamHI-cut *amyS* fragment. The integrity of the construct within *E. coli* TOP10 was analysed by DNA sequencing (Section 2.8.8), which showed there were no mutations or frame shifts present in *amySABDxhis*. Additionally, DNA sequencing confirmed that *dnaB* had been successfully excised.

3.10 Transformation and production of AmyS:ABDx:His

The p1623*amySABDxhis* expression vector was transformed into *B. megaterium* strains YYBm1 (Section 2.7.2). Colony growth of YYBm1 on tetracycline selective CR5-topagar (Section 2.2.5) indicated successful transformation of this strain with p1623*amySABDxhis*. Fifteen colonies were screened by colony PCR (Section 2.8.5), using primers targeting *amySABDxhis* sequence. Colony PCR of YYBm1 colonies resulted in a PCR product with molecular size of 2000 bp in 9 of the 15 colonies (Figure 27). This PCR product is consistent with the molecular size of *amySABDxhis*.

The integrity of the construct within *B. megaterium* YYBm1 was analysed by DNA sequencing (Section 2.8.8), which showed there were no mutations or frame shifts present in *amySABDxhis*.

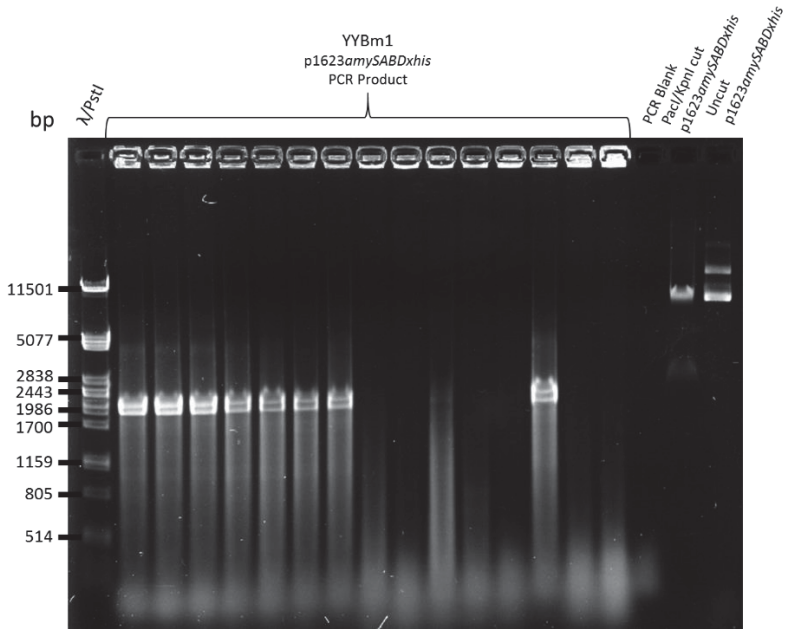

Figure 27. Confirmation of *B. megaterium* transformed with p1623*amySABDxhis*. Colony PCR products of *B. megaterium* YYBm1 transformed with p1623*amySABDxhis* analysed by 1% agarose gel electrophoresis. Colony PCR products of *B. megaterium* YYBm1 transformed with p1623*amySABDxhis* are labelled YYBm1 p1623*amySABDxhis* PCR product. The lane labelled PacI/KpnI-cut p1623*amySABDxhis* contains TOP10 isolated p1623*amySABDxhis* DNA hydrolysed by restriction endonucleases (REase) PacI and KpnI. The lane labelled Uncut p1623*amySABDxhis* contains p1623*amySABDxhis* DNA that has not been hydrolysed by restriction (REase). A blank PCR reaction mixture without DNA template is represented by PCR Blank. The lane labelled λ/PstI represents a DNA molecular size standard of Lambda phage DNA hydrolysed by REase PstI. Molecular size is given in base pairs (bp).

B. megaterium YYBm1 p1623*amySABDxhis* was used for protein production (Section 2.9.1), in which D-xylose was added to the growth media to a final concentration of 0.5% to induce production of AmyS:ABDx:His. Bacterial growth was monitored periodically until an OD_{600nm} of 6 was reached, at which point the culture was harvested. Following Section 2.9.2.1 for the collection of extracellular protein, ammonium sulfate at a saturation of 55% was used to precipitate proteins from the cell-free supernatant. The protein pellet was collected and resuspended in 100 mM Tris-HCl pH 8.4, and stored at -20˚C.

The bulk extracellular protein was quantified by a Bradford assay (Section 2.9.3) against a bovine serum albumin standard, which resulted in a bulk protein concentration of 0.5 mg/ml for YYBm1 p1623*amySABDxhis*.

Figure 28 shows the results of an anti-His-tag immunoblot (Section 2.10.2) and SDS-PAGE (Section 2.10.1) analysis of the extracellular and intracellular protein profiles of YYBm1 p1623*amySABDxhis* and p1623 empty vector. Shirin Ng supplied a confirmed His-tagged protein, AlgD:His, for use as a positive control for the immunoblot. SDS-PAGE analysis showed no unique bands between the extracellular protein profiles of YYBm1 p1623*amySABDxhis* and p1623empty. The concentration of the cell lysate fractions was too low to be adequately analysed by SDS-PAGE. AlgD:His was detected by anti-His-tag antibodies, whereas the immunoblot did not detect His-tag either intra- or extracellularly for YYBm1 p1623*amySABDxhis* or p1623empty, which indicates that *B. megaterium* YYBm1 p1623*amySABDxhis* was not producing AmyS:ABDx:His.

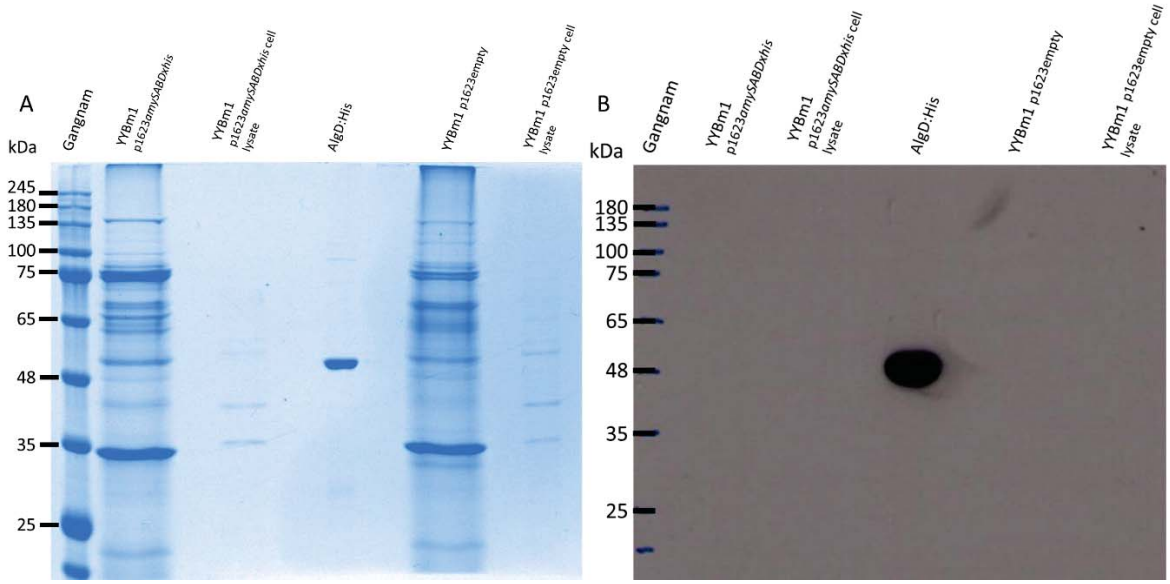

Figure 28. Protein analysis of *B. megaterium* transformed with p1623*amySABDxhis*. *A*. 10% SDS-PAGE analysis of the extracellular and cell lysate protein of *B. megaterium* YYBm1 transformed with p1623*amySABDxhis* and p1623 empty vector. *B*. Anti-His-tag immunoblot analysis of the extracellular and cell lysate protein profiles of *B. megaterium* YYBm1 transformed with p1623*amySABDxhis* and p1623 empty vector. The lane labelled Gangnam contains a MW standard GangNam-STAIN™ Pre-stained Protein Ladder. MW is given in kilodaltons (kDa).

CHAPTER FOUR
DISCUSSION

Biopolymers are an important group of biomaterials that have gained interest for the downstream processing of compounds as an alternative to traditional chromatographic techniques. Alginate is one of the foremost biopolymers in food, pharmaceutical and biomedical industries, and its ability for forming stable hydrogels has made it an excellent matrix for encapsulating and adsorbing compounds of interest. However, there have been no studies examining the potential for alginate to specifically immobilise and display target proteins.

The aim of this study was to generate a functionalised protein-displaying alginate. To this end, a recombinant protein that was capable of binding alginate and carrying out a secondary function was designed, and the product analysed for functionality. A cleavage module (DnaB) was placed between the alginate-binding protein (ABDx) and the target protein (AmyS) to enable the recovery of the target protein following display on alginate. In this way, a successful alginate-binding recombinant protein could have applications for target protein separation and enrichment.

4.1 Production of AmyS:DnaB:ABDx

B. megaterium was selected as the expression system for *amySdnaBABDx* due to its lack of endotoxins, naturally high secretion capacity, and established success producing exoenzymes, such as amylase (Terpe, 2006). These traits offered a comparable advantage over the more popular *E. coli* expression system, which produces endotoxins in most strains and is a poor secretor. In turn, *B. megaterium* strain YYBm1 was chosen because it is a deletion mutant for a major extracellular protease (*ΔnprM*) and for the proteins necessary to metabolise xylose (*ΔxylA*). *B. megaterium* strain MS941 was also selected as an expression system to increase the probability of a successful transformation, and subsequent expression of AmyS:DnaB:ABDx. Both YYBm1 and MS941 are deletion mutants of the parent strain DSM319. MS941 is a *ΔnprM* mutant, but it does not contain a deletion for *ΔxylA*, which means this strain retains the ability to metabolise xylose. Hence the method of protein production by

xylose induction was altered slightly for MS941 to include two extra additions of D-xylose: one at OD_{600nm} 1.0, and another at 2.0.

The results of extracellular protein analysis showed a band corresponding to a protein with a molecular weight (MW) of 85 kDa, which corresponds with the expected MW of AmyS:DnaB:ABDx (Figure 13). Additionally, when purification of the recombinant protein by alginate was attempted, a protein of similar MW was detected in the sample retained with the alginate (Figure 15). This suggested functionality of the recombinant protein alginate-binding domain (ABDx). Two additional bands with apparent MW of 56 kDa and 40 kDa were noted as unique to the YYBm1 p1623*amySdnaBABDx* extracellular protein profile, and most likely corresponded to the intein-cleaved domains: AmyS (55.8 kDa) and DnaB:ABDx (31.4 kDa) (Figure 13). This was not unexpected, as some low-level spontaneous intein cleavage is a known phenomenon, and since it appeared that concentration of the full-length recombinant protein was still high, this cleavage was not considered a significant issue (Volkmann *et al.*, 2009).

However, MALDI-TOF tryptic peptide mass analysis of the 85 kDa protein showed that this protein was not identical with AmyS:DnaB:ABDx, and instead was a match for peptidase S8, an extracellular protease with a similar MW (85.6kDa) to the recombinant protein (Appendix III). While peptide coverage was low at 37%, the score and identity were indicative that the protein being detected was peptidase S8. What was unambiguous, however, was that this protein was not AmyS:DnaB:ABDx. This raised a significant problem for using traditional methods of protein detection and isolation, such as SDS-PAGE, as the presence of the extracellular protease was potentially masking the detection of AmyS:DnaB:ABDx due to the similar size of each protein. In turn, the nature of peptidase S8 as an extracellular protease raised an issue of protein degradation, in which protease activity breaks down the recombinant. This would reduce the yield of full-length recombinant protein and make it harder to detect, especially given that intein-cleavage was occurring to an unknown degree.

As a further note on the analysis of recombinant protein production, *amySdnaBABDx* expression in *B. megaterium* MS941 was poor. Colony PCR confirmed the presence of *amySdnaBABDx* in MS941; however, protein production consistently yielded 3-fold less bulk protein than YYBm1, and the full-length recombinant protein was not detected by SDS-PAGE. Additionally, a starch degradation screen showed significantly less α-amylase activity for

extracellular protein from MS941 compared to YYBm1 (Figure 14). Due to these factors, MS941 was dropped as a recombinant protein production system. In this way, more resources could be devoted to optimising recombinant protein production in YYBm1.

4.2 Detection and isolation of AmyS:DnaB:ABDx

Several strategies were developed to detect and isolate AmyS:DnaB:ABDx. The first used anti-AlgX-antibodies in an immunoblot targeting the recombinant protein alginate-binding domain, which was derived from AlgX. Other strategies exploited the results of the starch degradation screen to aid with detection, as the extracellular protein of YYBm1 *amySdnaBABDx* was shown to have α-amylase activity. The first of these strategies analysed the extracellular protein by native PAGE followed by an α-amylase activity screen of the polyacrylamide gel. The second strategy sought to fractionate the extracellular proteins by one of two methods: (1) differential salting out, and (2) size exclusion chromatography, which could then be screened to detect α-amylase activity in each of the fractions.

4.2.1 Anti-AlgX immunoblot

The results of the anti-AlgX immunoblot showed problems detecting AmyS:DnaB:ABDx by targeting the alginate-binding domain. Full-length recombinant protein was not detected in the extracellular protein profiles of either YYBm1 or MS941 *amySdnaBABDx* (the decision to exclude MS941 as an expression system came after this immunoblot for the reasons described in Section 4.2. However, at this stage MS941 protein profiles were still being tested). A band corresponding to a protein with a molecular weight of 34 kDa was possibly detected in YYBm1 *amySdnaBABDx*, which could correspond with DnaB:ABDx region following intein-cleavage (Figure 16). However, this same band was unambiguously detected in both YYBm1 and MS941 p1623empty. This is unexpected as p1623empty is an empty vector control and thus lacks the *amySdnaBABDx* gene. Therefore anti-AlgX antibodies should not have been able to detect the ABDx domain in these samples. It is possible that that one sample could have been mistaken for another; however, this is considered unlikely because all containers, including flasks, Falcon® tubes, and Eppendorf® tubes were correctly labelled, and great care was taken with ensuring samples were correctly distributed. The more likely explanation for these

immunoblot results is that the p1623empty cultures were contaminated with p1623*amySdnaBABDx*, which could have occurred during inoculation of the growth media. While aseptic techniques were employed, flasks for both p1623empty and p1623*amySdnaBABDx* cultures were placed under the same laminar flow biohood during inoculation. One of the salient characteristics of *B. megaterium* is that this organism undergoes sporulation readily, and therefore the potential for aerosolised cells to persist outside of the growth media and to be passed onto a different container exists. Theoretically, it would take the growth of only one cell of YYBm1 or MS941 p1623*amySdnaBABDx* in the p1623empty growth media to produce a mixed culture. Such a mixed culture would invariably test positive for recombinant protein. To avoid such contamination in the future, the growth media was inoculated in separate biohoods if available, or at different times.

A problem with this hypothesis, however, is that recombinant protein expression in YYBm1 and MS941 p1623*amySdnaBABDx* cultures was almost non-detectable in the anti-AlgX immunoblot. If contamination occurred, it would be expected that ABDx domain would be detected equally in these expression profiles as for the empty vector. It should be noted that the immunoblot had significant background noise, which indicates that there was poor or inconsistent protein transfer during the blotting procedure. This could explain the absence of detection in the YYBm1 and MS941 p1623*amySdnaBABDx* samples.

Another possibility is that the anti-AlgX-antibody could be a factor contributing to the poor immunoblot results. The anti-AlgX antibody is a polyclonal antibody raised against *Pseudomonas aeruginosa* AlgX whole protein, and it is unknown which specific epitopes the antibody binds to (Robles-Price *et al.*, 2004). Antibody raised against whole protein could recognise multiple epitopes, including epitopes on the alginate-binding domain of AlgX or it may only recognise epitopes on the acetyltransferase domain, which is not a part of the recombinant protein design. Hence the bands detected in the immunoblot could be non-specific binding, or detection of an endogenous protein that shares homologous epitopes with AlgX. However, if non-specific binding was a factor, the antibody would not be expected to detect the same protein in both YYBm1 and MS941 p1623empty, and if it was detecting an endogenous protein the antibody would be expected to detect the same protein in all samples. Since neither is the case, the antibody is unlikely to be the cause of the immunoblot results, although it could still be a factor. An AlgX positive and negative control will need to

be sourced if an anti-AlgX immunoblot is repeated to confirm specificity of the antibody to alginate acetyltransferase. Such controls could be the envelope fraction of *P. aeruginosa* and the respective *P. aeruginosa ΔalgX*.

Assuming that the problems that had occurred with the anti-AlgX immunoblot were a result of contamination of the empty vector controls with *amySdnabABDx*-positive cultures, then analysis of the immunoblot indicates that the recombinant protein is being cleaved significantly by intein activity, as only a protein with a corresponding MW similar to DnaB:ABDx region was detected. Total intein cleavage is unexpected, although given that pH drops proportionally to bacterial growth, this could be caused by a significant pH drop in the growth media. Ssp DnaB intein activity occurs optimally at pH 6, which can be reached if the culture is allowed to grow for an extended period of time. Hence for all further experiments the growth medium was buffered to pH 7.4, excluding the sample used for native PAGE as this experiment was already underway at the time this decision was made.

4.2.2 Native PAGE analysis and protein renaturation

Detection of α-amylase activity and isolation of the recombinant protein by native PAGE led to inconsistent results. Addition of a starch solution to the native gel, followed by staining with Lugol's iodine showed strong α-amylase activity for the α-amylase control. Additionally, there was a band of starch degradation in the sample lane (Figure 17). However, the sample and negative control did not travel efficiently through the gel, and there was poor separation of the native protein marker. Both these factors made it difficult to relate the results of the α-amylase screen with a parallel gel that was stained with Coomassie® Brilliant Blue, and prevented isolation of the amylase-positive protein band. Native PAGE was repeated with an 8% polyacrylamide gel for a longer duration to overcome this issue. While an 8% gel did achieve significantly greater separation for the sample protein and the native protein marker, the gel failed to retain the starch solution and thus an α-amylase screen could not be successfully performed. A previous study that looked at co-polymerising SDS gels with starch indicated that in lower percentage gels (less than 10% polyacrylamide) there was a significant problem with starch leaking out of the gel before α-amylase activity could be screened (Martinez *et al.*, 2000).

Tabassum et al. (2014) had shown that α-amylase can be renatured from SDS-PAGE gels and then used in an α-amylase assay. Extracellular protein from YYBm1 p1623*amySdnaBABDx* and p1623empty, as well as an α-amylase control, underwent SDS-PAGE. The SDS gel was then used in the renaturing process and screened for α-amylase activity, following the same protocol as for the native gels. The results of the amylase screen showed starch degradation by *B. licheniformis* α-amylase, which indicates that the protein was successfully renatured (Figure 18). There was also some activity in the sample lane, which corresponds to a protein of around 60 kDa. This band is possibly the AmyS region of AmyS:DnaB:ABDx. There was no activity in bands of molecular weight consistent with the full-length recombinant protein. As with the results of the anti-AlgX immunoblot, native PAGE suggests that total intein cleavage occurred, which separated the recombinant protein between the AmyS and ABDx domains. This is a significant issue that negatively impacts yield and functionality of the recombinant protein.

4.2.3 Fractionation

Isolation of the recombinant protein through either solubility fractionation or size exclusion chromatography was unsuccessful. The first fractionation strategy utilised ammonium sulfate precipitation, in which proteins can be differentially salted out based on their solubility in a highly ionic solution. The solubility of a protein depends, in part, on its amino acid composition. By looking at the number of charged amino acid residues a protein contains, the relative solubility of that protein compared to a protein with a different composition can be inferred. The charged amino acid composition of peptidase S8 is Arg = 14, Asp = 52, Glu = 48, Lys = 78, whereas AmyS:DnaB:ABDx is Arg = 39, Asp = 54, Glu = 45, Lys = 48. Overall, peptidase S8 has greater charge, and thus can be expected to be slightly more soluble than AmyS:DnaB:ABDx in a solution that is highly ionic. By varying the concentration of ammonium sulfate in the solution, the proteins are fractionated based on solubility. Subsequently, the presence of AmyS:DnaB:ABDx in a given fraction can be detected through α-amylase activity of the α-amylase domain.

In practice, however, fractionation based on ammonium sulfate precipitation was unsuccessful. Alpha amylase activity was detected across a range of salt concentrations from 45 to 55%, and there was no observable difference in SDS-PAGE profiles between fractions in

this range (Figure 19). A significant problem with this method of fractionation is that the result is highly dependent on the way in which the ammonium sulfate is added to the solution. If the ammonium sulfate is added too quickly to a solution, or it is not mixed properly during addition, localised salt concentrations can form in solution as the ammonium sulfate does not dissolve uniformly. These localised concentrations can salt out proteins that are beyond the target solubility being fractionated for, leading to inaccurate fractionation.

Fractionation was re-attempted with variations to the technique, which included slower addition of ammonium sulfate and constant stirring of the solution. However, fractionation remained unsuccessful and α-amylase activity was still detected in fractions ranging from 45 to 55%.

A variation on technique that was not applied was using a saturated stock solution of ammonium sulfate. As indicated in Section 2.9.2.1, ammonium sulfate was added in solid form directly to the sample solution being fractionated. The use of a saturated stock solution is a more accurate method of achieving a specific concentration, and enables a significantly greater degree of control over the addition of the ammonium sulfate to the sample solution. However, this method can incur issues with volume as the maximum volume that can be centrifuged at one time is restricted. This requires that the sample be divided between multiple containers for collection, which negatively affects the protein yield. However, a saturated stock solution should have been used for this experiment, and it is strongly recommended for any future work with ammonium sulfate precipitation.

A second strategy utilising fractionation of the extracellular proteins based on size was developed with the goal of purifying and concentrating proteins in the relative size range of the full-length recombinant, i.e. 70 to 100 kDa. This fractionated protein sample could then be analysed by a lower percentage polyacrylamide gel, which allows for better separation and resolution of protein bands within this range. Ideally, this strategy enables the differentiation of proteins that have <2 kDa size difference, and therefore would allow for differentiating between the extracellular protease (85.6 kDa) and AmyS:DnaB:ABDx (87.2 kDa).

Analysing the extracellular protein profile using a lower percentage gel without doing fractionation first would be unlikely to give the band resolution necessary to differentiate protein bands within this range. This is because in an unfractionated sample, the

concentration of the proteins in the desired range would be diluted by the extraneous proteins. The bulk extracellular protein sample could be concentrated through ultrafiltration to mitigate this dilution; however, this strategy would then encounter problems with the amount of protein being loaded onto the gel. If the amount of protein being loaded is too high, there is the potential that the sample aggregates in the well and fails to migrate through the gel. In addition, overloading of the gel with sample causes significant smearing of the bands, which will drastically affect the ability to differentiate proteins.

To accomplish fractionation of proteins in the 70 – 100 kDa range, size exclusion chromatography (SEC) was used. Initially, the SEC results indicated a successful fractionation. The chromatogram showed a strong activity peak, which indicated protein was coming through the column, and twenty-seven 500 µl fractions were collected that fell within the range of these peaks. These fractions were screened for α-amylase activity, and out of 27, 11 fractions tested positive. However, the protein concentration of these fractions was too low to be quantified by a Bradford assay, and subsequently no bands were detected through SDS-PAGE. The concentration of the protein sample used for SEC was near the minimum threshold for gel filtration, which could explain the failure to detect bands through SDS-PAGE, as the fractions were too diluted. This result raises questions, however, since the concentration in the fractions was high enough to be screened for α-amylase activity, but was too low to be detected by a Bradford assay or SDS-PAGE.

A second gel filtration was undertaken using a sample that had been concentrated 7-fold (final 7.7 mg/ml). The resulting chromatogram showed a stronger and better aligned peak compared with the first chromatogram. The 33 fractions that were within the range of this peak were screened for α-amylase activity, and all tested negative. The lack of α-amylase activity is unlikely to be a problem associated with SEC or the gel filtration instruments, and is related to the culture from which this protein sample was collected. The protein used for the first SEC attempt was from a culture that had not been grown in a glucose-rich medium, whereas the protein used in the second gel filtration was derived from a culture that had been grown with 3% glucose. The addition of glucose to the medium was an attempt to inhibit production of peptidase S8. A previous study had shown that glucose at a concentration of 3% strongly inhibits the expression of extracellular proteases in *Bacillus* species (Wang *et al.*, 2006). While the results of an SDS-PAGE indicated that production of peptidase S8 was

strongly inhibited by the addition of glucose to the growth media, the experiment had failed to take into account that glucose is also a strong inhibitor of the xylose promoter (Terpe, 2006). It is very likely that the presence of glucose inhibited AmyS:DnaB:ABDx production, which is controlled by a xylose promoter.

Despite the increased protein concentration of the sample used for SEC, the concentration of the fractions was too low to be detected by Bradford assay and only a few bands were detectable by SDS-PAGE. None of these bands corresponded to the full-length recombinant protein, although this was expected given that AmyS:DnaB:ABDx production was likely inhibited by the presence of glucose in the growth medium. Furthermore, the bands corresponded to proteins with MW of less than 70 kDa, exclusively (Figure 20). This suggests that the peak seen in the chromatogram corresponds to proteins with a MW of less than 70 kDa. Hence proteins in the desired range of 70 – 100 kDa, in which the full-length recombinant protein would be located, have been excluded.

The difficulty with re-attempting size exclusion chromatography with a different protein sample and alternative column is that another attempt would encounter the same problem as previous gel filtrations. Despite scaling up protein production from 100 ml to 1000 ml of growth medium, a protein concentration could not be reached that would be sufficient for gel filtration. However, if SEC was re-attempted, it is strongly recommended that MW standards are used so that only proteins in the desired MW range are collected and analysed. Molecular weight standards were omitted in the initial strategy as a starch degradation screen was used to screen all fractions resulting from gel filtration for the recombinant protein.

Alternatives to size exclusion chromatography include membrane ultrafiltration with a molecular size cut-off (MWCO) and ion exchange chromatography (IEC). The recombinant protein has a net negative charge at pH 7, and therefore anion exchange chromatography would be used. However, given that the theoretical isoelectric point (pI) of AmyS:DnaB:ABDx is 6.17 (ExPasy, ProtParam), there is a potential issue when attempting to elute the protein from the positively charged column. The pH of the eluent would have to be decreased below the pI of the protein to switch the negative charge of AmyS:DnaB:ABDx to a net positive. At this point, pH would be low enough to induce intein activity, making recovery of the full-length recombinant protein difficult. Ultrafiltration would be able to fractionate proteins based on the MWCO of the column membrane, and could be used to achieve a concentrated

sample of extracellular proteins within 70 – 100 kDa. However, at the time that alternative methods were being considered, an ultrafiltration column with an appropriate MWCO was unavailable and would have had to have been ordered. While availability is not prohibitive, these alternatives were attempting to solve a problem to an experiment that in turn was trying to solve another problem. Protein fractionation was attempting to provide a solution to recombinant protein detection, and was practical solely because of the ready availability of the necessary instruments and reagents. Furthermore, fractionation would only be useful for the detection and isolation of the full-length recombinant protein. Detection of recombinant protein that had been truncated by protease or intein activity would not benefit from fractionation.

4.3 Generation of AmyS:DnaB:ABDx with a detectable marker and discovery of aberrant intein activity

A definitive method of detection and purification of AmyS:DnaB:ABDx was necessary. Detectable markers translationally fused with the target protein are a commonly used method of detecting and purifying recombinant protein. One such marker is a polyhistidine tag (His-tag), which is a block of histidine residues, typically 6, fused to the C- or N-terminus of the protein. The advantages of a His-tag are the availability of well-defined methods of detection and the ability to purify the protein through histidine affinity purification. Anti-polyhistidine-tag monoclonal antibodies are commercially available and are highly sensitive and specific to the polyhistidine motif. A 6xHis-tag was excluded from the initial recombinant protein design due to the uncertainty of how the marker would interact with the structure of the protein as well as its potential to mediate binding to the negatively charged alginate. There are reported problems with His-tags interfering with the proper folding of proteins and protein activity, which inhibits production of a functional recombinant protein (Bornhorst and Falke, 2000). However, the benefits of including a His-tag outweighed the associated risk to the recombinant protein structure and activity.

The first strategy to insert a His-tag into the hybrid gene sequence utilised primer dimers (Figure 8). However, this method was unsuccessful, despite experimenting with a sequential and a non-sequential restriction enzyme digestion, increasing the amount of

p1623*amySdnaBABDx* used, and having an experienced doctoral student attempt the restriction digest independently. The results of restriction fragment analysis strongly indicate that SapI did not have efficient restriction endonuclease (REase) activity. Given that fresh SapI failed to cut the expression vector, the problem is likely with the restriction site (*SapI*) itself, and would necessitate redesigning the cloning strategy using different restriction sites located within the hybrid gene.

The difficulty with repeating the primer dimer method is that this strategy is relatively novel, and therefore untested, within the laboratory group. While primer dimers had previously been used successfully by a member of the group, there was a dearth of experience in this area, and hence it is uncertain whether success could be achieved within a short timeframe. The unsuccessful attempts to His-tag using the primer-dimer method incurred a substantial cost in time, reagents and research budget. To attempt another primer dimer ligation, the primers would have to be redesigned around the new restriction sites. Since the success of the primer dimers themselves could not be verified, there was a significant risk that even with new restriction sites the insert and primer dimer would fail to ligate. This would place an additional burden on both time and reagents.

Due to this uncertainty and the desire to progress the project towards its goals, a gene fragment containing a His-tag sequence was designed, and then sent away to be synthesised by GenScript (Figure 9).

The addition of a His-tag to the C-terminus allowed for explicit detection of the recombinant protein, which was previously a major problem impacting the project. However, in the process, the His-tag has highlighted a significant issue with the Ssp DnaB mini-intein, which is a feature of the recombinant protein design used to facilitate recovery of the non-alginate binding portion of the protein. Specifically, the pH-sensitive intein was cleaving with complete efficiency even in alkaline conditions. While low-level spontaneous cleavage of intein has been reported, this would not account for 100% cleavage of the recombinant protein seen (Volkmann *et al.*, 2009).

The structures of the recombinant protein components were assessed, and a possible explanation for intein cleavage at raised pH is given. The alginate-binding domain of the acetyltransferase AlgX is folded such that the C-terminal is located very close to the N-

terminus of the domain (Figure 29) (Riley *et al.*, 2013). The proximity of the C-terminal His-tag to the intein could allow for interaction with residues involved in cleavage. Such interaction may alter the pKa values of these residues enough that cleavage can be induced even at increased pH (e.g. pH 8-9).

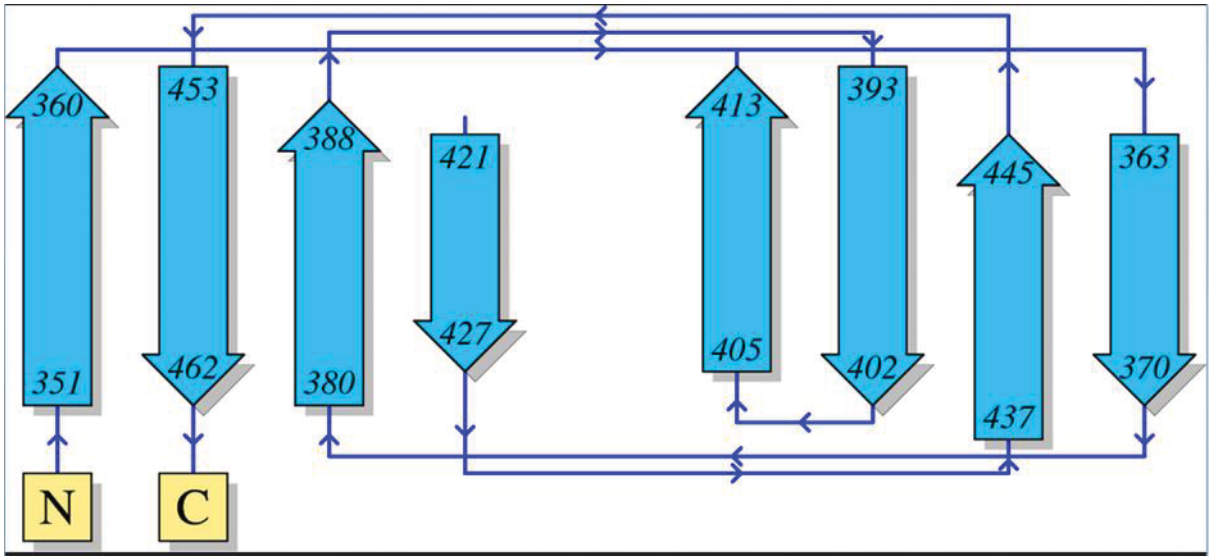

Figure 29. Structure of the C-terminal alginate-binding domain of AlgX. Topology representation of the C-terminal alginate-binding domain of *Pseudomonas aeruginosa* AlgX. N and C represent the N- and C- termini of the protein. Adapted from Riley *et al.* (2013).

If the His-tagged ABDx C-terminal domain is present in the extracellular protein fraction, then it must be exported as the full-length recombinant protein, given that the signal sequence is on the N-terminal of the AmyS domain. A logical argument against increased pH-sensitivity inducing cleavage is that physiological pH is 7.4. Thus the recombinant protein should cleave upon interaction with the cytosol. However, this is not the case because the signal sequence, YocH, mediates protein secretion through the type II secretion system. In type II secretion, folding does not occur until the protein is translocated into the extracellular space, and hence there can be no interaction between the His-tagged C-terminal and the intein until this stage.

Intein linkers, especially mini-inteins such as the one used in the recombinant protein (Ssp DnaB intein), are susceptible to mutation, which could also explain the altered pH-activity (Anraku and Satow, 2009). However, DNA sequencing of *amySdnaBABDxhis* isolated from *B.*

megaterium YYBm1 by colony PCR indicated high fidelity between the expected sequence and *dnaB*, which makes mutation of *dnaB* as the cause of altered activity unlikely.

Another possibility is that the Ssp DnaB intein is sensitive to more than one inducer. Cleavage in some inteins is achieved through the presence of a strong nucleophile, specifically dithiothreitol (DTT). DTT is used as a reducing agent in SDS-loading buffer during sample preparation for SDS-PAGE. Hence, if the Ssp DnaB intein is DTT-sensitive there is the potential that the problems being encountered with total intein cleavage could be a result of this sample preparation step. To investigate DTT as a factor, SDS-loading buffer was formulated without a reducing agent and used for sample preparation prior to SDS-PAGE.

There was no definitive result from this experiment. The presence of the C-terminus disulfide bridge in the ABDx domain may have caused aggregation of protein in the absence of a reducing agent, preventing mobilisation through a polyacrylamide gel (Figure 23). The presence of a lower band corresponding to the molecular weight (MW) of the cleaved domain, and yet no band around the expected MW of the full-length recombinant protein, would indicate that the aggregate is composed of only the cleaved domain. Therefore, a tentative conclusion can be made that the Ssp DnaB intein linker is not DTT-sensitive.

Various attempts were made to overcome total intein cleavage, which included varying the growth medium used, varying the pH buffer, and increasing pH to 9 and 10.

An alternative growth medium, trace metal mix A5 medium, was explored after it was recommended anecdotally as a superior medium for protein production compared to Luria-Bertani (LB). Previous attempts with A5 had shown that this medium is difficult to formulate, as the presence of divalent metal ions and phosphate cause insoluble metal phosphate precipitates to form, even when carefully mixed. This problem was overcome by combining the protocol for A5 medium with another medium that utilises metal salts, ZY5052. ZY5052 is also an auto-induction medium for lac promoters and was customised for a *xylA* promoter by exchanging D-xylose for α-lactose.

The custom A5 medium did show significant improvement for the growth rate of *B. megaterium*, with more than a 2-fold decrease in incubation time compared with LB. However, the A5 medium lacked any buffering capacity above pH 6.75, and thus was

unsuitable for production of the recombinant protein given the problems with intein cleavage.

Terrific Broth (Cold Spring Harbor) was recommended as an improved growth medium for protein production. An initial 100 ml culture demonstrated that Terrific Broth had an equal or better growth rate compared with the custom A5 medium (which in turn had a greater than 2-fold increase in growth rate compared with LB medium), while also possessing reasonable buffering capacity. Whereas A5 medium could not be buffered to any pH above 6.75, Terrific Broth could be buffered to n-1 pH, where n is the pH value of the buffer. For example, when a 100 ml culture was buffered with 1 M Tris-HCl pH 8.4, the resulting pH in the growth medium was 7.4.

B. megaterium can grow in a pH range of 3 to 11, which allowed for the use of two alternative buffers to raise pH to 9 or 10 in the Terrific Broth medium. 0.2 M borate buffer pH 9 and glycine sodium hydroxide buffer pH 10 were used, with pH in the growth media recorded over growth time. As previously noted, Terrific Broth has a buffering capacity of n-1, and hence the starting pH values of the borate and glycine buffered media were 7.98 and 9.0, respectively. The glycine buffered Terrific Broth culture failed to grow, whereas Terrific Broth borate yielded cleaved recombinant protein only. When repeated with LB media, pH of 9 and 10 were reached using borate and glycine buffer, respectively. However, there was no significant growth in either medium, which indicates the bacteria perform poorly in this pH range. This was possibly caused by the cells from the unbuffered overnight culture having entered the post-logarithmic phase of growth, and thus were too old to efficiently adapt to the raised pH. The growth time of the overnight culture could be better optimised to increase the probability of growth in alkaline media, and thus allow for the study of intein activity at pH range 9 – 10. However, the problem remains that while these variations may potentially solve some of the intein cleavage, the conditions necessary to achieve this pose a significant issue to down-stream production, collection, storage, and application. Ideally, the full-length recombinant protein should be produced, collected, stored, and applied under physiological conditions, i.e. pH 7.4.

To this end, Ssp DnaB mini-intein was removed from the recombinant protein. This was accomplished through PCR production of the two gene fragments around the intein sequence. Appropriate primers were used to create an in-frame restriction site on the 3’ end

of the amyS sequence and 5' end of the ABDx sequence, which was then digested and ligated into the p1623 expression vector (Figure 10).

4.4 Intein removal

The gene encoding Ssp DnaB mini-intein was successfully excised from the existing hybrid gene, leading to the generation of *amySABDxhis*. Restriction fragment analysis of plasmid isolated from transformed TOP10 *E. coli* indicated the presence of *amySABDxhis* (*sans dnaB*) as well as the functionality of the introduced *BamHI* restriction site, which was not previously present in the expression vector (Figure 26). DNA sequencing of *amySABDxhis* confirmed that there were no frame shifts or mutations, and that the *dnaB* sequence was no longer present in the hybrid gene, confirming successful excision of the intein encoding sequence.

However, transformed *B. megaterium* YYBm1 p1623*amySABDxhis* was unable to produce functional recombinant protein. Protein analysis by SDS-PAGE and anti-His-tag immunoblot was unable to detect AmyS:ABDx:His either intra- or extracellularly, and a starch degradation screen did not detect amylase activity in the extracellular protein of YYBm1 p1623*amySABDxhis* (Figure 28). Colony PCR confirmed the presence of *amySABDxhis* within transformed YYBm1, and DNA sequencing of the PCR product showed no frame shifts or mutations in the sequence of *amySABDxhis* that could explain why YYBm1 p1623*amySABDxhis* failed to produce the recombinant protein (Figure 27).

Further analysis of the recombinant protein sequence in collaboration with Prof. Geoffrey B. Jameson revealed a much greater problem with the protein. The structure of the C-terminal region of AlgX from *A. vinelandii* almost certainly involves the formation of a disulfide bond between the conserved C-terminal alginate-binding domain residue Cys466 and the conserved N-terminal acetyltransferase domain residue Cys348 by analogy to the disulfide bond observed for the equivalent residues Cys346 and Cys460 in *P. aeruginosa* (Figure 4) (Riley *et al.*, 2013). However, Cys348 was not included in the recombinant protein design, as it was thought to lie outside the C-terminal alginate-binding domain (ABDx) of interest. Riley *et al.* (2013) considered that the disulfide bond linked the catalytic domain of *P. aeruginosa* AlgX to the carbohydrate binding domain. Thus in the design of the recombinant fusion protein, it was thought that the alginate binding domain did not require this disulfide link.

However, the results clearly indicate that this disulfide link is critical to the stability of folding of the alginate binding domain of the fusion protein. This left only two cysteine residues present in the final recombinant AmyS:DnaB:ABDx fusion protein: (1) the alginate-binding domain cysteine, Cys781; and (2) Cys564 located within the intein (Appendix I). Because of the additional 99 amino acid residues between the cysteines of the recombinant protein compared with AlgX, of which many vary from the original AlgX sequence, it cannot be expected that a disulfide bond would link Cys564 and Cys781. And if one did, the alginate-binding domain structure may not be folded correctly, and would be unlikely to function.

Disulfide bond formation is assumed to occur in the recombinant protein due to the aggregation of the protein during the DTT-sensitivity test (Figure 23). However, the disulfide bond that led to this aggregation is more likely to be the result of protein denaturation during preparation for SDS-PAGE when the protein sample is heated to 95˚C (Section 2.10.1.1). The denatured protein would be free to form new linkages that could link the cysteine residues at this stage.

Furthermore, this oversight may have caused the unsuccessful production of intein-free recombinant protein. With the removal of intein, Cys564 is also eliminated, and hence the ABDx residue Cys781 (Cys627 in AmyS:ABDx:His) has no other cysteine to link to. Without a disulfide bond, the ABDx domain would be incapable of folding correctly, and without aberrant intein activity the α-amylase domain would not be cleaved off. The improperly folded ABDx domain could then disrupt the structure of the AmyS domain, leading to the improper folding of the entire protein. Proteins that do not fold correctly typically undergo rapid breakdown in the cytosol for recycling of peptides. This would explain why His-tag was not detected in the immunoblot (Figure 28), as the polyhistidine motif was hydrolysed in addition to the misfolded protein.

However, given the high efficiency of the xylose promoter, low-level detection of His-tag would still be expected intracellularly as the recombinant protein would be produced so long as the inducer is still present, even if the protein is non-functional. It is possible that during molecular cloning, the p1623 vector was damaged, which caused significant inhibition of *amySABDxhis* expression. In particular, if *xylA* was damaged and sensitivity to xylose was lost, recombinant protein production would be drastically reduced. The occurrence of one of these factors, or a combination of both, would result in the failure to produce a functional

recombinant protein. It is recommended that the p3stop1623hp vector should be sequenced to examine sequence fidelity and integrity, and the *amySABDxhis* insert should be transferred to fresh p1623 plasmid, or a different vector entirely. Saliently, the gene for the recombinant protein should be redesigned to include the critical cysteine residue corresponding to *P. aeruginosa* AlgX Cys346, or to eliminate the naked cysteine (Cys781) of the recombinant protein alginate binding domain by, for example, converting the cysteine residue to a serine.

4.5 Partial functionality of AmyS:DnaB:ABDx:His

Despite the problems posed by altered intein activity, it was instructive to assess the functionality of the different domains of AmyS:DnaB:ABDx:His. The functionality of either AmyS or ABDx, or both, gives a strong indication of the viability of the recombinant protein. If both domains were shown to be functional in cleaved form it would reflect positively on the functionality of a full-length recombinant protein *sans* intein.

Alpha amylase activity had been detected consistently in the extracellular protein of YYBm1 p1623*amySdnaBABDx*. In fact, the reliability of the starch degradation screen became such that entire strategies of recombinant protein detection and isolation were based around it. Starch degradation screens demonstrated that AmyS:DnaB:ABDx:His was α-amylase active, and therefore AmyS was functional. Additionally, α-amylase activity was known to be associated with the recombinant protein, and not with endogenous amylases of *B. megaterium,* as all *B. megaterium* strains transformed with an empty vector that did not contain the *amySdnaBABDx* gene tested negative for α-amylase activity. However, a quantitative assay was needed to fully assess the level of α-amylase activity shown by the AmyS domain.

The results of the maltose assay for α-amylase activity showed that the AmyS domain of the recombinant protein had activity of 1.4 u/mg of extracellular protein (Table 6). For comparison, the enzymatic activity of the α-amylase positive control was quantified as 10.2 u/mg of protein. The level of α-amylase activity of the AmyS domain is significant given that the recombinant protein has not been purified and was in a protein mixture. In this way, although 1 mg of total extracellular protein was used for the assay, significantly less than 1 mg of recombinant protein was present in the sample. The contribution to α-amylase activity

by endogenous amylases or other starch-degrading enzymes present in the extracellular protein of *B. megaterium* YYBm1 are minor, given that the extracellular protein of a YYBm1 transformant lacking *amySdnaBABDxhis* (p1623empty) demonstrated activity of 0.4 u/mg of extracellular protein. Therefore, the majority of activity seen in YYBm1 p1623*amySdnaBABDxhis* can be attributed to the presence of the hybrid gene.

Attempts to purify the recombinant protein using alginate beads were unsuccessful, indicating that the ABDx domain may not be functional. The results of the first alginate purification attempt of YYBm1 p1623*amySdnaBABDx* extracellular protein was initially promising (Figure 15). However, analysis of the protein detected after alginate purification showed it was not a match for the recombinant protein, and instead was identical with peptidase S8, an extracellular protease of *B. megaterium* (Appendix III). It is unclear why peptidase S8 was retained with the alginate beads, although it is possible that since the protease was overproduced, the concentration of peptidase S8 could have been sufficient to remain in the alginate solution even after multiple wash steps. Further alginate purification experiments with YYBm1 p1623*amySdnaBABDxhis* extracellular protein were also unsuccessful. An anti-His-tag immunoblot did not detect the His-tagged recombinant protein in the sample that had been purified by alginate beads, indicating the ABDx domain is non-functional. This is very likely to be due to the alginate-binding domain of the recombinant protein lacking a critical cysteine residue from AlgX, which prevents the formation of a disulfide bond (Riley *et al.*, 2013). The link between the two cysteines is almost certainly an essential structural element of AlgX, and hence the ABDx domain may be rendered non-functional without it.

4.6 Conclusion

In this study, a potential alginate-binding recombinant protein was produced from *B. megaterium* strains. Functionality of the α-amylase target protein domain was confirmed by multiple starch degradation screens and a quantitative maltose assay, which demonstrated a significant level of activity. However, identification of the full-length recombinant protein was substantially impaired by the presence of an overproduced extracellular protease, peptidase S8, which has a highly similar molecular weight compared to the recombinant protein, and

hence may have caused significant masking in traditional SDS-PAGE protein analysis. This difficulty detecting and isolating the recombinant protein, necessitated the addition of a detectable marker that could be used to efficiently identify the protein in a complex mixture. However, the detectable marker chosen, a block of six histidine residues (6xHis-tag), appears to strongly interact with the Ssp DnaB mini-intein, which is located between the N-terminal α-amylase domain (AmyS) and the C-terminal alginate-binding domain of AlgX (ABDx), due to the proximity of the C- and N-termini of ABDx. The intein was originally a part of the recombinant protein design as a mechanism of target protein recovery following display on alginate. However, interaction between the 6xHis-tag and intein causes aberrant intein activity. Specifically, the pH-sensitive intein is induced to cleave with complete efficiency at pH outside of the range at which Ssp DnaB is normally active (>pH 6-7). Total intein cleavage has prevented recovery of the full-length recombinant protein, and has therefore obstructed one of the aims of this study. PCR amplification was able to excise the intein-encoding gene, and the resulting hybrid gene *sans* intein was successfully transformed into *B. megaterium* YYBm1. However, the transformed *B. megaterium* YYBm1 was unable to produce the recombinant protein. Since a functional full-length recombinant protein has yet to be recovered, the alginate-binding function of the protein cannot be properly assessed. Preliminary alginate protein purifications have been unsuccessful so far, and a potentially critical cysteine residue, not included in the current protein design, has been identified as essential for the structure of the alginate-binding domain. However, it cannot be concluded that the alginate-binding domain is non-functional, and many potential solutions and avenues of study remain to be explored. That the α-amylase domain is not only functional, but also has a significant level of activity is cause for a positive outlook for the functionality of both domains in whole recombinant protein form.

4.7 Future directions

The failure to produce functional recombinant protein without intein leaves many questions unanswered. Can the full length recombinant protein be produced? Is it functional? What is the effect of not having intein as part of the recombinant protein? What caused intein hyperactivity? To answer these questions and accomplish the original aims of this study, several strategies are put forth in this section.

The first question that can be tackled is understanding why recombinant protein production was unsuccessful for YYBm1 p1623*amySABDxhis*. DNA sequencing of *amySABDxhis* indicated that there were no frame shifts or mutations to the sequence. However, analysis of the protein sequence revealed that the alginate-binding domain (ABDx) is missing a critical cysteine residue from AlgX, which is necessary to form a structurally significant disulfide bond (Riley *et al.*, 2013). In the case of AmyS:ABDx:His, the lack of a cysteine is likely causing the entire recombinant protein to be misfolded, preventing recovery of functional protein. The absence of the N-terminal AlgX cysteine is a grievous oversight that impacted on all the recombinant proteins produced during this study. Hence, before any other direction is taken, the recombinant protein needs to be redesigned or a gene fragment inserted to include the Cys348 residue of AlgX from *Azotobacter vinelandii* in the fusion protein alginate-binding domain.

Intein hyperactivity is suggested to be a result of the interaction between the polyhistidine tag and DnaB residues involved in intein cleavage. A study investigating this interaction is of high impact given the importance of both His-tags and mini-inteins in molecular biology and as tools of recombinant protein production. The hypothesis could be tested by using an alternative detectable marker for the recombinant protein, such as Strep- or FLAG-tag. Larger protein tags such as glutathione S-transferase (GST) or green fluorescent protein (GFP) should be avoided due to molecular weight constraints of the final recombinant protein, the effect these proteins will have on secretion, and the difficulty these tags present for comparison with the relatively small His-tag. A Strep-tag is optimal due to its small molecular weight and because streptavidin is biochemically almost inert. This makes it unlikely that the Strep-tag will interfere with protein folding, secretion or activity. A cloning strategy similar to the one used for His-tagging *amySdnaBABDx* can be used, in which a *BsrGI-KpnI* gene fragment that includes the Strep-tag is synthesised and inserted. As with the His-tag, the Strep-tag would be fused to the C-terminus of the recombinant protein.

Following protein analysis of both the His- and Strep-tagged recombinant proteins, the DnaB:ABDx:His region could be purified and concentrated for structural analysis by protein crystallography. By analysing the structure, the mechanism of interaction, if one exists, can be elucidated.

A problem, however, with the above strategy is that neither tagged recombinant proteins can be overproduced, given the presence of a pH-sensitive intein. Ssp DnaB intein undergoes complete cleavage at pH 6, under normal conditions. In this study, this problem was encountered when prolonged growth of *B. megaterium* caused the pH in the supernatant to fall below 6, even with sufficient buffering of the growth medium. Hence, as long as the recombinant protein is produced as an extracellular protein, the supernatant must be harvested before pH 6 is reached. This invariably means collecting protein during the middle of the logarithmic growth phase (OD_{600nm} 1-2), which in turn negatively impacts the protein yield. To overcome this problem, the signal sequence can be removed so that the recombinant protein is altered to be intracellular. However, the same strategy used for removing the *dnaB* sequence is not viable in this case. The amplified 5' fragment upstream of the signal sequence would be too small to be purified by gel electrophoresis (AGE). Instead a *PacI-BstBI* gene fragment that lacks the signal sequence could be synthesised and inserted into a PacI/BstBI-cut expression vector. Intracellular production has the advantage that physiological pH is constant (pH 7.4), and above the range for inducing intein cleavage. Additionally, intracellular production in *B. megaterium* YYBm1 prevents masking of the full-length recombinant protein by the extracellular protease, peptidase S8, which has previously been a significant issue. However, a notable drawback to intracellular production in *B. megaterium* is that cell compartments are typically reducing environments that inhibit the formation of disulfide bonds. Disulfide bond formation is essential for the structure and functionality of the alginate-binding domain.

Therefore, an alternative protein production system should be considered. The *Bacillus megaterium* production system has several advantages compared to the more commonly used *Escherichia coli*, which include naturally high secretion capacity, lack of endotoxin production, and precedent as an excellent producer of exoenzymes. However, the recombinant protein as it is currently designed is a poor fit for this system. As previously discussed, the presence of a pH-sensitive intein in an extracellular recombinant protein is a significant flaw. Protein yield is sacrificed either to underproduction because the supernatant was harvested prior to pH 6 being reached in the growth medium, or to intein cleavage because the supernatant was harvested after extended growth. Additionally, the molecular weight of the recombinant protein (87.2 kDa) is too close to the molecular weight of an

overproduced extracellular protease (85.6 kDa), which causes masking during SDS-PAGE analysis. Expression of peptidase S8 can be strongly inhibited either by a protease inhibitor or the presence of glucose in the growth medium. However, commercially available protease inhibitor is cost-prohibitive, and glucose strongly inhibits *XylA*, preventing xylose induction and recombinant protein production.

A suitable protein production system would be the Origami strain of *E. coli* (Novagen). Origami has mutations in both the thioredoxin mutase (*trxB*) and glutathione reductase (*gor*) genes, which greatly enhances disulfide bond formation in the cytoplasm. This is essential to the recombinant protein, as the cysteine residues of ABDx form a disulfide bond that is necessary for proper protein folding and alginate-binding activity. pETDuet-1 (Novagen) is a suitable plasmid for constructing the expression vector, and contains two multiple cloning sites, a T7 promotor, *lac* operon, and ampicillin resistance gene. The two cloning sites are advantageous as they allow for the expression of two hybrid genes. In this way, the same Origami transformant could be used to study the effect of two separate detectable markers on the recombinant protein, or the transformant could express hybrid genes that either possess or lack *dnaB*. Additionally, both His- and Strep-tags are appropriate for pETDuet-1. However, the hybrid gene will need to be optimised for expression in Origami, which includes the removal of the signal sequence as part of the recombinant protein design and codon optimisation of the Shine-Dalgarno sequence for *E. coli* expression. Additionally, Origami *E. coli* produces an endotoxin, LPS, which can represent a difficulty for licensing requirements in biotechnological and pharmaceutical applications. The problem associated with endotoxin production could be solved by generating a deletion mutant of Origami that does not produce LPS.

APPENDIX I
EXPRESSION VECTOR MAPS

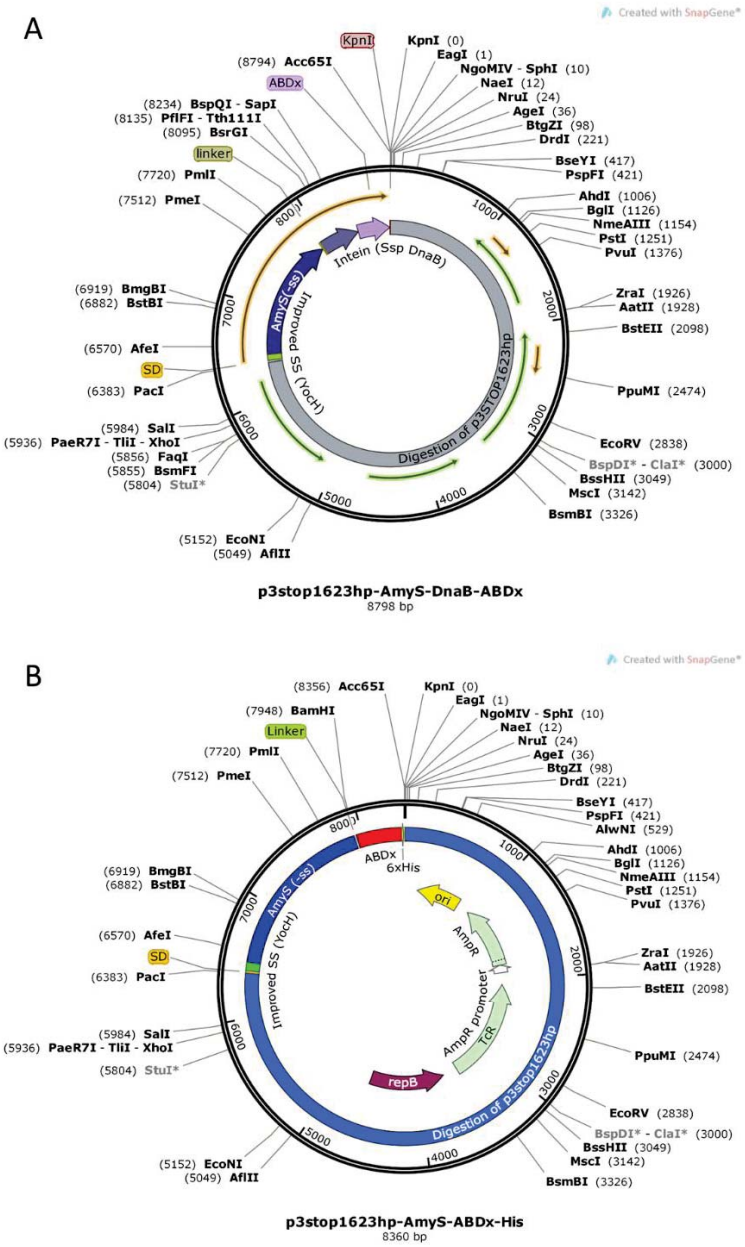

Figure 30. Sequence maps of expression vectors used in this study. *A*. Expression vector map of p1623*amySdnaBABDx* with features, including unique restriction sites. Size constraints means some features could not be displayed. *B.* Expression vector map of p1623*amySABDxhis* with features, including unique restriction sites, origin of replication (ori), β-lactamase gene *bla* promoter (AmpR promoter), β-lactamase gene *bla* (AmpR), tetracycline efflux protein gene *tetL* (TcR), and a RepB replication protein gene *repB* (repB).

DNA sequence of *amySdnaBABDx*, including translated sequence.

```
   1 TAACCAAGGAGGAGGTAGGAAAATGAAAAAGACAATGATTACGTTTAGCTTAGTTCTTAT 60
   1                       M  K  K  T  M  I  T  F  S  L  V  L  M  13
  61 GAGTTTATTTGGAGTGGCTTCTGGAGCAAGTGCAATGGCAGCAAATCTTAATGGAACACT 120
  14  S  L  F  G  V  A  S  G  A  S  A  M  A  A  N  L  N  G  T  L  33
 121 TATGCAATATTTTGAATGGTATATGCCTAACGATGGTCAACATTGGAAACGTCTTCAAAA 180
  34  M  Q  Y  F  E  W  Y  M  P  N  D  G  Q  H  W  K  R  L  Q  N  53
 181 CGATAGCGCTTATTTAGCAGAACATGGAATTACAGCTGTTTGGATTCCTCCAGCATATAA 240
  54  D  S  A  Y  L  A  E  H  G  I  T  A  V  W  I  P  P  A  Y  K  73
 241 GGGTACGAGTCAAGCTGATGTGGGATATGGTGCTTATGATCTTTATGATCTTGGAGAATT 300
  74  G  T  S  Q  A  D  V  G  Y  G  A  Y  D  L  Y  D  L  G  E  F  93
 301 TCATCAAAAAGGTACAGTACGAACGAAATATGGAACAAAAGGTGAACTTCAATCAGCTAT 360
  94  H  Q  K  G  T  V  R  T  K  Y  G  T  K  G  E  L  Q  S  A  I  113
 361 TAAATCTTTACATTCTCGTGATATTAACGTATATGGAGATGTAGTTATTAACCATAAAGG 420
 114  K  S  L  H  S  R  D  I  N  V  Y  G  D  V  V  I  N  H  K  G  133
 421 AGGTGCTGATGCAACAGAAGATGTTACGGCTGTGGAAGTAGATCCTGCTGATCGAAATCG 480
 134  G  A  D  A  T  E  D  V  T  A  V  E  V  D  P  A  D  R  N  R  153
 481 TGTAATTTCTGGAGAAGTTCGAATTAAAGCATGGACACATTTTCATTTTCCAGGACGTGG 540
 154  V  I  S  G  E  V  R  I  K  A  W  T  H  F  H  F  P  G  R  G  173
 541 TTCAACGTATAGTGATTTTAAATGGCATTGGTATCATTTTGATGGAACAGATTGGGATGA 600
 174  S  T  Y  S  D  F  K  W  H  W  Y  H  F  D  G  T  D  W  D  E  193
 601 AAGCCGAAAACTTAACCGTATTTATAAATTTCAAGGAAAAGCATGGGATTGGGAAGTTTC 660
 194  S  R  K  L  N  R  I  Y  K  F  Q  G  K  A  W  D  W  E  V  S  213
 661 TAACGAATTTGGTAACTATGATTATCTTATGTATGCAGATATTGATTATGATCATCCTGA 720
 214  N  E  F  G  N  Y  D  Y  L  M  Y  A  D  I  D  Y  D  H  P  D  233
 721 TGTGGTAGCTGAAATTAAAAGATGGGGAACATGGTATGCAAACGAATTACAACTTGATGG 780
 234  V  V  A  E  I  K  R  W  G  T  W  Y  A  N  E  L  Q  L  D  G  253
 781 TTTTCGACTTGATGCTGTAAAACATATTAAATTTTCATTTTTAAGAGATTGGGTTAACCA 840
 254  F  R  L  D  A  V  K  H  I  K  F  S  F  L  R  D  W  V  N  H  273
 841 TGTGCGAGAAAAAACAGGAAAAGAAATGTTTACGGTTGCTGAATATTGGTCTTATGATCT 900
 274  V  R  E  K  T  G  K  E  M  F  T  V  A  E  Y  W  S  Y  D  L  293
 901 TGGTGCACTTGAAAACTATCTTAACAAAACAAACTTTAACCATAGCGTATTTGATGTTCC 960
 294  G  A  L  E  N  Y  L  N  K  T  N  F  N  H  S  V  F  D  V  P  313
 961 ACTTCATTATCAATTTCATGCTGCATCTACACAAGGAGGTGGATATGATATGCGTAAACT 1020
 314  L  H  Y  Q  F  H  A  A  S  T  Q  G  G  G  Y  D  M  R  K  L  333
1021 TCTTAATTCAACGGTTGTGAGTAAACATCCTTTAAAAGCAGTGACATTTGTAGATAACCA 1080
 334  L  N  S  T  V  V  S  K  H  P  L  K  A  V  T  F  V  D  N  H  353
1081 TGATACGCAACCAGGACAATCTTTAGAATCTACAGTACAAACGTGGTTTAAACCTCTTGC 1140
 354  D  T  Q  P  G  Q  S  L  E  S  T  V  Q  T  W  F  K  P  L  A  373
1141 TTATGCATTTATTCTTACAAGAGAATCAGGTTATCCTCAAGTATTTTATGGTGATATGTA 1200
 374  Y  A  F  I  L  T  R  E  S  G  Y  P  Q  V  F  Y  G  D  M  Y  393
1201 TGGAACGAAAGGTGATAGTCAACGTGAAATTCCTGCTCTTAAACATAAAATTGAACCAAT 1260
 394  G  T  K  G  D  S  Q  R  E  I  P  A  L  K  H  K  I  E  P  I  413
1261 TCTTAAAGCAAGAAAACAATATGCTTATGGAGCACAACATGATTATTTTGATCATCATGA 1320
 414  L  K  A  R  K  Q  Y  A  Y  G  A  Q  H  D  Y  F  D  H  H  D  433
1321 TATTGTGGGATGGACACGTGAAGGAGATTCTTCAGTAGCTAATTCAGGATTAGCTGCACT 1380
 434  I  V  G  W  T  R  E  G  D  S  S  V  A  N  S  G  L  A  A  L  453
1381 TATTACGGATGGTCCTGGTGGAGCTAAAAGAATGTATGTAGGACGACAAAACGCAGGTGA 1440
 454  I  T  D  G  P  G  G  A  K  R  M  Y  V  G  R  Q  N  A  G  E  473
1441 AACATGGCATGATATTACGGGAAATAGATCAGAACCAGTAGTTATTAACAGTGAAGGATG 1500
 474  T  W  H  D  I  T  G  N  R  S  E  P  V  V  I  N  S  E  G  W  493
1501 GGGTGAATTTCATGTTAATGGTGGATCAGTTAGTATTTATGTGCAAAGAGGTGGAGGTGG 1560
 494  G  E  F  H  V  N  G  G  S  V  S  I  Y  V  Q  R  G  G  G  G  513
1561 AGGTGCTATTTCAGGAGATAGTTTAATTAGCCTTGCATCTACAGGTAAACGAGTATCTAT 1620
 514  G  A  I  S  G  D  S  L  I  S  L  A  S  T  G  K  R  V  S  I  533
1621 TAAAGATTTACTTGATGAAAAAGATTTTGAAATTTGGGCTATTAACGAACAAACAATGAA 1680
 534  K  D  L  L  D  E  K  D  F  E  I  W  A  I  N  E  Q  T  M  K  553
1681 ATTAGAAAGCGCAAAAGTTTCTCGTGTGTTTTGTACAGGTAAAAAATTAGTTTATATTCT 1740
 554  L  E  S  A  K  V  S  R  V  F  C  T  G  K  K  L  V  Y  I  L  573
```

```
1741 TAAAACGAGACTTGGTCGAACAATTAAAGCTACGGCAAACCATCGTTTTCTTACAATTGA 1800
 574  K  T  R  L  G  R  T  I  K  A  T  A  N  H  R  F  L  T  I  D  593
1801 TGGATGGAAAAGATTAGATGAATTATCACTTAAAGAACATATTGCTCTTCCTAGAAAATT 1860
 594  G  W  K  R  L  D  E  L  S  L  K  E  H  I  A  L  P  R  K  L  613
1861 AGAAAGTAGCTCTTTACAACTTAGTCCAGAAATTGAAAAACTTAGCCAATCTGATATTTA 1920
 614  E  S  S  S  L  Q  L  S  P  E  I  E  K  L  S  Q  S  D  I  Y  633
1921 TTGGGATTCAATTGTAAGTATTACAGAAACGGGAGTAGAAGAAGTTTTTGATTTAACAGT 1980
 634  W  D  S  I  V  S  I  T  E  T  G  V  E  E  V  F  D  L  T  V  653
1981 TCCTGGTCCACATAACTTTGTTGCAAACGATATTATTGTGCATAATAGCGGACGTAAAAC 2040
 654  P  G  P  H  N  F  V  A  N  D  I  I  V  H  N  S  G  R  K  T  673
2041 GGTGTTATCTCGTAAAGTAAAACTTCGTCAAGGTAGAAATGAAGTATTACTTAACTCAGC 2100
 674  V  L  S  R  K  V  K  L  R  Q  G  R  N  E  V  L  L  N  S  A  693
2101 TGCATTACCTATTCGTTCAGGAAGTTATGTGGCTGATGTAACATATAGCGATCCATCTGT 2160
 694  A  L  P  I  R  S  G  S  Y  V  A  D  V  T  Y  S  D  P  S  V  713
2161 TCATGAATTAAAAAACACGATTTGGTATATGAACGGACGTAGAGAACAACTTAAAATTGA 2220
 714  H  E  L  K  N  T  I  W  Y  M  N  G  R  R  E  Q  L  K  I  E  733
2221 ACAATCTAAAGCAGTAGATACAGGAGGTCGATATGTTTTTCAACTTCGTAACGATTCAGA 2280
 734  Q  S  K  A  V  D  T  G  G  R  Y  V  F  Q  L  R  N  D  S  D  753
2281 TTGGGCTGATCAACAATTTTTAAGTCTTGAAATTGAAGCACCTGAAGATATGCCACAAGG 2340
 754  W  A  D  Q  Q  F  L  S  L  E  I  E  A  P  E  D  M  P  Q  G  773
2341 ATTAGAAGTACAAGCAAGTATTTGTCAAGCAGCACCAGCAAAAGCAAGTCAATCTGTAGC 2400
 774  L  E  V  Q  A  S  I  C  Q  A  A  P  A  K  A  S  Q  S  V  A  793
2401 AGGACGATAAGGTAC 2415
 794  G  R  *                                                       795
```

DNA sequence of *amysABDxhis*, including translated sequence.

```
   1 TAACCAAGGAGGAGGTAGGAAAATGAAAAAGACAATGATTACGTTTAGCTTAGTTCTTAT 60
   1                       M  K  K  T  M  I  T  F  S  L  V  L  M  13
  61 GAGTTTATTTGGAGTGGCTTCTGGAGCAAGTGCAATGGCAGCAAATCTTAATGGAACACT 120
  14  S  L  F  G  V  A  S  G  A  S  A  M  A  A  N  L  N  G  T  L  33
 121 TATGCAATATTTTGAATGGTATATGCCTAACGATGGTCAACATTGGAAACGTCTTCAAAA 180
  34  M  Q  Y  F  E  W  Y  M  P  N  D  G  Q  H  W  K  R  L  Q  N  53
 181 CGATAGCGCTTATTTAGCAGAACATGGAATTACAGCTGTTTGGATTCCTCCAGCATATAA 240
  54  D  S  A  Y  L  A  E  H  G  I  T  A  V  W  I  P  P  A  Y  K  73
 241 GGGTACGAGTCAAGCTGATGTGGGATATGGTGCTTATGATCTTTATGATCTTGGAGAATT 300
  74  G  T  S  Q  A  D  V  G  Y  G  A  Y  D  L  Y  D  L  G  E  F  93
 301 TCATCAAAAAGGTACAGTACGAACGAAATATGGAACAAAAGGTGAACTTCAATCAGCTAT 360
  94  H  Q  K  G  T  V  R  T  K  Y  G  T  K  G  E  L  Q  S  A  I  113
 361 TAAATCTTTACATTCTCGTGATATTAACGTATATGGAGATGTAGTTATTAACCATAAAGG 420
 114  K  S  L  H  S  R  D  I  N  V  Y  G  D  V  V  I  N  H  K  G  133
 421 AGGTGCTGATGCAACAGAAGATGTTACGGCTGTGGAAGTAGATCCTGCTGATCGAAATCG 480
 134  G  A  D  A  T  E  D  V  T  A  V  E  V  D  P  A  D  R  N  R  153
 481 TGTAATTTCTGGAGAAGTTCGAATTAAAGCATGGACACATTTTCATTTTCCAGGACGTGG 540
 154  V  I  S  G  E  V  R  I  K  A  W  T  H  F  H  F  P  G  R  G  173
 541 TTCAACGTATAGTGATTTTAAATGGCATTGGTATCATTTTGATGGAACAGATTGGGATGA 600
 174  S  T  Y  S  D  F  K  W  H  W  Y  H  F  D  G  T  D  W  D  E  193
 601 AAGCCGAAAACTTAACCGTATTTATAAATTTCAAGGAAAAGCATGGGATTGGGAAGTTTC 660
 194  S  R  K  L  N  R  I  Y  K  F  Q  G  K  A  W  D  W  E  V  S  213
 661 TAACGAATTTGGTAACTATGATTATCTTATGTATGCAGATATTGATTATGATCATCCTGA 720
 214  N  E  F  G  N  Y  D  Y  L  M  Y  A  D  I  D  Y  D  H  P  D  233
 721 TGTGGTAGCTGAAATTAAAAGATGGGGAACATGGTATGCAAACGAATTACAACTTGATGG 780
 234  V  V  A  E  I  K  R  W  G  T  W  Y  A  N  E  L  Q  L  D  G  253
 781 TTTTCGACTTGATGCTGTAAAACATATTAAATTTTCATTTTTAAGAGATTGGGTTAACCA 840
 254  F  R  L  D  A  V  K  H  I  K  F  S  F  L  R  D  W  V  N  H  273
 841 TGTGCGAGAAAAAACAGGAAAAGAAATGTTTACGGTTGCTGAATATTGGTCTTATGATCT 900
 274  V  R  E  K  T  G  K  E  M  F  T  V  A  E  Y  W  S  Y  D  L  293
 901 TGGTGCACTTGAAAACTATCTTAACAAAACAAACTTTAACCATAGCGTATTTGATGTTCC 960
 294  G  A  L  E  N  Y  L  N  K  T  N  F  N  H  S  V  F  D  V  P  313
 961 ACTTCATTATCAATTTCATGCTGCATCTACACAAGGAGGTGGATATGATATGCGTAAACT 1020
 314  L  H  Y  Q  F  H  A  A  S  T  Q  G  G  G  Y  D  M  R  K  L  333
1021 TCTTAATTCAACGGTTGTGAGTAAACATCCTTTAAAAGCAGTGACATTTGTAGATAACCA 1080
 334  L  N  S  T  V  V  S  K  H  P  L  K  A  V  T  F  V  D  N  H  353
1081 TGATACGCAACCAGGACAATCTTTAGAATCTACAGTACAAACGTGGTTTAAACCTCTTGC 1140
 354  D  T  Q  P  G  Q  S  L  E  S  T  V  Q  T  W  F  K  P  L  A  373
1141 TTATGCATTTATTCTTACAAGAGAATCAGGTTATCCTCAAGTATTTTATGGTGATATGTA 1200
 374  Y  A  F  I  L  T  R  E  S  G  Y  P  Q  V  F  Y  G  D  M  Y  393
1201 TGGAACGAAAGGTGATAGTCAACGTGAAATTCCTGCTCTTAAACATAAAATTGAACCAAT 1260
 394  G  T  K  G  D  S  Q  R  E  I  P  A  L  K  H  K  I  E  P  I  413
1261 TCTTAAAGCAAGAAAACAATATGCTTATGGAGCACAACATGATTATTTTGATCATCATGA 1320
 414  L  K  A  R  K  Q  Y  A  Y  G  A  Q  H  D  Y  F  D  H  H  D  433
1321 TATTGTGGGATGGACACGTGAAGGAGATTCTTCAGTAGCTAATTCAGGATTAGCTGCACT 1380
 434  I  V  G  W  T  R  E  G  D  S  S  V  A  N  S  G  L  A  A  L  453
1381 TATTACGGATGGTCCTGGTGGAGCTAAAAGAATGTATGTAGGACGACAAAACGCAGGTGA 1440
 454  I  T  D  G  P  G  G  A  K  R  M  Y  V  G  R  Q  N  A  G  E  473
1441 AACATGGCATGATATTACGGGAAATAGATCAGAACCAGTAGTTATTAACAGTGAAGGATG 1500
 474  T  W  H  D  I  T  G  N  R  S  E  P  V  V  I  N  S  E  G  W  493
1501 GGGTGAATTTCATGTTAATGGTGGATCAGTTAGTATTTATGTGCAAAGAGGTGGAGGTGG 1560
 494  G  E  F  H  V  N  G  G  S  V  S  I  Y  V  Q  R  G  G  G  G  513
1561 AGGTAGCGGACGTAAAACGGTGTTATCTCGTAAAGTAAAACTTCGTCAAGGTAGAAATGA 1620
 514  G  S  G  R  K  T  V  L  S  R  K  V  K  L  R  Q  G  R  N  E  533
1621 AGTATTACTTAACTCAGCTGCATTACCTATTCGTTCAGGAAGTTATGTGGCTGATGTAAC 1680
 534  V  L  L  N  S  A  A  L  P  I  R  S  G  S  Y  V  A  D  V  T  553
```

```
1681 ATATAGCGATCCATCTGTTCATGAATTAAAAAACACGATTTGGTATATGAACGGACGTAG 1740
 554  Y  S  D  P  S  V  H  E  L  K  N  T  I  W  Y  M  N  G  R  R  573
1741 AGAACAACTTAAAATTGAACAATCTAAAGCAGTAGATACAGGAGGTCGATATGTTTTTCA 1800
 574  E  Q  L  K  I  E  Q  S  K  A  V  D  T  G  G  R  Y  V  F  Q  593
1801 ACTTCGTAACGATTCAGATTGGGCTGATCAACAATTTTTAAGTCTTGAAATTGAAGCACC 1860
 594  L  R  N  D  S  D  W  A  D  Q  Q  F  L  S  L  E  I  E  A  P  613
1861 TGAAGATATGCCACAAGGATTAGAAGTACAAGCAAGTATTTGTCAAGCAGCACCAGCAAA 1920
 614  E  D  M  P  Q  G  L  E  V  Q  A  S  I  C  Q  A  A  P  A  K  633
1921 AGCAAGTCAATCTGTAGCAGGACGACATCATCACCATCACCACTAAGGTAC 1971
 634  A  S  Q  S  V  A  G  R  H  H  H  H  H  H  *                 647
```

APPENDIX II
AMMONIUM SULFATE SATURATION TABLE

Table 7. Ammonium sulfate saturation table. Amount of solid ammonium sulfate in g needed to reach a given saturation percentage in 1 L of solution. Adapted from Dawson *et al.* (1986).

Initial concentration of ammonium sulfate (percentage saturation at 0 °C)	Percentage saturation at 0 °C																				
	Solid ammonium sulfate (g) to be added to 1 l of solution																				
	20	25	30	35	40	45	50	55	60	65	70	75	80	85	90	95	100
0	106	134	164	194	226	258	291	326	361	398	436	476	516	559	603	650	697
5	79	108	137	166	197	229	262	296	331	368	405	444	484	526	570	615	662
10	53	81	109	139	169	200	233	266	301	337	374	412	452	493	536	581	627
15	26	54	82	111	141	172	204	237	271	306	343	381	420	460	503	547	592
20	0	27	55	83	113	143	175	207	241	276	312	349	387	427	469	512	557
25		0	27	56	84	115	146	179	211	245	280	317	355	395	436	478	522
30			0	28	56	86	117	148	181	214	249	285	323	362	402	445	488
35				0	28	57	87	118	151	184	218	254	291	329	369	410	453
40					0	29	58	89	120	153	187	222	258	296	335	376	418
45						0	29	59	90	123	156	190	226	263	302	342	383
50							0	30	60	92	125	159	194	230	268	308	348
55								0	30	61	93	127	161	197	235	273	313
60									0	31	62	95	129	164	201	239	279
65										0	31	63	97	132	168	205	244
70											0	32	65	99	134	171	209
75												0	32	66	101	137	174
80													0	33	67	103	139
85														0	34	68	105
90															0	34	70
95																0	35
100																	0

APPENDIX III
MALDI-TOF PEPTIDE MASS ANALYSIS

MASCOT Search Results

Protein View: gi|502848054

peptidase S8 [Bacillus megaterium]

Database:	NCBInr
Score:	1680
Nominal mass (M_r):	85526
Calculated pI:	5.89
Taxonomy:	Bacillus megaterium

This protein sequence matches the following other entries:

- gi|295704293 from Bacillus megaterium DSM 319
- gi|294801952 from Bacillus megaterium DSM 319

Sequence similarity is available as an NCBI BLAST search of gi|502848054 against nr.

Search parameters

MS data file:	14156_B1.txt
Enzyme:	Trypsin: cuts C-term side of KR unless next residue is P.

Variable modifications: Oxidation (M), Carbamidomethyl (C), Deamidated (NQ)

Protein sequence coverage: 37%

Matched peptides shown in ***bold red***.

```
  1 MKKVSIRSVL STVAFSVALS SFAMGASANG NSKPALEPSL VKIQGDYNLK
 51 SAKKVKVIVE LNEESVAEAK KKGVAQSKGK IKKARDEVKK ELSKASKTSK
101 VKREYDQVFS GFSAELPAND LEKVASLPGV KAIYPSVEYH TTEVKSKEVS
151 AEEYGSEMDK SIYYVGADQA WKSGYTGKNM TVAVIDTGVD YDHPDLKSAF
201 EKYKGWDFVD DDKDPQETPA EDPKGEATTH GTHVAGTIAA DGKIKGVAPD
251 AHLLAYRVLG PGGTGTTEDV IAGIERAVED GADVMNLSLG DTINNPDLAT
301 SIALDWAMEE GVVAVTSNGN SGPANWTVGS PGTSREAISV GATQLPYNLY
351 KTTLTVDNAS YASAEVMGFP NEKALLDASG KKYEFVPVGL GKPEDFEGKD
401 VKGKVAVISR GDIAFVDKVD NAKKAGAVAT VIYNNVEGTI PDIPGTSLPS
451 IRLSKADGQA LAASLAKGSV TGSFTATFDQ TVDETMADFS SRGPVVDTWM
501 IKPDISAPGV DIISTVPTND PSNPHGYGSK QGTSMAAPHV AGAAALILQA
551 HPNYKVEDVK ASLMNTTELL RDRNGLVYPH NTQGAGSMRV VDAIKAKTLI
601 TPGSHSYGVF YKDKGKQVEK QSFKIKNLSN HSQKYSVKVK FKKSHQAIDV
651 KSTNDLVVNA GKTQKVNLNV KVDAGKLSPG YYEGTITVSN NKETYDVPTI
701 LFVKEPDYPR VTSAYVDVLG NGSFEYGSYL PGGAEKLSYY IYDATLEKGE
751 LLSSYTNVEK GFSSATWDGK INGEALPPGT YYLYAEAVKA GQTTGSLGEF
801 EIK
```

MASCOT Search Results

Protein View: gi|502848054

peptidase S8 [Bacillus megaterium]

Database:	NCBInr
Score:	991
Nominal mass (M_r):	85526
Calculated pI:	5.89
Taxonomy:	Bacillus megaterium

This protein sequence matches the following other entries:

- gi|295704293 from Bacillus megaterium DSM 319
- gi|294801952 from Bacillus megaterium DSM 319

Sequence similarity is available as an NCBI BLAST search of gi|502848054 against nr.

Search parameters

MS data file:	14156_B2.txt
Enzyme:	Trypsin: cuts C-term side of KR unless next residue is P.

Variable modifications: Oxidation (M), Carbamidomethyl (C), Deamidated (NQ)

Protein sequence coverage: 22%

Matched peptides shown in ***bold red***.

```
  1 MKKVSIRSVL STVAFSVALS SFAMGASANG NSKPALEPSL VKIQGDYNLK
 51 SAKKVKVIVE LNEESVAEAK KKGVAQSKGK IKKARDEVKK ELSKASKTSK
101 VKREYDQVFS GFSAELPAND LEKVASLPGV KAIYPSVEYH TTEVKSKEVS
151 AEEYGSEMDK SIYYVGADQA WKSGYTGKNM TVAVIDTGVD YDHPDLKSAF
201 EKYKGWDFVD DDKDPQETPA EDPKGEATTH GTHVAGTIAA DGKIKGVAPD
251 AHLLAYRVLG PGGTGTTEDV IAGIERAVED GADVMNLSLG DTINNPDLAT
301 SIALDWAMEE GVVAVTSNGN SGPANWTVGS PGTSREAISV GATQLPYNLY
351 KTTLTVDNAS YASAEVMGFP NEKALLDASG KKYEFVPVGL GKPEDFEGKD
401 VKGKVAVISR GDIAFVDKVD NAKKAGAVAT VIYNNVEGTI PDIPGTSLPS
451 IRLSKADGQA LAASLAKGSV TGSFTATFDQ TVDETMADFS SRGPVVDTWM
501 IKPDISAPGV DIISTVPTND PSNPHGYGSK QGTSMAAPHV AGAAALILQA
551 HPNYKVEDVK ASLMNTTELL RDRNGLVYPH NTQGAGSMRV VDAIKAKTLI
601 TPGSHSYGVF YKDKGKQVEK QSFKIKNLSN HSQKYSVKVK FKKSHQAIDV
651 KSTNDLVVNA GKTQKVNLNV KVDAGKLSPG YYEGTITVSN NKETYDVPTI
701 LFVKEPDYPR VTSAYVDVLG NGSFEYGSYL PGGAEKLSYY IYDATLEKGE
751 LLSSYTNVEK GFSSATWDGK INGEALPPGT YYLYAEAVKA GQTTGSLGEF
801 EIK
```

APPENDIX IV
SIZE EXCLUSION CHROMATOGRAPHY

A

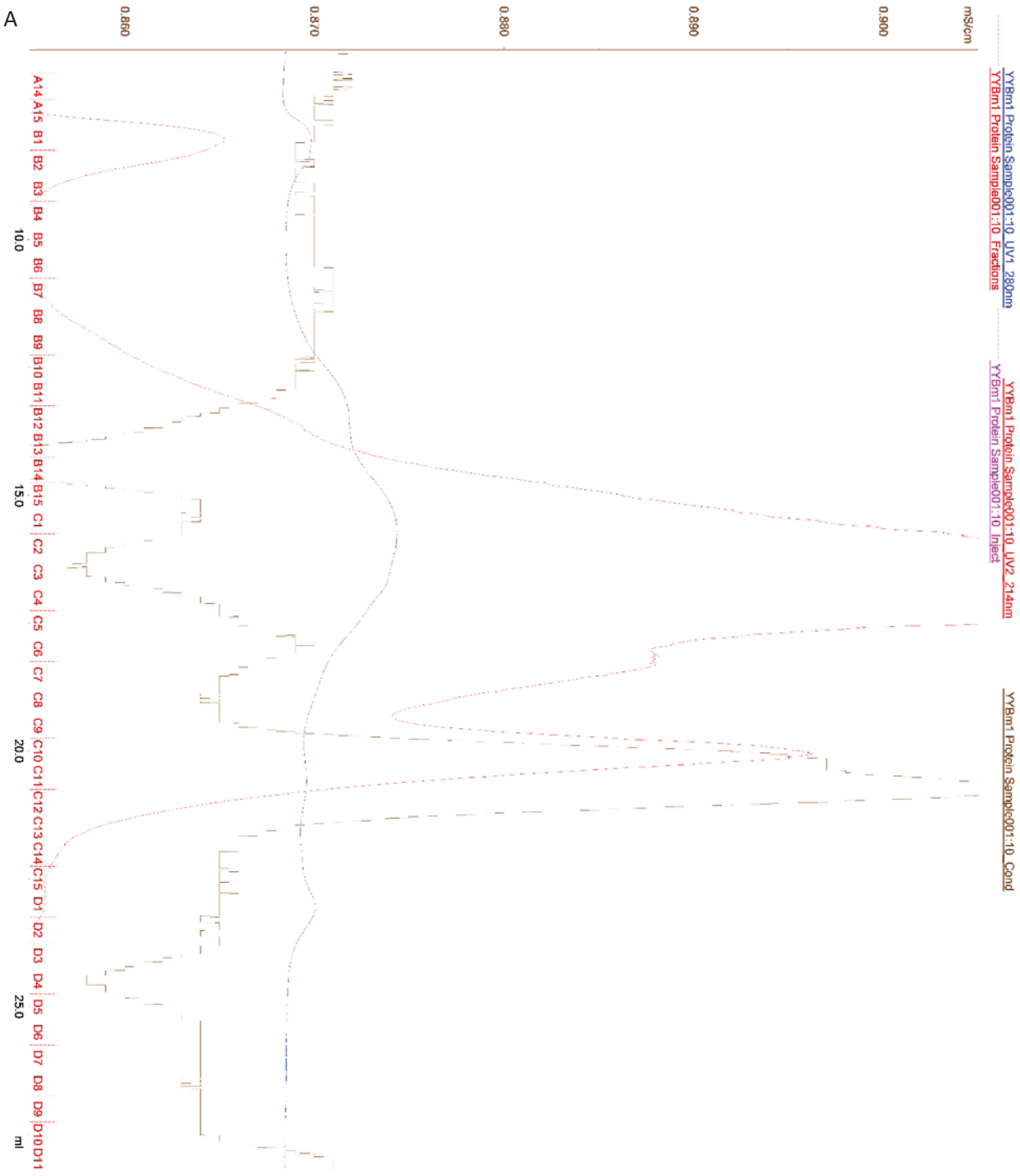

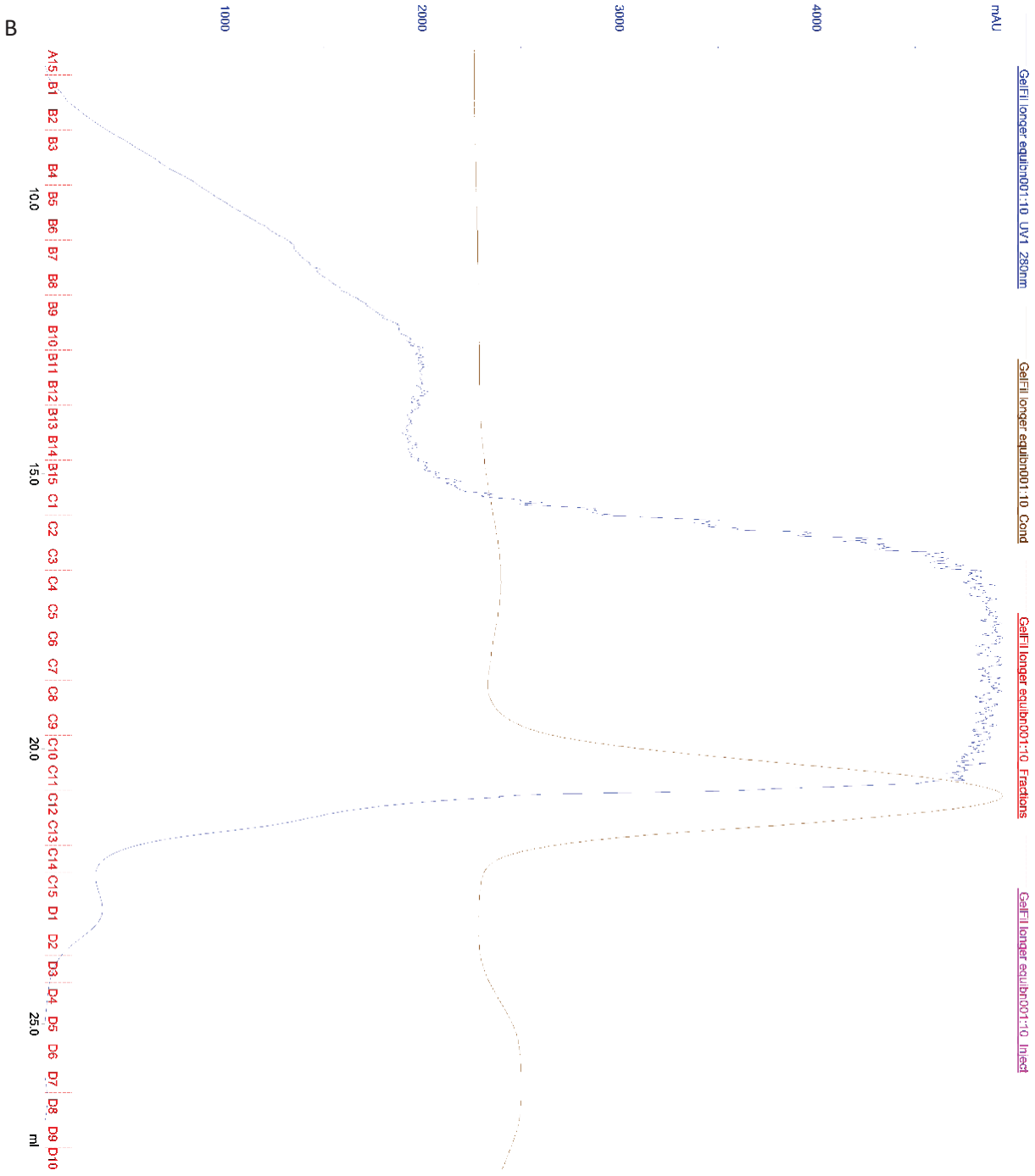

Figure 31. Protein fractionation by gel filtration chromatography. Chromatogram of protein fractions from *B. megaterium* YYBm1 transformed with p1623*amySdnaBABDx* generated by size exclusion chromatography.

References

Albrecht, M. T. & Schiller, N. L. 2005. Alginate lyase (AlgL) activity is required for alginate biosynthesis in Pseudomonas aeruginosa. *J Bacteriol,* 187**,** 3869-72. Available: DOI 10.1128/JB.187.11.3869-3872.2005.

Anraku, Y., Mizutani, R. & Satow, Y. 2005. Protein splicing: its discovery and structural insight into novel chemical mechanisms. *IUBMB Life,* 57**,** 563-74. Available: DOI 10.1080/15216540500215499.

Anraku, Y. & Satow, Y. 2009. Reflections on protein splicing: structures, functions and mechanisms. *Proc Jpn Acad Ser B Phys Biol Sci,* 85**,** 409-21.

Baker, P., Ricer, T., Moynihan, P. J., Kitova, E. N., Walvoort, M. T., Little, D. J., Whitney, J. C., Dawson, K., Weadge, J. T., Robinson, H., Ohman, D. E., Codee, J. D., Klassen, J. S., Clarke, A. J. & Howell, P. L. 2014. P. aeruginosa SGNH hydrolase-like proteins AlgJ and AlgX have similar topology but separate and distinct roles in alginate acetylation. *PLoS Pathog,* 10**,** e1004334. Available: DOI 10.1371/journal.ppat.1004334.

Bornhorst, J. A. & Falke, J. J. 2000. Purification of proteins using polyhistidine affinity tags. *Methods Enzymol,* 326**,** 245-54.

Boyd, A. & Chakrabarty, A. M. 1995. Pseudomonas aeruginosa biofilms: role of the alginate exopolysaccharide. *J Ind Microbiol,* 15**,** 162-8.

Bunk, B., Schulz, A., Stammen, S., Munch, R., Warren, M. J., Rohde, M., Jahn, D. & Biedendieck, R. 2010. A short story about a big magic bug. *Bioeng Bugs,* 1**,** 85-91. Available: DOI 10.4161/bbug.1.2.11101.

Castro, G. R., Chen, J., Panilaitis, B. & Kaplan, D. L. 2009. Emulsan-alginate beads for protein adsorption. *J Biomater Sci Polym Ed,* 20**,** 411-26. Available: DOI 10.1163/156856209X416449.

Castro, G. R., Kamdar, R. R., Panilaitis, B. & Kaplan, D. L. 2005. Triggered release of proteins from emulsan-alginate beads. *J Control Release,* 109**,** 149-57. Available: DOI 10.1016/j.jconrel.2005.09.042.

Chen, S., Parlane, N. A., Lee, J., Wedlock, D. N., Buddle, B. M. & Rehm, B. H. 2014. New skin test for detection of bovine tuberculosis on the basis of antigen-displaying polyester inclusions produced by recombinant Escherichia coli. *Appl Environ Microbiol,* 80**,** 2526-35. Available: DOI 10.1128/AEM.04168-13.

Chitnis, C. E. & Ohman, D. E. 1993. Genetic analysis of the alginate biosynthetic gene cluster of Pseudomonas aeruginosa shows evidence of an operonic structure. *Mol Microbiol,* 8**,** 583-93.

Chong, S., Mersha, F. B., Comb, D. G., Scott, M. E., Landry, D., Vence, L. M., Perler, F. B., Benner, J., Kucera, R. B., Hirvonen, C. A., Pelletier, J. J., Paulus, H. & Xu, M. Q. 1997. Single-column purification of free recombinant proteins using a self-cleavable affinity tag derived from a protein splicing element. *Gene,* 192**,** 271-81.

David, M., Günther, H. & Röper, H. 1987. Catalytic properties of Bacillus megaterium amylase. *Starch,* 39**,** 436-440.

Dawson, R. M. C., Elliott, D. C., Elliott, W. H. & Jones, K. M. 1986. *Data for biochemical research,* Oxford, United Kingdom, Clarendon Press.

De Moraes, M. A., Silva, M. F., Weska, R. F. & Beppu, M. M. 2014. Silk fibroin and sodium alginate blend: miscibility and physical characteristics. *Mater Sci Eng C Mater Biol Appl,* 40**,** 85-91. Available: DOI 10.1016/j.msec.2014.03.047.

Demain, A. L. & Vaishnav, P. 2009. Production of recombinant proteins by microbes and higher organisms. *Biotechnol Adv,* 27**,** 297-306. Available: DOI 10.1016/j.biotechadv.2009.01.008.

Doig, P., Smith, N. R., Todd, T. & Irvin, R. T. 1987. Characterization of the binding of Pseudomonas aeruginosa alginate to human epithelial cells. *Infect Immun,* 55**,** 1517-22.
Franklin, M. J., Chitnis, C. E., Gacesa, P., Sonesson, A., White, D. C. & Ohman, D. E. 1994. Pseudomonas aeruginosa AlgG is a polymer level alginate C5-mannuronan epimerase. *J Bacteriol,* 176**,** 1821-30.
Franklin, M. J., Nivens, D. E., Weadge, J. T. & Howell, P. L. 2011. Biosynthesis of the Pseudomonas aeruginosa Extracellular Polysaccharides, Alginate, Pel, and Psl. *Front Microbiol,* 2**,** 167. Available: DOI 10.3389/fmicb.2011.00167.
Franklin, M. J. & Ohman, D. E. 1993. Identification of algF in the alginate biosynthetic gene cluster of Pseudomonas aeruginosa which is required for alginate acetylation. *J Bacteriol,* 175**,** 5057-65.
Franklin, M. J. & Ohman, D. E. 1996. Identification of algI and algJ in the Pseudomonas aeruginosa alginate biosynthetic gene cluster which are required for alginate O acetylation. *J Bacteriol,* 178**,** 2186-95.
Gottschalk, U. 2008. Bioseparation in antibody manufacturing: the good, the bad and the ugly. *Biotechnol Prog,* 24**,** 496-503. Available: DOI 10.1021/bp070452g.
Grage, K., Peters, V. & Rehm, B. H. 2011. Recombinant protein production by in vivo polymer inclusion display. *Appl Environ Microbiol,* 77**,** 6706-9. Available: DOI 10.1128/AEM.05953-11.
Grage, K. & Rehm, B. H. 2008. In vivo production of scFv-displaying biopolymer beads using a self-assembly-promoting fusion partner. *Bioconjug Chem,* 19**,** 254-62. Available: DOI 10.1021/bc7003473.
Gutsche, J., Remminghorst, U. & Rehm, B. H. 2006. Biochemical analysis of alginate biosynthesis protein AlgX from Pseudomonas aeruginosa: purification of an AlgX-MucD (AlgY) protein complex. *Biochimie,* 88**,** 245-51. Available: DOI 10.1016/j.biochi.2005.06.003.
Haki, G. D. & Rakshit, S. K. 2003. Developments in industrially important thermostable enzymes: a review. *Bioresour Technol,* 89**,** 17-34.
Hanahan, D. 1983. Studies on transformation of Escherichia coli with plasmids. *J Mol Biol,* 166**,** 557-80.
Hay, I. D., Du, J., Reyes, P. R. & Rehm, B. H. 2015. In vivo polyester immobilized sortase for tagless protein purification. *Microb Cell Fact,* 14**,** 190. Available: DOI 10.1186/s12934-015-0385-3.
Hay, I. D., Ur Rehman, Z., Moradali, M. F., Wang, Y. & Rehm, B. H. 2013. Microbial alginate production, modification and its applications. *Microb Biotechnol,* 6**,** 637-50. Available: DOI 10.1111/1751-7915.12076.
Laemmli, U. K. 1970. Cleavage of structural proteins during the assembly of the head of bacteriophage T4. *Nature,* 227**,** 680-5.
Langer, E. 2012. Key downstream problems decline while industry continues to demand new technologies.: BioProcess International. Available: http://www.bioprocessintl.com/downstream-processing/chromatography/key-downstream-problems-decline-while-industry-continues-to-demand-new-technologies-329015/.
Leonard, L., Gharsallaoui, A., Ouaali, F., Degraeve, P., Wache, Y., Saurel, R. & Oulahal, N. 2013. Preferential localization of Lactococcus lactis cells entrapped in a caseinate/alginate phase separated system. *Colloids Surf B Biointerfaces,* 109**,** 266-72. Available: DOI 10.1016/j.colsurfb.2013.03.005.
Liu, Y., Fan, S., Liu, X., Zhang, Z., Wang, J., Wang, Z. & Lu, F. 2014. A highly active alpha amylase from Bacillus licheniformis: directed evolution, enzyme characterization and structural analysis. *J Microbiol Biotechnol,* 24**,** 898-904.
Luo, J., Choulet, J. & Samuelson, J. C. 2009. Rational design of a fusion partner for membrane protein expression in E. coli. *Protein Sci,* 18**,** 1735-44. Available: DOI 10.1002/pro.189.
Martinez, T. F., Alarcon, F. J., Diaz-Lopez, M. & Moyano, F. J. 2000. Improved detection of amylase activity by sodium dodecyl sulfate-polyacrylamide gel electrophoresis with copolymerized

starch. *Electrophoresis,* 21**,** 2940-3. Available: DOI 10.1002/1522-2683(20000801)21:14<2940::AID-ELPS2940>3.0.CO;2-S.
Miraula, M., Enculescu, C., Schenk, G. & Mitić, N. 2015. Inteins—a focus on the biotechnological applications of splicing-promoting proteins. *American Journal of Molecular Biology,* 5**,** 42-56. Available: DOI 10.4236/ajmb.2015.52005.
Moraes, M. & Beppu, M. 2013. Biocomposite membranes of sodium alginate and silk fibroin fibers for biomedical applications. *Journal of Applied Polymer Science,* 130**,** 3451-3457. Available: DOI 10.1002/app.39598.
Nivens, D. E., Ohman, D. E., Williams, J. & Franklin, M. J. 2001. Role of alginate and its O acetylation in formation of Pseudomonas aeruginosa microcolonies and biofilms. *J Bacteriol,* 183**,** 1047-57. Available: DOI 10.1128/JB.183.3.1047-1057.2001.
O'toole, G., Kaplan, H. B. & Kolter, R. 2000. Biofilm formation as microbial development. *Annu Rev Microbiol,* 54**,** 49-79. Available: DOI 10.1146/annurev.micro.54.1.49.
Park, D., Jagtap, S. & Nair, S. K. 2014. Structure of a PL17 family alginate lyase demonstrates functional similarities among exotype depolymerases. *J Biol Chem,* 289**,** 8645-55. Available: DOI 10.1074/jbc.M113.531111.
Parlane, N. A., Chen, S., Jones, G. J., Vordermeier, H. M., Wedlock, D. N., Rehm, B. H. & Buddle, B. M. 2015. Display of Antigens on Polyester Inclusions Lowers the Antigen Concentration Required for a Bovine Tuberculosis Skin Test. *Clin Vaccine Immunol,* 23**,** 19-26. Available: DOI 10.1128/CVI.00462-15.
Paul, W. & Sharma, C. 2004. Chitosan and alginate wound dressings: a short review. *Trends in Biomaterials and Artificial Organs,* 18**,** 18-23.
Qin, Y., Fang, Z., Pan, F., Zhao, Y., Li, H., Wu, H. & Meng, X. 2012. Significance of Tyr302, His235 and Asp194 in the alpha-amylase from Bacillus licheniformis. *Biotechnol Lett,* 34**,** 895-9. Available: DOI 10.1007/s10529-011-0843-x.
Ramadas, M., Paul, W., Dileep, K. J., Anitha, Y. & Sharma, C. P. 2000. Lipoinsulin encapsulated alginate-chitosan capsules: intestinal delivery in diabetic rats. *J Microencapsul,* 17**,** 405-11. Available: DOI 10.1080/026520400405660.
Rasiah, I. A. & Rehm, B. H. 2009. One-step production of immobilized alpha-amylase in recombinant Escherichia coli. *Appl Environ Microbiol,* 75**,** 2012-6. Available: DOI 10.1128/AEM.02782-08.
Rehm, B. H. 2010. Bacterial polymers: biosynthesis, modifications and applications. *Nat Rev Microbiol,* 8**,** 578-92. Available: DOI 10.1038/nrmicro2354.
Rehm, B. H., Boheim, G., Tommassen, J. & Winkler, U. K. 1994. Overexpression of algE in Escherichia coli: subcellular localization, purification, and ion channel properties. *J Bacteriol,* 176**,** 5639-47.
Rehman, Z. U., Wang, Y., Moradali, M. F., Hay, I. D. & Rehm, B. H. 2013. Insights into the assembly of the alginate biosynthesis machinery in Pseudomonas aeruginosa. *Appl Environ Microbiol,* 79**,** 3264-72. Available: DOI 10.1128/AEM.00460-13.
Remminghorst, U. & Rehm, B. H. 2006. Bacterial alginates: from biosynthesis to applications. *Biotechnol Lett,* 28**,** 1701-12. Available: DOI 10.1007/s10529-006-9156-x.
Riley, L. M., Weadge, J. T., Baker, P., Robinson, H., Codee, J. D., Tipton, P. A., Ohman, D. E. & Howell, P. L. 2013. Structural and functional characterization of Pseudomonas aeruginosa AlgX: role of AlgX in alginate acetylation. *J Biol Chem,* 288**,** 22299-314. Available: DOI 10.1074/jbc.M113.484931.
Robles-Price, A., Wong, T. Y., Sletta, H., Valla, S. & Schiller, N. L. 2004. AlgX is a periplasmic protein required for alginate biosynthesis in Pseudomonas aeruginosa. *J Bacteriol,* 186**,** 7369-77. Available: DOI 10.1128/JB.186.21.7369-7377.2004.
Sambrook, J., Fritsch, E. F. & Maniatis, T. 1989. *Molecular cloning: a laboratory manual,* Cold Spring Harbor, NY, Cold Spring Harbor Laboratory Press.

Shankar, S., Ye, R. W., Schlictman, D. & Chakrabarty, A. M. 1995. Exopolysaccharide alginate synthesis in Pseudomonas aeruginosa: enzymology and regulation of gene expression. *Adv Enzymol Relat Areas Mol Biol,* 70**,** 221-55.

Shimoyama, T., Itoh, K., Kobayashi, M., Miyazaki, S., D'emanuele, A. & Attwood, D. 2012. Oral liquid in situ gelling methylcellulose/alginate formulations for sustained drug delivery to dysphagic patients. *Drug Dev Ind Pharm,* 38**,** 952-60. Available: DOI 10.3109/03639045.2011.634809.

Silva, M., Yamanaka, B., Taniwaki, M. & Kieckbusch, T. 2012. Evaluation of the antimicrobial potential of alginate and alginate/chitosan films containing potassium sorbate and natamycin. *Packaging Technology and Science,* 26**,** 479-492.

Simpson, R. 2006. Bulk precipitation of proteins by ammonium sulfate. Cold Spring Harbor. Available: http://cshprotocols.cshlp.org/content/2006/1/pdb.prot4308.citation.

Skoog, D. A. 2006. *Principles of Instrumental Analysis,* Belmont, California, Thompson Brooks/Cole.

Sun, J. Y., Zhao, X., Illeperuma, W. R., Chaudhuri, O., Oh, K. H., Mooney, D. J., Vlassak, J. J. & Suo, Z. 2012. Highly stretchable and tough hydrogels. *Nature,* 489**,** 133-6. Available: DOI 10.1038/nature11409.

Svanem, B. I., Strand, W. I., Ertesvag, H., Skjak-Braek, G., Hartmann, M., Barbeyron, T. & Valla, S. 2001. The catalytic activities of the bifunctional Azotobacter vinelandii mannuronan C-5-epimerase and alginate lyase AlgE7 probably originate from the same active site in the enzyme. *J Biol Chem,* 276**,** 31542-50. Available: DOI 10.1074/jbc.M102562200.

Tabassum, R., Khaliq, S., Rajoka, M. I. & Agblevor, F. 2014. Solid State Fermentation of a Raw Starch Digesting Alkaline Alpha-Amylase from Bacillus licheniformis RT7PE1 and Its Characteristics. *Biotechnol Res Int,* 2014**,** 495384. Available: DOI 10.1155/2014/495384.

Terpe, K. 2006. Overview of bacterial expression systems for heterologous protein production: from molecular and biochemical fundamentals to commercial systems. *Appl Microbiol Biotechnol,* 72**,** 211-22. Available: DOI 10.1007/s00253-006-0465-8.

Tielen, P., Strathmann, M., Jaeger, K. E., Flemming, H. C. & Wingender, J. 2005. Alginate acetylation influences initial surface colonization by mucoid Pseudomonas aeruginosa. *Microbiol Res,* 160**,** 165-76. Available: DOI 10.1016/j.micres.2004.11.003.

Uchino, K., Saito, T., Gebauer, B. & Jendrossek, D. 2007. Isolated poly(3-hydroxybutyrate) (PHB) granules are complex bacterial organelles catalyzing formation of PHB from acetyl coenzyme A (CoA) and degradation of PHB to acetyl-CoA. *J Bacteriol,* 189**,** 8250-6. Available: DOI 10.1128/JB.00752-07.

Vary, P. S., Biedendieck, R., Fuerch, T., Meinhardt, F., Rohde, M., Deckwer, W. D. & Jahn, D. 2007. Bacillus megaterium--from simple soil bacterium to industrial protein production host. *Appl Microbiol Biotechnol,* 76**,** 957-67. Available: DOI 10.1007/s00253-007-1089-3.

Volkmann, G. & Iwai, H. 2010. Protein trans-splicing and its use in structural biology: opportunities and limitations. *Mol Biosyst,* 6**,** 2110-21. Available: DOI 10.1039/c0mb00034e.

Volkmann, G. & Mootz, H. D. 2013. Recent progress in intein research: from mechanism to directed evolution and applications. *Cell Mol Life Sci,* 70**,** 1185-206. Available: DOI 10.1007/s00018-012-1120-4.

Volkmann, G., Sun, W. & Liu, X. Q. 2009. Controllable protein cleavages through intein fragment complementation. *Protein Sci,* 18**,** 2393-402. Available: DOI 10.1002/pro.249.

Wang, W., Hollmann, R. & Deckwer, W. D. 2006. Comparative proteomic analysis of high cell density cultivations with two recombinant Bacillus megaterium strains for the production of a heterologous dextransucrase. *Proteome Sci,* 4**,** 19. Available: DOI 10.1186/1477-5956-4-19.

Weadge, J. T., Yip, P. P., Robinson, H., Arnett, K., Tipton, P. A. & Howell, P. L. 2010. Expression, purification, crystallization and preliminary X-ray analysis of Pseudomonas aeruginosa AlgX. *Acta Crystallogr Sect F Struct Biol Cryst Commun,* 66**,** 588-91. Available: DOI 10.1107/S1744309110011851.

Wolfram, F., Kitova, E. N., Robinson, H., Walvoort, M. T., Codee, J. D., Klassen, J. S. & Howell, P. L. 2014. Catalytic mechanism and mode of action of the periplasmic alginate epimerase AlgG. *J Biol Chem,* 289**,** 6006-19. Available: DOI 10.1074/jbc.M113.533158.

Zhu, B. & Yin, H. 2015. Alginate lyase: Review of major sources and classification, properties, structure-function analysis and applications. *Bioengineered,* 6**,** 125-31. Available: DOI 10.1080/21655979.2015.1030543.